Durham University

Durham E-Theses

Re-Os Systematics of Crude Oil and Re-Os Petroleum System Geochronology

LIU, JUNJIE

How to cite:

LIU, JUNJIE (2017) *Re-Os Systematics of Crude Oil and Re-Os Petroleum System Geochronology*, Durham theses, Durham University. Available at Durham E-Theses Online: http://etheses.dur.ac.uk/12296/

Use policy

The full-text may be used and/or reproduced, and given to third parties in any format or medium, without prior permission or charge, for personal research or study, educational, or not-for-profit purposes provided that:

- a full bibliographic reference is made to the original source
- a link is made to the metadata record in Durham E-Theses
- the full-text is not changed in any way

The full-text must not be sold in any format or medium without the formal permission of the copyright holders.

Please consult the full Durham E-Theses policy for further details.

Academic Support Office, The Palatine Centre, Durham University, Stockton Road, Durham, DH1 3LE
e-mail: e-theses.admin@durham.ac.uk Tel: +44 0191 334 6107
http://etheses.dur.ac.uk

Abstract

Junjie LIU (刘俊杰)

Re-Os Systematics of Crude Oil and Re-Os Petroleum System Geochronology

Re and Os are present in many crude oils in measurable abundances. The Re-Os geochronometer has successfully constrained the timing of oil generation, thermochemical sulphate reduction and thermal alteration of crude oil for petroleum systems worldwide. The Os isotope composition has also been used as an oil-source correlation tool.

This thesis firstly presents two petroleum matrix-matched Re-Os measurement reference materials: the RM8505 crude oil and ~ 90 g homogeneous asphaltene powder isolated from the RM8505 crude oil. The Re-Os data are from the repeated measurements of these samples via the Carius Tube - Isotope Dilution - Negative Thermal Ionization Mass Spectrometry methodology. The normal distribution and low relative standard deviation of the abundance and isotopic data ensure them to be appropriate petroleum matrix-matched reference materials for Re-Os measurements.

A Re-Os age of 66 ± 31 Ma was defined by the Duvernay-sourced oil asphaltene fractions from Western Canada sedimentary basin. This age is in excellent agreement with the main-stage hydrocarbon generation of Duvernay Formation based on basin modelling. Further, this study supports Os isotope composition as a valid oil-source tracer and the hypothesis that the oil $^{187}Os/^{188}Os$ composition is inherited from the source unit during oil generation. This study shows limited or no influence of the Re-Os systematics of crude oil through the interaction of basinal fluids.

The progressively precipitated asphaltene fractions of six oil samples exhibit a decrease in Re and Os abundance, and diverse $^{187}Re/^{188}Os$ and $^{187}Os/^{188}Os$ patterns. This study proposes that Re and Os in crude oil are to be bound in multiple free compounds and such molecules occluded/absorbed in the asphaltene aggregate structure. No combination of the fractions of a crude oil can consistently yield geologically meaningful Re-Os age for all of the six oil samples, either the progressively precipitated asphaltene fractions or the asphaltenes and maltenes separated by *n*-alkanes. As such, obtaining geologically meaningful Re-Os dates from a single oil may not be viable for many oils.

Re-Os Systematics of Crude Oil and Re-Os Petroleum System Geochronology

Junjie LIU

刘俊杰

A thesis submitted in partial fulfilment of the requirements for the degree of

Doctor of Philosophy at Durham University

Department of Earth Sciences

Durham University

2017

Table of Contents

Abstract 1
Table of Contents 5
List of Tables 9
List of Figures 11
List of Abbreviations 15
Declaration 17
Acknowledgement 19

Chapter 1 Introduction
1.1 The presence of Re and Os in petroleum system 21
1.2 The Re-Os elemental and isotopic systematics within crude oil 22
1.3 The application of Re-Os geochronometer to petroleum systems 23
1.3.1 The Re-Os geochronology of petroleum systems 23
1.3.2 Oil-source correlation with Os isotope composition 25
1.4 Research rationale 25
1.4.1 Petroleum Re-Os analysis reference material 26
1.4.2 Re-Os dating of the crude oil generation of Duvernay petroleum system 26
1.4.3 Re-Os elemental and isotopic systematics within crude oil 27
1.5 Thesis outline 28
1.5.1 Chapter Two: A matrix matched reference material for validating petroleum Re-Os analysis 28
1.5.2 Chapter Three: Re-Os geochronology and oil-source correlation of Duvernay petroleum system, Western Canada sedimentary basin: Implications for the application of the Re-Os geochronometer to petroleum systems 28
1.5.3 Chapter Four: Further evaluation of the Re-Os systematics of crude oil: Implications for Re-Os geochronology of petroleum systems 29
1.5.4 Chapter Five: Conclusions and future work 29
1.6 References 31

Chapter 2 A matrix matched reference material for validating petroleum Re-Os analysis
2.1 Introduction 33
2.2 Samples preparation 35

2.3 Analytical procedure 37
2.4 Results and discussion 38
2.4.1 RM8505 whole oil Re and Os and comparison with previous studies 38
2.4.2 Re and Os data of the individually separated asphaltene and maltene from RM8505 40
2.4.3 Asphaltene and maltene mass balance and isotopic characteristics 41
2.4.4 Homogenized asphaltene 42
2.4.5 Comparing whole oil, individually separated asphaltene and homogenized asphaltene as reference material 43
2.5 Summary 44
2.6 References 45
Tables 49
Figures 60

Chapter 3 Re-Os geochronology and oil-source correlation of the Duvernay petroleum system, Western Canada sedimentary basin: Implications for the application of the Re-Os geochronometer to petroleum systems
3.1 Introduction 77
3.2 Geological setting 81
3.3 Sample preparation and analysis methodology 84
3.3.1 Oil samples 84
3.3.2 Source rock 85
3.3.3 Gas chromatography and biomarker analyses of crude oil and source rock extracts 85
3.3.4 Re-Os analyses 86
3.4 Results 87
3.4.1 Asphaltene Re-Os data 88
3.4.2 Re-Os data for organic-rich intervals of the Duvernay Formation 88
3.4.3 Organic geochemistry of crude oil and source rock 89
3.5 Discussion 91
3.5.1 Petroleum Re-Os geochronology 91
3.5.2 $^{187}Os/^{188}Os$ composition oil-source fingerprinting 92
3.5.3 Oil Re-Os systematics: effect of oil-water contact 96
3.6 Conclusions 97
3.7 References 99

Tables 105
Figures 116

Chapter 4 Further evaluation of the Re-Os systematics of crude oil: Implications for Re-Os geochronology of petroleum systems
4.1 Introduction 143
4.2 Samples and analytical protocols 145
4.2.1 The samples 145
4.2.2 Sample preparation 147
4.2.3 Re-Os analyses of the samples 149
4.3 Results 150
4.3.1 The progressive precipitation of asphaltene and the separation of crude oil by *n*-alkanes 150
4.3.2 Re and Os elemental abundances and distribution in the fractions of oil 151
4.3.3 Re-Os isotopic systematics 154
4.4 Discussion 156
4.4.1 The residence of Re and Os in crude oil and asphaltene 156
4.4.2 Insights to Re-Os behaviour in oil based on the Re-Os isotopic systematics of crude oil fractions 159
4.4.3 Re-Os geochronology from the fractions of crude oil 160
4.5 Conclusion 163
4.6 References 165
Tables 171
Figures 190

Chapter 5 Conclusions and prospects
5.1 Petroleum matrix-matched Re-Os analysis reference materials 209
5.2 Re-Os geochronology and oil-source correlation of Duvernay petroleum system 210
5.3 Re-Os elemental and isotopic systematics during the fractionation of crude oil and asphaltene 211
5.4 References 213

List of Tables

Chapter 2

Table 2.1 Total procedural blanks of rhenium and osmium, and $^{187}Os/^{188}Os$ composition during the study. 49

Table 2.2 Rhenium and osmium abundances and isotopic ratios of RM8505 whole oil. 50 - 52

Table 2.3 Rhenium and osmium abundances and isotopic ratios of the individually separated asphaltene fractions from RM8505. 53 - 54

Table 2.4 Rhenium and osmium abundances and isotopic ratios of the individually separated maltene fractions from RM8505. 55 - 56

Table 2.5 Rhenium and osmium abundances and isotopic ratios of the homogenized asphaltene samples. 57

Table 2.6 Asphaltene and maltene mass percentage and their Re and Os proportion of their sum, i.e. the whole oil. 58 - 59

Chapter 3

Table 3.1 Well locations and reservoir formations of the oil samples of this study. 105

Table 3.2 Re-Os data synopsis for the Duvernay Formation shale samples from multiple locations (wells) and their Os_i (378.5 Ma) and Os_g (66 Ma) values. 106 - 108

Table 3.3 Re-Os data synopsis for asphaltene fractions of the oil samples from the Duvernay petroleum system and their Os_i (66 Ma) values. 109 - 110

Table 3.4 The compounds represented by the peak annotations in the geochemistry figures (Figures 3.8 - 3.10). 111

Table 3.5 Re-Os data and calculated $^{187}Os/^{188}Os$ composition at 66 Ma for other oil prone strata of the WCSB. 112 - 115

Chapter 4

Table 4.1 Details of the bulk asphaltene, solvent/precipitant volume and the progressively precipitated fractions of asphaltene. 171

Table 4.2 The separation of crude oils by *n*-alkanes (*n*-C_5, *n*-C_6, *n*-C_7, *n*-C_8, *n*-C_9 and *n*-C_{10}) and dichloromethane and methanol of Derby, Federal, Viking-Morel, Persian, Purisima and RM8505 oil samples. 172 - 173

Table 4.3 Re-Os data synopsis for the progressively precipitated asphaltene fractions and the whole oil, *n*-heptane asphaltene and maltene for the six oils. The mass balance calculation of Re, unradiogenic Os (^{192}Os) and radiogenic ^{187}Os for the progressive precipitation is also presented. See text for discussion. 174 - 180

Table 4.4 Re-Os data synopsis for the asphaltene fractions separated by *n*-alkane-dichloromethane-methanol from the six oil samples. 181 - 182

Table 4.5 Re-Os data synopsis for the maltene fractions separated by *n*-alkane-dichloromethane-methanol from the six oil samples. 183 - 184

Table 4.6 The sum of Re and Os of asphaltenes and maltenes separated by *n*-alkanes, and the percentage they account for of the crude oil. 185 - 187

Table 4.7 Geochronology of the fractions of the six crude oil samples in this study. 188 - 189

List of Figures

Chapter 2

Figure 2.1 Linearized probability plots (top) and histograms and probability density curves (bottom) of RM8505 whole oil Re-Os data. 60 - 61

Figure 2.2 Linearized probability plots (top) and histograms and probability density curves (bottom) for individually separated asphaltene Re-Os data. 62 - 63

Figure 2.3 Linearized probability plots (top) and histograms and probability density curves (bottom) of separated maltene Re-Os data. 64 - 65

Figure 2.4 Comparison of the Re and Os abundances of RM8505 whole oil, asphaltene and maltene. 66 - 67

Figure 2.5 Comparison of the Re-Os isotopic compositions of the RM8505 whole oil, asphaltene and maltene. 68 - 69

Figure 2.6 Mass balance of asphaltene-maltene separation and Re-Os budget of RM8505 oil: a) mass percentages of asphaltene and maltene; b) Re budget of RM8505 oil separated asphaltene and maltene fractions; c) Os budget of RM8505 oil separated asphaltene and maltene fractions; d) Re percentages of asphaltene and maltene within oil; and e) Os percentages of asphaltene and maltene within oil. 70 - 71

Figure 2.7 Comparison of the Re-Os isotopic compositions of asphaltene, crude oil and maltene of previously studied oils: a) seven oils from Selby *et al*. (2007) and b) selected data of three oils from Georgiev *et al*. (2016). 72 - 73

Figure 2.8 Linearized probability plots (top) and histograms and probability density curves (bottom) of the homogenized asphaltene Re-Os data. 74 - 75

Chapter 3

Figure 3.1 Map of the study area showing the location of the oil and Duvernay Formation shale samples used in this study (modified from Fowler et al. 2001 with the permission of Canadian Society of Petroleum Geologists). 116 - 117

Figure 3.2 Devonian stratigraphy of the study area, south-central Alberta (modified from Li et al. 1998 and Fowler et al. 2001). 118 - 119

Figure 3.3 Migration of the Duvernay Formation generated oil (Modified from Switzer et al. 1994). 120 - 121

Figure 3.4 Asphaltene content versus asphaltene Re (ppb) and unradiogenic Os (ppt, represented by ^{192}Os) abundance of the Duvernay oils. 122 - 123

Figure 3.5 $^{187}Re/^{188}Os$ vs $^{187}Os/^{188}Os$ plot for the asphaltene fractions of the Duvernay oil. 124 - 125

Figure 3.6 The individually calculated Os_i values of asphaltene samples of the Duvernay oil. 126 - 127

Figure 3.7 Duvernay Formation total organic carbon (TOC), Re and unradiogenic Os (^{192}Os as representative) abundances, and calculated $^{187}Os/^{188}Os$ compositions at the time of deposition (Os_i, 378.5 Ma) and oil generation (Os_g, 66 Ma). 128 - 129

Figure 3.8a Representative gas chromatograms showing distributions of: 1) gasoline range hydrocarbons and 2) normal alkanes and isoprenoids in low (sample L02221), medium (sample L02155) and high (sample L02177) maturity Duvernay-sourced crude oils. 130 - 131

Figure 3.8b Representative gas chromatograms showing distributions of: 3) terpanes and 4) steranes in low (sample L02221), medium (sample L02155) and high (sample L02177) maturity Duvernay-sourced crude oils. 132 - 133

Figure 3.9 Saturate fraction gas chromatograms showing distributions of 1) normal alkanes and isoprenoids, 2) terpanes and 3) steranes in low and high maturity Duvernay Formation organic extracts. 134 - 135

Figure 3.10 Oil-source correlation of a Nisku crude oil from Wood River field (within the Bashaw reef complex, 10-28-42-23W4, sample L02203) and Duvernay Formation organic extract from 13-14-35-25W4. 136 - 137

Figure 3.11 $^{187}Re/^{188}Os$ vs $^{187}Os/^{188}Os$ plots for the Duvernay formation. A) core 10-27-57-21W4; B) core 16-18-52-5W5; C) core 14-29-48-6W5; D) core 2-6-47-4W5;

and E) all data including samples from references (Selby et al., 2007; Finlay et al., 2012). 138 - 139

Figure 3.12 Comparison of the currently available $^{187}Os/^{188}Os$ compositions at 66 Ma for the WCSB Phanerozoic organic-rich intervals with the Duvernay shale Os_g and oil Os_i values. 140 - 141

Chapter 4

Figure 4.1 The modified Yen model of asphaltene molecule, aggregate and cluster structure (Mullins, 2010). 190 - 191

Figure 4.2 Free metal complexes and the absorption and occlusion by asphaltene aggregates (Modified from Snowdon et al. 2016). 192 - 193

Figure 4.3 The procedure of asphaltene progressive precipitation. . 194 - 195

Figure 4.4 Mass percentages of the progressively precipitated fractions of the asphaltenes. 196 - 197

Figure 4.5 Asphaltene (a) and maltene (b) percentages separated by *n*-alkane-DCM-methanol and their total (c). 198 - 199

Figure 4.6 Normalized Re and Os abundances of the fractions of Derby oil, Federal oil and Viking-Morel oil. 200 - 201

Figure 4.7 Normalized Re and Os abundances of Persian oil, Purisima oil and RM8505 oil. 202 - 203

Figure 4.8 The Re-Os isotopic ratios of Derby oil, Federal oil and Viking-Morel oil. 204 - 205

Figure 4.9 The Re-Os isotopic ratios of Persian oil, Purisima oil and RM8505 oil. 206 - 207

List of Abbreviations

Os_i	– Initial $^{187}Os/^{188}Os$ at the time of rock deposition or oil generation	25
Os_g	– $^{187}Os/^{188}Os$ of source rock at the time of oil generation	25
NIST	– National Institute of Standards and Technology	28
RM8505	– Research Material 8505	28
rpm	– Round per minute	36
MSWD	– Mean standard weighted distribution	42
WCSB	– Western Canada sedimentary basin	81
ppb	– Part per billion (ng/g)	88
ppt	– Part per trillion (pg/g)	88

Declaration

I declare that this thesis, which I submit for the degree of Doctor of Philosophy at Durham University, is my own work and the contained material has never been submitted for a degree in this or any other institution previously.

Junjie Liu

Durham University

July, 2017

© The copyright of this thesis rests with the author. No quotation from it should be published without the author's prior written consent and information derived from it should be acknowledged.

Acknowledgement

If consider only the scientific struggle that I have had throughout this PhD, it is not hard for me to understand why it would be the last degree people wish to get. As such it would not have been possible for me to accomplish it without the massive support and guidance that I received.

Firstly, I would like to acknowledge my supervisor Professor David Selby and the sources of funding. Profound gratitude goes to Dave for being very dedicated to his role and sharing his expertise so willingly. Dave has been both being meticulous on the experiments and writings and being open-minded – he allows me to try to interpret the data in the way wildly as I can see today. Also, this research is only made possible by the research funding from the petroleum company Total, a Durham University tuition waiver and a China Scholarship Council grant: and many thanks to Dave for his role in securing them (the funds).

Importantly, I would like to thank my collaborators and reviewer who have also contributed to this work. Dr Honggang Zhou and Dr Magali Pujol, thank you for your deep involvement in my research and the insightful discussions. Dr Mark Obermajer and Dr Andy Mort, thank you for your contributions to the experiments and writing and the help for my presentations of the work. Dr Paul Lillis, thank you for your persistent help with the samples and your comments and advices on writing. Professor Andrew Aplin and Professor Ken McCaffrey, thank you for being my PhD progress reviewers. Many thanks go to Professor Erdem Idiz and Professor Andrew Aplin for being my examiners. Professor Chris Greenwell, thank you very much for your inspiration on my projects and the massive support of lab work.

I have also been benefited hugely from the people from the lab, especially Dr Joanna Hesselink, Miss Antonia Hofmann and Dr Edward Dempsey who have provided the much needed instruction and help on the lab works. Xiang, Adam and Zeyang, your wits and company are a great part of the pleasure of the lab time, many thanks to you. Also, many thanks go to all my friends in Durham, Beijing and my hometown for your unending support which kept me going. Thank you to the friends in Durham, especially to Li Li, Sheng, Hongliang, Lijun, Ma Zhao, the Huangs, Guangquan, Huizhe, Ning, Xiaolin, Wenyan, and Seunghee and Loraine The Beautiful for the

company, entertainment and encouragement. Special thanks go to Huifei, Meiyan, Li Li and Yanzhong for your support both academically and personally.

Without the support from my beloved family I could never have come to Durham and conduct this PhD. Thanks for my parents and siblings for your supports on every decision I have made and many thanks to my nieces and nephew for your unconditional love.

Finally, thanks to everyone who helps me in any way during or before this PhD although I have not mentioned you specifically.

Chapter 1 Introduction

In addition to the collection of techniques available today, e.g. basin modelling and biomarker analysis, the rhenium-osmium (Re-Os) isotope system provides a novel and powerful tool to determine the timing of crude oil generation and trace the source of oil (Selby et al., 2005; Selby and Creaser, 2005; Selby et al., 2007; Finlay et al., 2011; Finlay et al., 2012; Rooney et al., 2012; Lillis and Selby, 2013; Cumming et al., 2014). The research presented in this thesis aims to improve the understanding of the Re-Os geochronometer in the dating of crude oil generation and also the elemental (abundance) and isotopic (ratios) systematics of Re and Os in crude oil. This introductory chapter presents brief background of Re-Os studies in the dating of crude oil generation and the rationale of the research of this thesis.

1.1 The presence of Re and Os in petroleum system

Rhenium and osmium have long been found to be present in bitumens and crude oils in measurable concentrations (Poplavko et al., 1974; Barre et al., 1995; Selby et al., 2007). The origin of Re and Os in crude oil and bitumen is thought to be either the source rock of crude oil (Rooney et al., 2012; Cumming et al., 2014) and/or formation water in contact with oil (Mahdaoui et al., 2015) and/or carrier and reservoir rocks.

The organic-rich sedimentary intervals, where the crude oils are originated from, are commonly enriched in Re and Os in comparison to the upper continental crust which has the average concentrations of 198 pg/g Re and 31 pg/g Os (Peucker-Ehrenbrink and Jahn, 2001). Hydrous pyrolysis experiments have been conducted on Type I, II-S and III kerogen source rocks (Rooney et al., 2012; Cumming et al., 2014). These experiments showed that Re and Os were transferred to the generated oil during thermal maturation, although the majority of them still remained in the source rock. Simultaneously, the generated oil also inherited the Os isotopic composition of the source rock. However, the abundances of Re and Os of the artificially generated oil are relatively low compared to those of natural crude oil. The authors suggested that the transfer of Re and Os is kinetically controlled and attributed the low abundances in generated oils to the difference in hydrous pyrolysis experiment conditions with the natural generation of oil, i.e. short time, high temperature and the formation of insoluble phase during the experiments.

In an oil-water contact experiment, Re and Os transferred rapidly and massively to the oil from the water phase of a wide range of Re and Os concentration under different temperatures (Mahdaoui et al., 2015). According to the calculation of the authors, it is possible that all of the Re and Os in crude oil can be transferred from the basinal fluids in contact with oil. Thus, the authors proposed that formation water can possibly be the main origin of the Re and Os in crude oil and the limited transfer of these elements from source rock to generated oil during the hydrous pyrolysis may not simply be the artefact of the experiments. Based on this proposal, the authors also proposed the mechanism of Os isotopic composition homogenization and fractionation of Re/Os ratios, which are the basic conditions for the Re-Os geochronometer to serve.

1.2 The Re-Os elemental and isotopic systematics within crude oil

The residence of Re and Os within crude oil was firstly examined by separating 17 worldwide oils into asphaltene and maltene fractions (Selby et al., 2007). It was shown that asphaltene is the main carrier of the Re (> 90%) and Os (> 83%) in crude oil. As a result, the crude oil Re-Os isotopic ratios are largely dominated by the asphaltene fraction. Their similarity allows the use of asphaltene as a substitute of whole oil to obtain Re-Os isotopic ratios of better precision than the crude oils. This substitution is especially important in the application of this tool to oils with low Re and Os abundances. Meanwhile, the Re-Os isotope compositions of the maltene fraction were shown to be either similar to or higher or lower than the asphaltene fraction of a crude oil (Selby et al., 2007; Georgiev et al., 2016). Selby et al. (2007), suggesting the possibility of multiple complexes for Re and Os in crude oil, including metalloporphyrins.

The residence and isotopic systematics of Re and Os in crude oil was further revealed by the Re-Os analyses taken on the progressive precipitated sub-fractions of asphaltene (Mahdaoui et al., 2013). The Re and Os abundances of the precipitated asphaltene sub-fractions decrease during the progressive precipitation while the Re/Os elemental and $^{187}Os/^{188}Os$ ratios remain constant except for the last few fractions. Thus, the authors argued that the natural loss of asphaltene in petroleum systems has little influence on Re/Os elemental and $^{187}Os/^{188}Os$ ratios and that the similar decreasing profile of Re and Os indicates similar binding properties of Re and Os in asphaltene.

1.3 The application of Re-Os geochronometer to petroleum systems

1.3.1 The Re-Os geochronology of petroleum systems

For an oil or gas accumulation to be formed, the essential elements (source, reservoir and seal etc.) and processes (trap formation and oil generation-expulsion-migration) should match both spatially and temporally (Magoon and Beaumont, 1999). Establishing an accurate and precise age of the hydrocarbon generation, a critical moment of petroleum system, is important for understanding the evolution of a petroleum system and for exploration. The presence of measurable Re and Os in many crude oils provides the primary foundation for the constraints of the petroleum generation timings via the Re-Os geochronometer. Indeed, it has been demonstrated to be a viable radiometric tool for directly dating of oil generation and the Os isotope composition is also a robust inorganic oil-source correlation tool.

The inaugural successful Re-Os dating of petroleum samples yielding reasonable age determinations is achieved by Selby et al. (2005). It was taken on the open-space filling and coating bitumen of a Zn-Pb deposit. The multiple bitumen samples yields a Re-Os age of 374 Ma with reasonable spread of data points on an isochron. This age is indistinguishable with the sphalerite Rb-Sr date and paleomagnetic date of both the Zn-Pb mineralization, revealing the relationship between Pb–Zn mineralization and bitumen formation, and the potential of the Re-Os isotope system to pinpoint the important timings of crude oil evolution. Shortly after, Re-Os data of bitumen samples defined a date of 112 Ma for the emplacement of the Alberta oil sand deposit (Selby and Creaser, 2005). This Re-Os date supports the basin model of Riediger et al. (2001) indicating the main source to be the Devonian-Mississippian Exshaw Formation in the Peace River Embayment area with oil generation happened between about 110 and 80 Ma, which is earlier in contrast to some other models though, e.g. Berbesi et al. (2012), indicating the Lower Jurassic Gordondale member to be the main sources with oil generation during Laramide orogeny (~ 60 Ma). The 68 ± 13 Ma Re-Os date defined by the United Kingdom Atlantic margin petroleum system oils is consistent with both the relative (basin models) and absolute ($^{40}Ar/^{39}Ar$ K-feldspar cement geochronology) timing of oil generation (Finlay et al., 2011).

The Re-Os analysis on the crude oil from Phosphoria petroleum system, Bighorn basin, USA defines a Miocene age of 9.24 ± 0.39 Ma for the oils experienced thermochemical sulphate reduction (TSR) and a Late Triassic age of 211 ± 21 Ma for the oils which haven't been effected by TSR (Lillis and Selby, 2013). The Miocene age corresponds to the end of a period of uplift, inferred to indicate the end of TSR. The Late Triassic age corresponds to the early stage of oil generation, i.e. the bitumen generation before main stage of crude oil generation. The Re-Os analysis on the crude oil from Green River petroleum system, Uinta basin, USA is the first lacustrine petroleum system Re-Os study and determined an oil generation age of 19 ± 14 Ma (Cumming et al., 2014).

Secondary alteration processes have different effects on the Re-Os isotopic systematics of crude oil samples and also the geochronology. There are evidences of various degree of biodegradation for oils samples in many of the aforementioned studies (Selby et al., 2005; Selby and Creaser, 2005; Selby et al., 2007; Finlay et al., 2011; Lillis and Selby, 2013), however, the Re-Os geochronology has not been heavily hampered – biodegradation preferentially removes the light fractions of crude oil leaving the main carrier of Re and Os, the asphaltene fraction, largely untouched. Involvement of Re-Os data from oils experienced TSR has led to high uncertainty of the Re-Os oil generation age and the TSR event itself can also be recorded by the Re-Os clock (Lillis and Selby, 2013). The Re-Os work on low-maturity bitumen and pyrobitumen from the western margin of Xuefeng uplift, southern China, yields both the initial crude oil generation age (430 Ma) and the cessation of thermal cracking (70 Ma), i.e. the end of gas and pyrobitumen generation, respectively (Ge et al., 2016). For both TSR and thermal cracking the Re-Os systematics of hydrocarbons have been shown to reset.

All of the studies introduced above use multiple oil or bitumen samples to obtain Re-Os age. The work of Georgiev et al. (2016) on Triassic–Jurassic Sicily oils firstly obtained Re-Os dates with the maltenes and asphaltenes from single sample of crude oil. The asphaltene and maltene fractions were separated with a series of *n*-alkanes from a single crude oil sample to seek for the necessary spread in Re-Os isotopic compositions to form an isochron. A Re-Os date (~ 200 Ma) was defined by some of the maltenes of a Streppenosa oil and interpreted by the authors to be the timing of oil generation.

1.3.2 Oil-source correlation with Os isotope composition

Re-Os analyses on crude oil have also provided an additional inorganic tool to the collection of oil-source correlation techniques. Hydrous pyrolysis experiments on organic-rich sedimentary rocks (Rooney et al., 2012; Cumming et al., 2014) have shown that during thermal maturation, the generated oil inherits the Os isotope composition of the source rock. This relationship is employed in many of the aforementioned studies for oil-source correlation by comparing the $^{187}Os/^{188}Os$ of oil and source rock at the time of oil generation, i.e. the oil Os_i (initial) and source rock Os_g (generation).

Selby et al. (2005) attempted to identify the source of the bitumen in the Zn-Pb deposit from the several regional potential source rocks, however, firm conclusion on the main source was unachieved because of the very limited sampling of source rocks. Selby and Creaser (2005) precluded a possible Cretaceous source to be the main source of Alberta oil sand bitumen and recommended that the source rock should be more than 100 million years older than the oil generation based on the $^{187}Os/^{188}Os$ values of the bitumen and Palaeozoic-Mesozoic seawater, i.e. the initial $^{187}Os/^{188}Os$ of the Palaeozoic-Mesozoic source rocks. The Late Jurassic Kimmeridge clay Formation and not that of the Middle Jurassic shales were identified as the source of UKAM oil by comparing their Os isotope composition with that of the oils (Finlay et al., 2011). Effective oil-source correlation in lacustrine systems using Os isotopes is exemplified by Cumming et al. (2014). The $^{187}Os/^{188}Os$ values of source rocks and oils coupled with Pt/Pd values permitted the fingerprinting of United Kingdom Atlantic margin oil and West Canadian oil sands to their sources (Finlay et al., 2012).

1.4 Research rationale

The research presented in this thesis aims to improve the understandings of Re-Os geochronometer in the dating of crude oil generation and also the elemental (abundance) and isotopic (ratios) systematics of Re and Os in crude oil. This thesis comprises the work of 1) developing matrix matched reference materials for petroleum Re-Os analysis, 2) validating the ability of Re-Os geochronometer to constrain the timing of crude oil generation with the instance of Duvernay petroleum system of Western Canada sedimentary basin, and 3) exploring the Re-Os elemental

and isotopic systematics within crude oil by the fractionation of crude oil and asphaltenes.

1.4.1 Petroleum Re-Os analysis reference material

There has been more than a decade of continuous Re-Os research undertaken on petroleum samples since the inaugural successful application of Re-Os analyses on petroleum systems (bitumen of the Polaris MVT deposit, Canada, Selby et al. (2005)) to explore the application and understand their geochemical behaviour(s). However, there is still not a matrix matched reference material for the validation of petroleum Re-Os analysis prior to this study. Such a reference material is in need as it is of critical importance for the inter- and intra-laboratory comparison and for the validation of analysis methodology. Higher precision and faster analytical protocols are always the pursuit of researchers. Improvement of the current Re-Os analysis chemical procedures, especially regarding the sample digestion, is necessary if extending this Re-Os tool to crude oil with low Re and Os contents is also the expectation of researchers.

1.4.2 Re-Os dating of the crude oil generation of Duvernay petroleum system

The Re-Os geochronometer has been applied to many petroleum systems worldwide prior to this study on Duvernay petroleum system of Western Canada sedimentary basin. The influences of some secondary alteration processes after oil generation, e.g. thermal cracking, thermochemical sulphate reduction, etc., have also been discussed to various extent (Selby et al., 2005; Selby and Creaser, 2005; Selby et al., 2007; Finlay et al., 2011; Lillis and Selby, 2013; Ge et al., 2016). However, the understanding of using Re-Os as petroleum generation geochronometer and oil-source tracer are often compromised by the lack of understanding, or their intrinsic complex geological characteristics, of the studied petroleum systems. The source units of some of the preciously studied petroleum systems are often unclear or the mix of two or more, and/or very thick (e.g. Green River Formation, ~ 3000 m) organic-rich intervals (Selby and Creaser, 2005; Lillis and Selby, 2013; Cumming et al., 2014). Debates exist on maturation timings or there are multiple stages of oil generation (e.g. Finlay et al., 2011). Both multiple sources and multiple generation stages of oil are likely to lead to a large range of initial $^{187}Os/^{188}Os$ compositions of the generated oils. Some oil samples are also altered, e.g. by biodegradation, thermal cracking, and thermochemical sulphate reduction, for which the disturbance on oil

Re-Os systematics and the implications for geochronology have been discussed, but still need verification with more examples. Possible impact of water-bearing Re and Os on the crude oil Re-Os systematics is proposed, but not verified with real examples as yet. It is also not sure if Re-Os still gives the oil generation age when the maturation happens long after the source rock deposition, where the initial $^{187}Os/^{188}Os$ compositions of the generated oil is highly likely to possess a large range and make it difficult to establish an isochron. It is suspected that the Re-Os geochronology for petroleum systems can possibly be confined to the scenario where oil generates shortly after source rock deposition (Mahdaoui et al., 2013).

Given the uncertainties of the previous instances, Chapter Three presents a Re-Os study on a well-understood petroleum system, the Duvernay petroleum system of Western Canada sedimentary basin, which provides ideal conditions for the examination of the Re-Os isotopic systematics as a geochronometer of oil generation and an oil-source correlation tool. The oils of the Leduc and Nisku reservoir of Duvernay petroleum system are originated from a single source unit, i.e. the Late Devonian Duvernay formation (~ 378 Ma). Consensus is reached on the main phase of oil generation to be during the Late Cretaceous to Eocene Laramide Orogeny (Deroo et al., 1977; Creaney and Allan, 1990; Bustin, 1991; Berbesi et al., 2012). It had been a long time (~ 300 million years) since the source rock deposition to the main oil generation stage. Also, there has seldom been any secondary alteration for the areas of the oil sampling, i.e. biodegradation, thermal cracking or thermochemical sulphate reduction.

1.4.3 Re-Os elemental and isotopic systematics within crude oil

Although the Re-Os systematics within asphaltene has been studied through the progressive precipitation of two asphaltenes (Mahdaoui et al., 2013), the worldwide crude oils and asphaltenes are substantially complex and diverse. It is possible that different Re-Os elemental and isotopic systematics patterns of the progressively precipitated asphaltene could exist and be disclosed through the study of more samples. Improving data precision can also probably reveal more hidden details. Further interpretation of Re and Os residence and the implications can also be proposed based on the understanding of asphaltene aggregation and precipitation.

It will also be worthwhile to examine the difference in asphaltene and maltene yields from the separation of a crude oil by different *n*-alkanes, and the resultant Re and Os abundance and isotopic composition. On this basis, if the determination of geological timings of petroleum systems via the Re-Os analyses on the fractions of a single oil can be extensively applied or not will also be examined.

1.5 Thesis outline

This thesis consists of this introductory chapter, three main chapters which will be presented in the format of individual papers (which have been published, or currently in review), and a conclusion chapter.

1.5.1 Chapter Two: A matrix matched reference material for validating petroleum Re-Os analysis

This work is done on a commercially available crude oil sample, the National Institute of Standards and Technology (NIST) Research Material 8505 (RM8505), and a homogeneous asphaltene sample (~90 g) isolated from the RM8505 oil. The data were obtained through repeated Re-Os analysis via the Carius Tube – Isotope Dilution – Negative Thermal Ionisation Mass Spectrometry (ID-NTIMS). The Re and Os abundances and isotopic ratio datasets were evaluated to establish if they follow a normal distribution, which is expected for reference materials if sufficient data are obtained (Meisel and Moser, 2004; Ludwig, 2012) – and the dispersion of data through standard deviation.

The sample preparation, Re-Os analyses laboratory work, data processing and evaluation of this study were carried out by the author. This chapter was written by myself with comments and suggestions from Professor David Selby. A version of this chapter co-authored with David Selby has been submitted to *Geostandards and Geoanalytical Research* and is currently accepted pending revision.

1.5.2 Chapter Three: Re-Os geochronology and oil-source correlation of Duvernay petroleum system, Western Canada sedimentary basin: Implications for the application of the Re-Os geochronometer to petroleum systems

Organic geochemical analyses were performed on the Leduc-Nisku oils and the Duvernay formation shale extracts. Re-Os analyses were taken on the Duvernay-sourced oils and Duvernay shales. Oil and shale Re-Os isotopic data were regressed

by Isoplot (Ludwig, 2012) for isochrons to obtain Re-Os ages. Oil initial $^{187}Os/^{188}Os$ values (Os_i, at 66 Ma, the Re-Os crude oil generation age), Duvernay formation and four other organic-rich intervals of Western Canada sedimentary basin $^{187}Os/^{188}Os$ values at oil generation (Os_g, 66 Ma) were calculated and compared to examine the ability of Os isotope composition distinguishing the source rock of oil. The influence of basinal fluids on oil Re-Os systematics has also been discussed based on the extensive basinal fluids studies.

The oil and shale samples were collected from the Geological Survey of Canada, Calgary. The Re-Os analyses laboratory work and data processing and evaluation of this study were carried out by the author. Geochemical analyses and evaluation were carried out by Mark Obermajer and Andy Mort of Geological Survey of Canada, Calgary. This chapter was written by myself with comments and suggestions from Professor David Selby, Dr Paul Lillis and Mark Obermajer. A version of this chapter co-authored by David Selby, Mark Obermajer and Andy Mort has been accepted for publication by *AAPG Bulletin*.

1.5.3 Chapter Four: Further evaluation of the Re-Os systematics of crude oil: Implications for Re-Os geochronology of petroleum systems

Six oils from different localities were fractionated in two ways to study the Re-Os systematics within crude oil. One way is that they were separated by *n*-C_7 into asphaltenes and maltenes, and the asphaltenes were further fractionated into eight or nine fractions with the changing ratio mix of *n*-C_7 and dichloromethane. The other way is that the six oils were separated by a series of *n*-alkanes from *n*-C_5 to *n*-C_{10}. The Re and Os residence domains in crude oil are proposed. The role of asphaltene aggregation and precipitation in the observed Re-Os systematics within crude oil and the geochronology implications are discussed.

The samples are from NIST, US Geological Survey and petroleum company, Total. The sample preparation, Re-Os laboratory work, data processing and evaluation of this study were carried out by myself. The chapter was written by myself with comments and suggestions from Professor David Selby. A version of this chapter will be submitted to *Geochimica et Cosmochimica Acta* co-authored by David Selby, Paul G. Lillis, Honggang Zhou and Magali Pujol.

1.5.4 Chapter Five: Conclusions and future work

The final chapter presents a summary of the work outlined in all the chapters. Further, this chapter presents suggestions for possible future work based on the findings of this thesis and the inspiration from previous research.

1.6 References

Barre, A., A. Prinzhofer, and C. Allegre, 1995, Osmium isotopes in the organic matter of crude oil and asphaltenes: Terra Abs, v. 7, p. 199.

Berbesi, L. A., R. di Primio, Z. Anka, B. Horsfield, and D. K. Higley, 2012, Source rock contributions to the Lower Cretaceous heavy oil accumulations in Alberta: A basin modeling study: AAPG bulletin, v. 96, no. 7, p. 1211-1234.

Bustin, R., 1991, Organic maturity in the western Canada sedimentary basin: International Journal of Coal Geology, v. 19, no. 1, p. 319-358.

Creaney, S., and J. Allan, 1990, Hydrocarbon generation and migration in the Western Canada Sedimentary Basin: Geological Society, London, Special Publications, v. 50, no. 1, p. 189-202.

Cumming, V. M., D. Selby, P. G. Lillis, and M. D. Lewan, 2014, Re–Os geochronology and Os isotope fingerprinting of petroleum sourced from a Type I lacustrine kerogen: Insights from the natural Green River petroleum system in the Uinta Basin and hydrous pyrolysis experiments: Geochimica et Cosmochimica Acta, v. 138, p. 32-56.

Deroo, G., T. G. Powell, B. Tissot, and R. G. McCrossan, 1977, The origin and migration of petroleum in the Western Canadian Sedimentary Basin, Alberta: a geochemical and thermal maturation study.

Finlay, A. J., D. Selby, and M. J. Osborne, 2011, Re-Os geochronology and fingerprinting of United Kingdom Atlantic margin oil: Temporal implications for regional petroleum systems: Geology, v. 39, no. 5, p. 475-478.

Finlay, A. J., D. Selby, and M. J. Osborne, 2012, Petroleum source rock identification of United Kingdom Atlantic Margin oil fields and the Western Canadian Oil Sands using Platinum, Palladium, Osmium and Rhenium: Implications for global petroleum systems: Earth and Planetary Science Letters, v. 313-314, p. 95-104.

Ge, X., C. Shen, D. Selby, D. Deng, and L. Mei, 2016, Apatite fission-track and Re-Os geochronology of the Xuefeng uplift, China: Temporal implications for dry gas associated hydrocarbon systems: Geology, p. G37666. 37661.

Georgiev, S. V., H. J. Stein, J. L. Hannah, R. Galimberti, M. Nali, G. Yang, and A. Zimmerman, 2016, Re-Os dating of maltenes and asphaltenes within single samples of crude oil: Geochimica Et Cosmochimica Acta, v. 179, p. 53-75.

Lillis, P. G., and D. Selby, 2013, Evaluation of the rhenium–osmium geochronometer in the Phosphoria petroleum system, Bighorn Basin of Wyoming and Montana, USA: Geochimica et Cosmochimica Acta, v. 118, p. 312-330.

Ludwig, K., 2012, User's manual for Isoplot version 3.75-4.15: a geochronological toolkit for Microsoft: Excel Berkley Geochronological Center Special Publication, no. 5.

Magoon, L. B., and E. A. Beaumont, 1999, Treatise of Petroleum Geology/Handbook of Petroleum Geology: Exploring for Oil and Gas Traps. Chapter 3: Petroleum Systems.

Mahdaoui, F., R. Michels, L. Reisberg, M. Pujol, and Y. Poirier, 2015, Behavior of Re and Os during contact between an aqueous solution and oil: Consequences for the application of the Re–Os geochronometer to petroleum: Geochimica et Cosmochimica Acta, v. 158, p. 1-21.

Mahdaoui, F., L. Reisberg, R. Michels, Y. Hautevelle, Y. Poirier, and J.-P. Girard, 2013, Effect of the progressive precipitation of petroleum asphaltenes on the Re–Os radioisotope system: Chemical Geology, v. 358, p. 90-100.

Meisel, T., and J. Moser, 2004, Reference materials for geochemical PGE analysis: new analytical data for Ru, Rh, Pd, Os, Ir, Pt and Re by isotope dilution ICP-MS in 11 geological reference materials: Chemical Geology, v. 208, no. 1-4, p. 319-338.

Peucker-Ehrenbrink, B., and B.-M. Jahn, 2001, Rhenium-osmium isotope systematics and platinum group element concentrations: Loess and the upper continental crust: Geochemistry, Geophysics, Geosystems, v. 2, no. 10, p. n/a-n/a.

Poplavko, Y., V. Ivanov, T. Karasik, A. Miller, V. Orekhov, S. Taliyev, Y. Tarkhov, and V. Fadeyeva, 1974, On the concentration of rhenium in petroleum, petroleum bitumens and oil shales: Geochemistry International, v. 11, no. 5, p. 969-972.

Riediger, C. L., S. Ness, M. Fowler, and N. T. Akpulat, 2001, Timing of oil generation and migration, northeastern British Columbia and southern Alberta—Significance for understanding the development of the eastern Alberta tar sands deposits (abs.): AAPG Annual Convention Official Program, v. 10, p: A168.

Rooney, A. D., D. Selby, M. D. Lewan, P. G. Lillis, and J.-P. Houzay, 2012, Evaluating Re–Os systematics in organic-rich sedimentary rocks in response to petroleum generation using hydrous pyrolysis experiments: Geochimica et Cosmochimica Acta, v. 77, p. 275-291.

Selby, D., R. Creaser, K. Dewing, and M. Fowler, 2005, Evaluation of bitumen as a Re–Os geochronometer for hydrocarbon maturation and migration: A test case from the Polaris MVT deposit, Canada: Earth and Planetary Science Letters, v. 235, no. 1-2, p. 1-15.

Selby, D., and R. A. Creaser, 2005, Direct radiometric dating of hydrocarbon deposits using rhenium-osmium isotopes: Science, v. 308, no. 5726, p. 1293-1295.

Selby, D., R. A. Creaser, and M. G. Fowler, 2007, Re–Os elemental and isotopic systematics in crude oils: Geochimica et Cosmochimica Acta, v. 71, no. 2, p. 378-386.

Chapter 2 A matrix matched reference material for validating petroleum Re-Os analysis

A version of this chapter co-authored with David Selby has been submitted to Geostandards and Geoanalytical Research and is currently accepted pending revision.

2.1 Introduction

Since its inaugural application to the Polaris Mississippi Valley Type Pb-Zn deposit (Selby et al., 2005) and the Giant Oil Sands of Alberta, Canada (Selby and Creaser, 2005), the rhenium-osmium (Re-Os) radioisotope system has been applied to many petroleum systems worldwide (Selby et al., 2007; Finlay et al., 2010; Finlay et al., 2011; Cumming et al., 2012; Finlay et al., 2012; Rooney et al., 2012; Lillis and Selby, 2013; Cumming et al., 2014; Ge et al., 2016; Georgiev et al., 2016). These studies have demonstrated that the Re-Os isotope systematics of petroleum (crude oil, bitumen) have the ability to directly date the processes related to petroleum generation and evolution, and also provide insights into the source of the petroleum. Laboratory studies have also been carried out on the Re-Os isotope systematics of crude oil fractions (Selby et al., 2007; Mahdaoui et al., 2013; Mahdaoui et al., 2015; Georgiev et al., 2016). These studies have discussed the possible influences of geological processes on the Re-Os systematics of petroleum and its application to petroleum systems, e.g. the timing of oil generation, the precipitation of asphaltene, and the effect of contact with basinal fluids.

Previous Re-Os petroleum studies have utilized a wide range of sample types. They include not only conventional crude oil, but also the altered forms, e.g. bitumen of different origins. The Re-Os analysis procedures were initially setup for rock samples, e.g. sulphides and organic-rich mudrocks (Cohen et al., 1999; Reisberg and Meisel, 2002; Marques, 2013; Zimmerman et al., 2014) and then adapted for the specific characteristics of petroleum samples (Selby et al., 2005; Mahdaoui et al., 2013; Sen and Peucker-Ehrenbrink, 2014; Georgiev et al., 2016). In general, current petroleum Re-Os analysis protocols adopt similar chemical purification procedures among different laboratories with the main differences being the digestion (i.e.

choice of vessels and acids) and mass spectrometry (N-TIMS and ICP-MS) methods. The two noteworthy characteristics of petroleum samples that the protocols have to deal with are the low concentrations of Re (≤1 ng g^{-1}) and Os (~10 pg g^{-1}) of many oils (see Selby et al., 2007) and the high pressure during the digestion.

Petroleum samples are usually digested in closed-system (Carius tubes and Anton Paar High Pressure Asher (HPA-S) vessels) with strong oxidizing acids. The digestion process should ensure the complete destruction of the organic matrix and the achievement of the highest oxidation state (OsO_4) of all Os, to permit the equilibrium of the sample and spike Os. The most commonly used digestion reagent is concentrated nitric and hydrochloric acid in the form of inverse *aqua regia*. The addition of hydrogen peroxide is demonstrated to increase the efficiency of sample digestion and the mass spectrometer Os signal (Li et al., 2011). However, it also increases the risk of Carius tube rupture during digestion. The low Re and Os concentrations of many crude oils require a large amount of sample and low procedural blanks to obtain accurate and precise data. However, the high pressure generated by the formation of carbon dioxide during the digestion process limits the amount of sample that can be handled with the current digestion technique. The HPA-S method has been used to digest up to 0.45 g of crude oil effectively (Georgiev et al., 2016) and it can also digest samples in short times (overnight or ~2-3 hrs). Further, a recent study presents the design of re-useable Carius tubes (Qi et al., 2013). Both Carius tubes and HPA-S methods can yield low blanks, with the blanks primarily controlled by the reagents used. Importantly, reuse of digestion vessels increase the probability of variable blanks, which can hamper the application of most appropriate blank correction. When tubes are not reused, the Carius tube - inverse aqua regia methodology typically yields low Re and Os blanks across different labs, e.g. generally lower than 10 pg for Re and 50 - 200 fg for Os (e.g. Cumming et al., 2014 and this study, Table 2.1), less than 3 pg Re and 2 pg Os (Steven et al., 2015), and 3.7 ± 4.7 pg Re and 340 ± 226 fg Os (Georgiev et al., 2016).

After sample digestion and spike-sample equilibration, the Os fractions are typically extracted with an organic solvent and purified by micro-distillation (Cohen and Waters, 1996; Birck et al., 1997), with the Re fractions being purified by anion exchange chromatography (Morgan et al., 1991; Selby and Creaser, 2001). The Re and Os isotope compositions of the purified Re and Os fractions from samples are

determined by Negative Thermal Ionization Mass Spectrometry (N-TIMS) and/or (Multi-Collector) Inductively Coupled Plasma Mass Spectrometry (MC-ICP-MS/ICP-MS) (Creaser et al. 1991; Völkening et al., 1991; Reisberg and Meisel, 2002; Meisel et al., 2003; Walczyk, 2004; Nowell et al., 2008). The MC-ICP-MS/ICP-MS permits faster isotope mass determination and simpler elemental purification chemistry. However, the N-TIMS methodology is a more appropriate reference technique for Os isotopic measurement because of its advantage on precision, which is especially important for oils that often possess low abundances of Os.

The pursuit of simple, rapid, accurate and precise Re-Os measurement of petroleum and the demand for both inter- and intra- laboratory calibration are driven by the increasing interest and application of petroleum Re-Os analysis. Considering the unique nature of petroleum samples, e.g. easy to digest, significant CO_2 generated during digestion and typically low Re and Os abundance, a matrix-matched reference material is needed for petroleum Re-Os analysis method development and validation. Some progress has already been made (Sen and Peucker-Ehrenbrink, 2014). In this study, we present Re-Os data for the National Institute of Standards and Technology (NIST) 8505 crude oil and a homogeneous asphaltene sample (~90 g) isolated from the RM8505 oil, to demonstrate their use as appropriate petroleum matrix-matched reference materials for Re-Os analysis. These two samples are repeatedly analysed for their Re and Os abundance and isotope composition via the Carius Tube - Isotope Dilution - NTIMS methodology. In addition, based on the Re-Os analysis of individually separated asphaltene and maltene fractions in this study, we further confirm that asphaltene is the main carrier of Re and Os within crude oils, and that there is negligible Re and Os in the volatile fraction (at 80 °C) of this oil.

2.2 Samples preparation

The U.S. National Institute of Standards and Technology (NIST) vanadium Research Material 8505 (RM8505) is a Venezuelan crude oil with currently (year of 2017) over 100 bottles of 250 ml in stock. The oil was produced in 1983 and received from Scallop Petroleum Company, a subsidiary of Royal Dutch Shell. No geological details concerning the origin of this oil are available. The predominant source rocks (95% source of Venezuelan's crude oil) of Venezuela are the Upper Cretaceous (Cenomanian-Turonian-Coniacian, 100 – 86 Ma) La Luna Formation and its age

equivalents, with only minor contributions from Palaeocene, Eocene and Miocene source rocks (James, 1990, 2000; Summa et al., 2003). Oil generation from the La Luna Formation is considered to have occurred from the Early Eocene onwards (≤ 56 Ma), with the majority of the oil having been generated since the Miocene (James, 2000; Summa et al., 2003).

In this study, four sample types are repeatedly analysed for their Re-Os abundance and isotope compositions, i.e. the RM8505 crude whole oil, the individually separated asphaltene and maltene fractions from 8505, and a homogenized asphaltene sample. Five bottles of RM8505 crude oil were used and subtitled A, B, C, D and E.

The asphaltene is defined as the insoluble fraction of oil in *n*-alkanes and the maltene is the soluble fraction. The separation in this study is done by adding 40 ml of *n*-heptane to ~ 1 g of whole oil (Speight, 2004; Selby et al., 2007). The *n*-heptane and crude oil were thoroughly mixed and left on a rocker overnight at room temperature. The next day the mixture was centrifuged at 3500 rpm for 15 minutes. The precipitated asphaltene was separated by decanting the maltene-bearing *n*-heptane. The asphaltene fraction was transferred to a glass vial using chloroform and dried at 60 °C. The maltene fractions were recovered by evaporating the *n*-heptane at 80 °C in a glass vial.

To produce the homogenized asphaltene powder, the asphaltene fraction of ~ 1000 g of RM8505 oil from all five bottles was isolated and homogenized. The isolation procedure of the asphaltene is generally the same as the *n*-heptane method described above. The difference is that the *n*-heptane asphaltene-maltene mixture was filtered through 0.45 μm Whatman glass microfibre filter instead of being centrifuged. The dried asphaltene was ground to fine powder (< 212 μm) using an agate pestle and mortar, homogenized, and then evenly distributed into 12 glass bottles with 7.5g of asphaltene placed into each bottle. This amount asphaltene will permit 50 analyses if using 150 mg aliquots per Re-Os analysis.

For bottle A, six Re-Os analyses on each of the whole oil, individually separated asphaltene and maltene fractions were conducted. For bottles B, C, D, and E, three Re-Os analyses were carried out for each of the three sample types from every bottle. The asphaltene and maltene samples represent paired petroleum fractions from the

separation of ~ 1 g crude oil by *n*-heptane. They are not separated from the whole oil Re-Os analysis samples from the same bottle. In total we present the data of eighteen Re-Os analyses of each sample type for the five bottles. In addition, Re-Os analyses were performed on two samples taken from each of the twelve bottles of homogenized asphaltene powder.

2.3 Analytical procedure

The Re and Os abundances and Re-Os isotopic systematics were determined by the Isotope Dilution – Negative Thermal Ionisation Mass Spectrometry (ID-NTIMS) method at Durham University in the Laboratory for Source Rock and Sulphide Geochronology and Geochemistry (a member of the Durham Geochemistry Centre). The analytical protocols are based on those developed in previous studies (Creaser et al., 1991; Shirey and Walker, 1995; Birck et al., 1997; Selby and Creaser, 2001; Selby et al., 2007).

The mass of samples used for each Re-Os analysis were ~150 mg of whole oil and maltene, ~120 mg of the individually separated asphaltene and ~150 mg for the homogenized asphaltene powder. The solid asphaltenes were weighed using weighing paper. The viscous crude oil and maltene were weighed in small glass vials (~3 ml and 4.5 g) and then transferred into a pre-cleaned (with step 1 by 5% H_2O_2, step 2 by 8 mol l^{-1} HNO_3, step 3 by MilliQ water) Carius tubes with the aid of ~ 1 ml chloroform, which was evaporated at 60˚C.

After adding a known amount of ^{185}Re + ^{190}Os mixed tracer solution, the samples were dissolved and equilibrated in Carius tubes using inverse *aqua regia* (3 ml 12 mol l^{-1} HCl + 6 ml 16 mol l^{-1} HNO_3) at 220 °C for 24 hrs. A solvent extraction methodology was used to isolate the Os from the digested solution using 3 x 3 ml aliquots of chloroform. The Os was then back-extracted from chloroform with 3 ml 9N HBr solution at room temperature on a rocker overnight. Then separated HBr solution was evaporated to dryness, with the remaining Os fraction further purified by micro-distillation using the CrO_3-H_2SO_4-HBr technique. The purified Os fraction was loaded onto Pt wire filament and covered with ~0.3 µl of NaOH-$Ba(OH)_2$ activator solution. Following the extraction of Os, the acid medium was evaporated to dryness with the Re fraction purified by anion exchange chromatography. The eluted solution containing Re was evaporated to dryness and the Re was loaded onto

a Ni wire filament with ~0.5 µl $Ba(NO_3)_2$ activator solution. The Re and Os isotopic measurements were conducted on a Thermo Scientific TRITON mass spectrometer via ion-counting using a secondary electron multiplier in peak-hopping mode for all Os and maltene Re, and static Faraday collection for oil and asphaltene Re. The measured oxide ratios for Os and Re were corrected for isobaric oxygen interferences to obtain metal ratios, which were then corrected for mass fractionation using a $^{192}Os/^{188}Os$ value of 3.08761 (Nier, 1937) and a $^{185}Re/^{187}Re$ value of 0.59738 (Gramlich *et al*., 1973), spike contributions and blank. The total procedural blanks during the study are 1.90 ± 0.97 picograms for Re and 73 ± 19 femtograms for Os, with an average $^{187}Os/^{188}Os$ of 0.24 ± 0.03 (2 SD, n = 7; Table 2.1). An in-house Os control solution, DROsS, yields an average $^{187}Os/^{188}Os$ of 0.1611 ± 0.0004 (1 σ, *n* = 126) being identical to previously reported values (Nowell et al., 2008; Cumming et al., 2014 and references therein). The in-house Re standard solution yields an average $^{185}Re/^{187}Re$ of 0.5989 ± 0.0019 (1 σ, *n* = 116) which is used for the correction of mass fractionation in comparison with the accepted $^{185}Re/^{187}Re$ value of 0.5974 (Gramlich et al., 1973). The final 2 standard error level absolute uncertainties presented for the Re and Os data (Tables 2.2 - 2.5) were calculated by full error propagation of uncertainties in the Re and Os mass spectrometry measurements, blank values, weighing, isotopic compositions, spike calibrations, and the reproducibility of the standard Re and Os values.

2.4 Results and discussion

The Re and Os abundances and $^{187}Re/^{188}Os$ and $^{187}Os/^{188}Os$ compositions are presented in Tables 2.2 - 2.5 and Figures 2.1 - 2.5. The standard deviation (SD) and the relative standard deviation (RSD) are included as indication of data variability. Linearized probability plots are constructed with *Isoplot* (v 4.15). A normal distribution of the results is expected if sufficient data are obtained (Meisel and Moser, 2004), in which case data points should be dispersed closely to a linear trend with a slope of 1 on a linearized probability plot (Ludwig, 2012). In addition, histograms and probability density curves presented here also indicate the range and distribution pattern of the Re-Os data, although their shapes depend partially on the choice of bins and axis scale.

2.4.1 RM8505 whole oil Re and Os and comparison with previous studies

The RM8505 whole oil Re and Os abundances and isotopic ratios are presented in Table 2.2 and Figure 2.1. The results of two whole oil analyses of RM8505 by Georgiev et al. (2016) are also presented on the figures where appropriate for comparison.

The eighteen RM8505 whole oil samples in this study range from 1.69 to 2.15 ng g^{-1} Re and 20.96 to 27.02 pg g^{-1} total Os, with the $^{187}Re/^{188}Os$ values ranging from 435.4 to 473.8 and $^{187}Os/^{188}Os$ compositions from 1.479 to 1.540. The average values are 1.95 ± 0.25 ng g^{-1} for Re, 24.4 ± 3.5 pg g^{-1} for Os, 454 ± 21 for $^{187}Re/^{188}Os$ and 1.517 ± 0.043 for $^{187}Os/^{188}Os$. These average values are very similar to the median values, thus indicating a symmetrical distribution of the data. The linearized probability plots of the Re-Os data show that the Re-Os abundance and isotopic ratio data points are distributed along linear trends with slopes of ~1 (0.95 ~ 1.02) indicating a similar to normal distribution of the data set. The histograms and the probability density curves of the isotopic ratios are clearly similar to a normal distribution, although this is less so for the Re and Os abundances. Besides the choice of the bins, the less than normal distribution of the Re and Os abundance data is also due to the better reproducibility of the isotopic ratios compared to the Re and Os abundances, which is also reflected by the lower RSD values for isotopic ratio measurements.

The RM8505 crude oil has also previously been analysed for Re-Os data by Sen and Peucker-Ehrenbrink (2014) and Georgiev et al. (2016). Although slightly different methods were applied, the results of these studies are consistent with the results of the present study. These studies both applied HPA-S digestion instead of the Carius tube method. In addition, Sen and Peucker-Ehrenbrink (2014) also sparged the OsO_4 of the digested solution directly into MC-ICPMS for measurement of the Os isotope composition. The six analyses of Sen and Peucker-Ehrenbrink (2014) yield Re abundances and Os abundances of RM8505 of 2.9 ± 1.5 ng g^{-1} and 28 ± 4 pg g^{-1}, respectively, with $^{187}Os/^{188}Os$ compositions of 1.62 ± 0.15. Although spreading over a relatively large range due to the incomplete digestion as indicated by the authors, the results are broadly consistent with the results of the present study. The Re and Os abundances of the two analyses of Georgiev et al. (2016) are slightly higher than the present study (2.28 and 2.30 vs 1.95 ± 0.25 ng g^{-1} Re; ~ 31.0 and 29.3 vs 24.4 ± 3.5 pg g^{-1} Os). However, the $^{187}Os/^{188}Os$ compositions are identical (1.455 and 1.515 vs

1.517 ± 0.043), with one of the $^{187}Re/^{188}Os$ values being nominally lower than this study (419 and 443 vs 454 ± 21). It is reasonable that variation on the abundance values is encountered given the possible heterogeneity of this heavy oil as presented in this study, and importantly, that absolute Re and Os abundances are highly dependent on the measurement methodology, e.g., weighing procedures, evaporation, etc.

2.4.2 Re and Os data of the individually separated asphaltene and maltene from RM8505

The Re and Os abundances and isotopic compositions of the individually separated asphaltene and maltene samples (eighteen of each type) from the RM8505 whole oil are presented in Tables 2.3 - 2.4, and Figures 2.2 - 2.3, respectively. The asphaltene fraction possess Re and total Os abundances from 13.47 to 14.56 ng g^{-1} and from 137.35 to 153.15 pg g^{-1}, respectively. The $^{187}Re/^{188}Os$ and $^{187}Os/^{188}Os$ values of the asphaltene range from 552.9 to 570.2 and 1.575 to 1.648, respectively. The average values are 14.04 ± 0.79 ng g^{-1} for Re, 145 ± 10 pg g^{-1} for total Os, 556 ± 18 for $^{187}Re/^{188}Os$ and 1.611 ± 0.046 for $^{187}Os/^{188}Os$. The maltene fractions range from 0.22 to 0.27 ng g^{-1} Re and from 7.78 to 8.89 pg g^{-1} total Os, with $^{187}Re/^{188}Os$ values between 143.8 and 183.4 and $^{187}Os/^{188}Os$ compositions between 1.088 and 1.280. The average values are 0.25 ± 0.04 ng g^{-1} for Re, 8.41 ± 0.70 pg g^{-1} for total Os, 161 ± 26 for $^{187}Re/^{188}Os$ and 1.199 ± 0.094 for $^{187}Os/^{188}Os$. All of the Re-Os data averages for the asphaltene and maltene fractions are similar to the corresponding median values.

The Re-Os data show linear trends on the linearized probability plots, with slopes of ~1 (0.97 ~ 1.02). The histograms and the probability density curves of maltenes Re-Os abundances and isotopic ratios are very similar to normal distributions. Those of asphaltene isotopic ratios are similar to normal distributions; however, more data are needed before this can be affirmed for asphaltene Re and Os abundances. The lower RSD values of the isotopic compositions indicate better data reproducibility than for the Re and Os abundances for asphaltenes. The RSD values of maltenes are generally higher than those of the asphaltene and whole oil samples. Overall the Re and Os abundances RSD values decrease from maltene to whole oil to asphaltene. This phenomenon indicates the increase in the data reproducibility and precision,

which corresponds to the increased levels of Re and Os abundance, and the increase of sample to blank ratios.

2.4.3 Asphaltene and maltene mass balance and isotopic characteristics

2.4.3.1 Asphaltene and maltene separation of RM8505

The asphaltene and maltene fractions of RM8505 account for an average of ~13% and ~79% of the mass of crude oil (Table 2.6; Figure 2.6a). The average of ~8% loss of sample during this separation process can largely be attributed to the loss of volatile light fractions and any water present during the drying of samples. For example, heating 0.3 g of RM8505 crude oil at 80 °C for 10 days yields a mass loss of 4.4%. Further, additional minor sample loss can be accounted for during sample transfer, and additionally evaporation to remove the $CHCl_3$ used to transfer the sample.

2.4.3.2 Re and Os abundances and isotopic composition of asphaltene and maltene

The elemental abundance sums of every pair of asphaltene and maltene separated from the same oil, weighted by their mass percentage, are from 1.86 to 2.11 ng g^{-1} Re and from 23.1 to 26.75 pg g^{-1} Os (Figure 2.6b-c; Table 2.6). These values are indistinguishable from the Re and Os contents of whole oil (Table 2.2), indicating good mass balance and no significant Re or Os loss with the evaporated fractions (Figure 2.6b-c). Further, good mass balance of radiogenic ^{187}Os is also reached for the asphaltene-maltene separation process (Tables 2.2 and 2.6). Disregarding any possible Re and Os in the volatile components, the asphaltene fraction accounts for the majority of the Re and Os of whole oil (the total of the separated asphaltene and maltene), i.e. ~ 90% Re and ~ 74% Os, with the remaining Re and Os (~ 10% Re and ~ 26% Os) being bound in the maltene fraction (Table 2.6; Figure 2.6d-e). This observation is consistent with previous studies (Selby et al., 2007; Rooney et al., 2012; Lillis and Selby, 2013; Cumming et al., 2014; Georgiev et al., 2016).

The $^{187}Re/^{188}Os$ and $^{187}Os/^{188}Os$ compositions of the asphaltenes are closer to those of the RM8505 crude oils when compared with the maltenes (Figure 2.5). It is typical that the Re-Os isotope systematics of whole oils are dominated by that of the asphaltene fractions as a direct result of the asphaltene fraction housing the majority of the Re and Os abundance of a crude oil (Figure 2.6; Selby et al., 2007). The asphaltene and crude oil of the same oil exhibit either identical or similar $^{187}Re/^{188}Os$

and $^{187}Os/^{188}Os$ compositions within uncertainty of the oils studied by Selby et al. (2007). However, in contrast, the Re-Os isotope compositions of the maltene fraction can be similar, within uncertainty, to that of the whole oil and the asphaltene, but often differ significantly from that of the crude oil and asphaltene. The available data show that the maltene fractions can possess both lower $^{187}Re/^{188}Os$ and $^{187}Os/^{188}Os$ and/or lower $^{187}Re/^{188}Os$ and similar to higher $^{187}Os/^{188}Os$ to that of the whole oil and asphaltene fraction (Figure 2.7; Selby et al., 2007; Georgiev et al., 2016; this study). The explanation for the differences in the Re-Os isotope systematics of the maltene to that of the asphaltene and whole crude oil is currently not known.

The RM8505 whole oil, asphaltene and maltene Re-Os isotope compositions define a line of best-fit that determines a Re-Os date of 62.7 ± 5.7 Ma (n = 54, initial $^{187}Os/^{188}Os$ = 1.030 ± 0.051, MSWD = 0.31). However, without detailed information with respect to the source of RM8505 and accurate estimates of its generation age from the source, it is challenging to fully interpret the date given by the Re-Os isotope compositions of the whole oil, asphaltene and maltene of RM8505. This Re-Os date is older and only overlaps with the timing of the initial oil generation of the Venezuelan source rocks, i.e. Early Eocene, when uncertainty is considered. As such, it is difficult to relate the Re-Os date to the known timing of any geological process associated with the Venezuelan petroleum systems, i.e., oil generation and the deposition of the source rock. In fact, we consider the outcome of the line of best-fit of the Re-Os isotope data to be the result of fractionation of Re and Os between the asphaltene and maltene of RM8505 crude oil. However, any interpretation of the collective use of the Re-Os systematics of crude oil, asphaltene, and maltene from a single oil with respect to Re-Os geochronology of the petroleum system should be treated with caution before a more thorough knowledge of the Re and Os geochemistry of a crude oil is obtained.

2.4.4 Homogenized asphaltene

The Re-Os data of two different batches of the homogenized asphaltene (2×12, 2 samples from each bottle) are presented in Table 2.5 and Figure 2.8. The Re-Os data for these asphaltene analyses range from 16.18 to 17.01 ng g^{-1} for Re and from 161.18 to 169.64 pg g^{-1} for total Os, with the $^{187}Re/^{188}Os$ values being between 558.0 and 591.7 and the $^{187}Os/^{188}Os$ compositions being between 1.612 and 1.665. The average values of the Re-Os data, which are very similar to their medians, are 16.52

± 0.48 ng g^{-1} for Re, 166.0 ± 4.4 pg g^{-1} for total Os, 574 ± 17 for $^{187}Re/^{188}Os$ and 1.640 ± 0.025 for $^{187}Os/^{188}Os$. The linearized probability plots, histograms and probability density curves illustrate the similar to normal distribution of the data.

2.4.5 Comparing whole oil, individually separated asphaltene and homogenized asphaltene as reference material

Crude oil is a highly complex mixture of thousands of organic compounds and also water and minerals in many cases (Berridge et al., 1968). The intrinsic heterogeneity of liquid crude oil is a major problem for the reproducibility of elemental abundances and isotopic measurements (Heilmann et al., 2009; Ventura et al., 2015; e.g. Fe). This is reflected by the difference in Re-Os characteristics of whole oil samples in this study (Table 2.2). For example, there is heterogeneity among the RM8505 bottles analysed in this study: bottle A contains less asphaltene and lower Re and Os abundances than the other bottles. Among all the analyses of the crude oil, the variations in the Re and Os abundances account for as high as ~27% and 29% of the lowest values, respectively. However, the highest variations in the $^{187}Re/^{188}Os$ and $^{187}Os/^{188}Os$ data are relatively low (9% and 4% of the lowest values, respectively). In addition to the heterogeneity of the Re-Os bearing organic compounds in RM8505, different water contents of the sampled oils could have also contributed to the variation of crude oil Re-Os elemental abundances. Considering the good data quality of the $^{187}Re/^{188}Os$ and $^{187}Os/^{188}Os$ measurements, the direct analysis of the RM8505 whole oil can serve as a good reference material for Re-Os isotopic ratios.

Another way to reduce the effect of liquid oil heterogeneity is to use fine solid bitumen/asphaltene powder, which is easier to homogenize and keep homogenized. The bitumen/asphaltene powder will still have typical petroleum sample Re and Os abundances, and keeps the character of petroleum samples with respect to generating carbon dioxide during digestion. In fact, the ~ 90 g asphaltene in the form of homogenized fine solid powder yields the lowest Re-Os abundance and isotopic data RSD values of all sample types in this study. This confirms the ability of solid asphaltene powder to reduce the influence of liquid crude oil heterogeneity. The standard deviation values are also significantly reduced from the individually separated asphaltenes – each of which is from ~ 1 g of crude oil in this study and subject to the variation of asphaltene separation process (e.g. Table 2.6). The

homogenized asphaltene can serve as a good reference material for both Re and Os abundance and isotopic ratio determination.

2.5 Summary

The Re-Os elemental abundances and isotopic ratio data of RM8505 whole oil and the homogenized asphaltene in this study, which were obtained via Carius Tube - Isotope Dilution - NTIMS methodology, entitle them as suitable matrix-matched reference material for petroleum Re-Os measurements. The Re-Os data and close to normal distribution and the RSD values are low. The establishment of these matrix-matched reference materials should facilitate inter- and intra-laboratory comparison and method validation with regards to petroleum Re-Os measurements.

2.6 References

Berridge, S., M. Thew, and A. Loriston-Clarke, 1968, The formation and stability of emulsions of water in crude petroleum and similar stocks: Journal of the Institute of Petroleum, v. 54, no. 539, p. 333-357.

Birck, J. L., M. R. Barman, and F. Capmas, 1997, Re-Os Isotopic Measurements at the Femtomole Level in Natural Samples: Geostandards and Geoanalytical Research, v. 21, no. 1, p. 19-27.

Cohen, A. S., A. L. Coe, J. M. Bartlett, and C. J. Hawkesworth, 1999, Precise Re–Os ages of organic-rich mudrocks and the Os isotope composition of Jurassic seawater: Earth and Planetary Science Letters, v. 167, no. 3-4, p. 159-173.

Cohen, A. S., and F. G. Waters, 1996, Separation of osmium from geological materials by solvent extraction for analysis by thermal ionisation mass spectrometry: Analytica Chimica Acta, v. 332, no. 2, p. 269-275.

Creaser, R. A., D. A. Papanastassiou, and G. J. Wasserburg, 1991, Negative thermal ion mass spectrometry of osmium, rhenium and iridium: Geochimica et Cosmochimica Acta, v. 55, no. 1, p. 397-401.

Cumming, V. M., D. Selby, and P. G. Lillis, 2012, Re–Os geochronology of the lacustrine Green River Formation: Insights into direct depositional dating of lacustrine successions, Re–Os systematics and paleocontinental weathering: Earth and Planetary Science Letters, v. 359-360, p. 194-205.

Cumming, V. M., D. Selby, P. G. Lillis, and M. D. Lewan, 2014, Re–Os geochronology and Os isotope fingerprinting of petroleum sourced from a Type I lacustrine kerogen: Insights from the natural Green River petroleum system in the Uinta Basin and hydrous pyrolysis experiments: Geochimica et Cosmochimica Acta, v. 138, p. 32-56.

Finlay, A. J., D. Selby, and M. J. Osborne, 2011, Re-Os geochronology and fingerprinting of United Kingdom Atlantic margin oil: Temporal implications for regional petroleum systems: Geology, v. 39, no. 5, p. 475-478.

Finlay, A. J., D. Selby, and M. J. Osborne, 2012, Petroleum source rock identification of United Kingdom Atlantic Margin oil fields and the Western Canadian Oil Sands using Platinum, Palladium, Osmium and Rhenium: Implications for global petroleum systems: Earth and Planetary Science Letters, v. 313-314, p. 95-104.

Finlay, A. J., D. Selby, M. J. Osborne, and D. Finucane, 2010, Fault-charged mantle-fluid contamination of United Kingdom North Sea oils: Insights from Re-Os isotopes: Geology, v. 38, no. 11, p. 979-982.

Ge, X., Shen, C., D. Selby, D. Deng, and L. Mei, 2016, Apatite fission-track and Re-Os geochronology of the Xuefeng uplift, China: Temporal implications for dry gas associated hydrocarbon systems: Geology, v. 44, no. 6, p. 491-494.

Georgiev, S. V., H. J. Stein, J. L. Hannah, R. Galimberti, M. Nali, G. Yang, and A. Zimmerman, 2016, Re-Os dating of maltenes and asphaltenes within single samples of crude oil: Geochimica Et Cosmochimica Acta, v. 179, p. 53-75.

Gramlich, J. W., T. J. Murphy, E. L. Garner, and W. R. Shields, 1973, Absolute isotopic abundance ratio and atomic weight of a reference sample of rhenium: J. Res. Natl. Bur. Stand. A, v. 77, p. 691-698.

Heilmann, J., S. F. Boulyga, and K. G. Heumann, 2009, Development of an isotope dilution laser ablation ICP-MS method for multi-element determination in crude and fuel oil samples: Journal of Analytical Atomic Spectrometry, v. 24, no. 4, p. 385-390.

James, K., 1990, The Venezuelan hydrocarbon habitat: Geological Society, London, Special Publications, v. 50, no. 1, p. 9-35.
James, K., 2000, The Venezuelan hydrocarbon habitat, part 1: tectonics, structure, palaeogeography and source rocks: Journal of Petroleum Geology, v. 23, no. 1, p. 5-53.
Li, C., W.J. Qu, D.H. Wang, Z.H. Chen, A.D. Du, and C.Q. Zhang, 2011, Dissolving Experimental Research of Re-Os Isotope System for Bitumen Samples: Rock and Mineral Analysis, v. 30, no. 6, p. 688-694.
Lillis, P. G., and D. Selby, 2013, Evaluation of the rhenium–osmium geochronometer in the Phosphoria petroleum system, Bighorn Basin of Wyoming and Montana, USA: Geochimica et Cosmochimica Acta, v. 118, p. 312-330.
Ludwig, K., 2012, User's manual for Isoplot version 3.75-4.15: a geochronological toolkit for Microsoft: Excel Berkley Geochronological Center Special Publication, no. 5.
Mahdaoui, F., R. Michels, L. Reisberg, M. Pujol, and Y. Poirier, 2015, Behavior of Re and Os during contact between an aqueous solution and oil: Consequences for the application of the Re–Os geochronometer to petroleum: Geochimica et Cosmochimica Acta, v. 158, p. 1-21.
Mahdaoui, F., L. Reisberg, R. Michels, Y. Hautevelle, Y. Poirier, and J.P. Girard, 2013, Effect of the progressive precipitation of petroleum asphaltenes on the Re–Os radioisotope system: Chemical Geology, v. 358, p. 90-100.
Marques, J. C., 2013, Overview on the Re-Os isotopic method and its application on ore deposits and organic-rich rocks: Geochimica Brasiliensis, v. 26, no. 1.
Meisel, T., and J. Moser, 2004, Reference materials for geochemical PGE analysis: new analytical data for Ru, Rh, Pd, Os, Ir, Pt and Re by isotope dilution ICP-MS in 11 geological reference materials: Chemical Geology, v. 208, no. 1-4, p. 319-338.
Meisel, T., L. Reisberg, J. Moser, J. Carignan, F. Melcher, and G. Brügmann, 2003, Re–Os systematics of UB-N, a serpentinized peridotite reference material: Chemical Geology, v. 201, no. 1, p. 161-179.
Morgan, J., D. Golightly, and A. Dorrzapf, 1991, Methods for the separation of rhenium, osmium and molybdenum applicable to isotope geochemistry: Talanta, v. 38, no. 3, p. 259-265.
Nier, A. O., 1937, The isotopic constitution of osmium: Physical Review, v. 52, no. 8, p. 885.
Nowell, G., A. Luguet, D. Pearson, and M. Horstwood, 2008, Precise and accurate $^{186}Os/^{188}Os$ and $^{187}Os/^{188}Os$ measurements by multi-collector plasma ionisation mass spectrometry (MC-ICP-MS) part I: Solution analyses: Chemical Geology, v. 248, no. 3, p. 363-393.
Qi, L., J.F. Gao, M.F. Zhou, and J. Hu, 2013, The Design of Re-usable Carius Tubes for the Determination of Rhenium, Osmium and Platinum-Group Elements in Geological Samples: Geostandards and Geoanalytical Research, v. 37, no. 3, p. 345-351.
Reisberg, L., and T. Meisel, 2002, The Re-Os Isotopic System: A Review of Analytical Techniques: Geostandards Newsletter, v. 26, no. 3, p. 249-267.
Rooney, A. D., D. Selby, M. D. Lewan, P. G. Lillis, and J.-P. Houzay, 2012, Evaluating Re–Os systematics in organic-rich sedimentary rocks in response to petroleum generation using hydrous pyrolysis experiments: Geochimica et Cosmochimica Acta, v. 77, p. 275-291.

Selby, D., R. Creaser, K. Dewing, and M. Fowler, 2005, Evaluation of bitumen as a Re–Os geochronometer for hydrocarbon maturation and migration: A test case from the Polaris MVT deposit, Canada: Earth and Planetary Science Letters, v. 235, no. 1-2, p. 1-15.

Selby, D., and R. A. Creaser, 2001, Re-Os geochronology and systematics in molybdenite from the Endako porphyry molybdenum deposit, British Columbia, Canada: Economic Geology, v. 96, no. 1, p. 197-204.

Selby, D., and R. A. Creaser, 2005, Direct radiometric dating of hydrocarbon deposits using rhenium-osmium isotopes: Science, v. 308, no. 5726, p. 1293-1295.

Selby, D., R. A. Creaser, and M. G. Fowler, 2007, Re–Os elemental and isotopic systematics in crude oils: Geochimica et Cosmochimica Acta, v. 71, no. 2, p. 378-386.

Sen, I. S., and B. Peucker-Ehrenbrink, 2014, Determination of Osmium Concentrations and $^{187}Os/^{188}Os$ of Crude Oils and Source Rocks by Coupling High-Pressure, High-Temperature Digestion with Sparging OsO_4 into a Multicollector Inductively Coupled Plasma Mass Spectrometer: Analytical chemistry, v. 86, no. 6, p. 2982-2988.

Shirey, S. B., and R. J. Walker, 1995, Carius tube digestion for low-blank rhenium-osmium analysis: Analytical Chemistry, v. 67, no. 13, p. 2136-2141.

Speight, J., 2004, Petroleum Asphaltenes-Part 1: Asphaltenes, resins and the structure of petroleum: Oil & gas science and technology, v. 59, no. 5, p. 467-477.

Steven, N., R. Creaser, K. Wulff, A. Kisters, B. Eglington, and J. Miller, 2015, Implications of high-precision Re-Os molybdenite dating of the Navachab orogenic gold deposit, Namibia: Geochemistry: Exploration, Environment, Analysis, v. 15, no. 2-3, p. 125-130.

Summa, L., E. Goodman, M. Richardson, I. Norton, and A. Green, 2003, Hydrocarbon systems of Northeastern Venezuela: plate through molecular scale-analysis of the genesis and evolution of the Eastern Venezuela Basin: Marine and Petroleum Geology, v. 20, no. 3, p. 323-349.

Ventura, G. T., L. Gall, C. Siebert, J. Prytulak, P. Szatmari, M. Hürlimann, and A. N. Halliday, 2015, The stable isotope composition of vanadium, nickel, and molybdenum in crude oils: Applied Geochemistry, v. 59, p. 104-117.

Völkening, J., T. Walczyk, and K.G. Heumann, 1991, Osmium isotope ratio determination by negative thermal ion mass spectrometry: International Journal of Mass Spectrometry and Ion Processes, v. 105, no. 2, p. 147–159.

Walczyk, T., 2004, TIMS versus multicollector-ICP-MS: coexistence or struggle for survival?: Analytical and bioanalytical chemistry, v. 378, no. 2, p. 229-231.

Zimmerman, A., H. J. Stein, J. W. Morgan, R. J. Markey, and Y. Watanabe, 2014, Re–Os geochronology of the El Salvador porphyry Cu–Mo deposit, Chile: Tracking analytical improvements in accuracy and precision over the past decade: Geochimica et Cosmochimica Acta, v. 131, p. 13-32.

Table 2.1 Total procedural blanks of rhenium and osmium, and $^{187}Os/^{188}Os$ composition during the study.

Blank ID	Re (pg)	±	Os (fg)	±	$^{187}Re/^{188}Os$	±	$^{187}Os/^{188}Os$	±	rho
RO539-13	1.61	0.03	64.60	0.36	121.4	2.3	0.227	0.005	0.29
RO549-4	1.63	0.03	98.78	0.67	81.3	1.5	0.302	0.009	0.21
RO560-19	1.53	0.02	38.96	0.69	216.6	7.6	1.255	0.063	0.56
RO560-21	9.76	0.16	95.3	14.1	527	183	0.64	0.36	0.61
RO631-7	5.82	0.09	89.35	0.47	317.9	5.9	0.230	0.004	0.29
RO713-7	3.70	0.06	52.47	4.44	356.4	70.9	0.495	0.141	0.69
RO728-6	2.16	0.03	46.43	5.84	225.4	62.8	0.168	0.242	0.19

Table 2.2 Rhenium and osmium abundances and isotopic ratios of RM8505 whole oil.

Sample	Re		Os		^{187}Os						
	(ng g^{-1})	±	(pg g^{-1})	±	(pg g^{-1})	±	^{187}Re/^{188}Os	±	^{187}Os/^{188}Os	±	rho
A	1.86	0.04	22.5	0.9	3.81	0.15	474	43	1.54	0.18	0.72
A	1.69	0.04	21.0	0.8	3.54	0.14	459	42	1.53	0.18	0.72
A	1.88	0.04	23.4	0.9	3.96	0.16	458	41	1.53	0.18	0.72
A	1.84	0.04	22.9	0.9	3.87	0.16	456	41	1.53	0.18	0.72
A	1.94	0.04	24.3	1.0	4.08	0.16	455	41	1.52	0.18	0.72
A	1.77	0.04	22.2	0.9	3.75	0.15	454	42	1.53	0.18	0.72
average of A:	1.83		22.7		3.83		459		1.53		
B	2.15	0.04	27.0	1.1	4.51	0.18	454	40	1.51	0.18	0.71
B	2.06	0.04	26.0	1.0	4.28	0.17	450	40	1.49	0.18	0.71
B	2.09	0.04	26.8	1.0	4.40	0.18	442	39	1.48	0.17	0.71
average of B:	2.10		26.6		4.40		449		1.49		
C	1.94	0.04	25.0	1.0	4.18	0.17	441	40	1.51	0.18	0.71
C	1.88	0.04	23.6	1.0	4.01	0.16	453	41	1.52	0.18	0.72
C	1.88	0.04	23.6	1.0	3.95	0.16	454	41	1.54	0.18	0.72
average of C:	1.90		24.1		4.05		449		1.52		

To be continued.

Continue:

Sample	Re		Os		^{187}Os						
	(ng g^{-1})	±	(pg g^{-1})	±	(pg g^{-1})	±	^{187}Re/^{188}Os	±	^{187}Os/^{188}Os	±	rho
D	1.94	0.04	24.4	1.0	4.12	0.17	454	41	1.53	0.18	0.72
D	2.03	0.04	26.3	1.0	4.25	0.17	439	39	1.49	0.18	0.71
D	1.97	0.04	25.7	1.0	4.33	0.17	435	39	1.49	0.18	0.71
average of D:	1.98		25.5		4.23		443		1.50		
E	2.05	0.04	25.4	1.0	4.29	0.17	460	41	1.53	0.18	0.72
E	2.01	0.04	24.8	1.0	4.20	0.17	461	41	1.54	0.18	0.72
E	2.06	0.04	24.8	1.0	4.10	0.17	472	42	1.50	0.18	0.72
average of E:	2.04		25.0		4.20		464		1.52		
median of all	1.94		24.6		4.11		454		1.52		
average of all	1.95		24.4		4.09		454		1.52		
SD of all	0.12		1.7		0.25		10		0.02		
RSD of all	6.16%		6.79%		6.05%		2.22%		1.34%		

To be continued.

Continue:

Sample	Re		Os		^{187}Os						
	(ng g^{-1})	±	(pg g^{-1})	±	(pg g^{-1})	±	^{187}Re/^{188}Os	±	^{187}Os/^{188}Os	±	rho
Georgiev et al. (2016)											
SVG-1	2.30	0.03	31.0	0.1			419	7	1.455	0.007	0.170
SVG-2	2.28	0.03	29.3	0.1			443	8	1.515	0.008	0.149
Sen and Peucker-Ehrenbrink (2014)											
8505_1	5.1		21.7	0.4					1.77	0.03	
8505_2	1.9		28.9	0.5					1.69	0.04	
8505_2 rpt			27.9	0.7					1.74	0.07	
8505_3	1.9		27.4	0.4					1.53	0.04	
8505_4	2.7		35.6	0.5					1.67	0.03	
8505_5			28.8	0.5					1.55	0.02	
8505_6			27.0	0.4					1.36	0.02	

Table 2.3 Rhenium and osmium abundances and isotopic ratios of the individually separated asphaltene fractions from RM8505.

Sample	Re		Os		^{187}Os						
	(ng g^{-1})	±	(pg g^{-1})	±	(pg g^{-1})	±	^{187}Re/^{188}Os	±	^{187}Os/^{188}Os	±	rho
A 1	13.68	0.07	140.3	1.8	24.92	0.25	562	12	1.63	0.05	0.71
A 2	13.54	0.07	138.6	1.8	24.74	0.25	564	12	1.64	0.05	0.71
A 3	13.47	0.06	137.4	1.8	24.53	0.25	566	12	1.64	0.05	0.71
A 4	13.61	0.07	138.8	1.8	24.79	0.25	566	12	1.64	0.05	0.71
A 5	13.71	0.07	139.7	1.8	24.93	0.25	566	12	1.64	0.05	0.71
A 6	14.56	0.06	147.5	1.9	26.45	0.27	570	12	1.65	0.05	0.71
average of A:	13.76		140.4		25.06		566		1.64		
B 1	14.50	0.06	153.2	2.0	26.81	0.27	544	12	1.60	0.05	0.70
B 2	13.73	0.06	143.4	1.7	25.06	0.25	550	12	1.60	0.05	0.71
B 3	13.96	0.06	145.2	1.9	25.64	0.26	553	12	1.62	0.05	0.71
average of B:	14.06		147.3		25.83		549		1.60		
C 1	14.19	0.06	147.8	1.9	25.86	0.26	551	12	1.60	0.05	0.71
C 2	14.28	0.06	148.4	1.9	25.65	0.26	551	12	1.58	0.05	0.71
C 3	14.00	0.06	148.2	1.9	26.07	0.26	543	12	1.61	0.05	0.71
average of C:	14.15		148.2		25.86		548		1.59		

To be continued.

Continue:

Sample	Re		Os		^{187}Os						
	(ng g^{-1})	±	(pg g^{-1})	±	(pg g^{-1})	±	^{187}Re/^{188}Os	±	^{187}Os/^{188}Os	±	rho
D 1	14.17	0.06	149.1	1.9	26.11	0.26	546	12	1.60	0.05	0.71
D 2	14.55	0.07	152.6	2.0	26.59	0.27	547	12	1.59	0.05	0.71
D 3	13.77	0.06	143.6	1.9	25.16	0.25	551	12	1.60	0.05	0.71
average of D:	14.16		148.4		25.95		548		1.60		
E 1	14.26	0.06	148.0	1.9	25.75	0.26	552	12	1.59	0.05	0.70
E 2	14.31	0.07	148.1	1.9	25.90	0.26	555	12	1.60	0.05	0.71
E 3	14.50	0.07	147.5	1.9	25.82	0.26	565	12	1.60	0.05	0.71
average of E:	14.36		147.9		25.82		557		1.60		
median of all	14.08		147.5		25.70		553		1.60		
average of all	14.04		145.4		25.60		556		1.61		
SD of all	0.37		4.8		0.68		9		0.02		
RSD of all	2.65%		3.30%		2.65%		1.56%		1.35%		

Table 2.4 Rhenium and osmium abundances and isotopic ratios of the individually separated maltene fractions from RM8505.

Sample	Re		Os		^{187}Os						
	(ng g^{-1})	±	(pg g^{-1})	±	(pg g^{-1})	±	^{187}Re/^{188}Os	±	^{187}Os/^{188}Os	±	rho
A 1	0.25	0.04	8.08	0.42	1.15	0.03	173	34	1.25	0.19	0.52
A 2	0.26	0.04	8.69	0.45	1.20	0.03	163	32	1.21	0.18	0.50
A 3	0.25	0.04	7.78	0.42	1.09	0.03	179	36	1.22	0.19	0.53
A 4	0.27	0.04	8.69	0.44	1.21	0.03	172	32	1.22	0.18	0.52
A 5	0.27	0.04	8.15	0.42	1.18	0.03	183	34	1.28	0.19	0.54
A 6	0.27	0.04	8.24	0.43	1.17	0.03	183	35	1.24	0.18	0.54
average of A:	0.26		8.27		1.17		176		1.24		
B 1	0.23	0.04	8.16	0.45	1.13	0.05	155	36	1.22	0.19	0.48
B 2	0.23	0.04	8.09	0.42	1.10	0.05	153	32	1.18	0.18	0.48
B 3	0.23	0.04	8.41	0.43	1.10	0.05	148	31	1.13	0.17	0.47
average of B:	0.23		8.22		1.11		152		1.18		
C 1	0.24	0.04	8.68	0.44	1.18	0.05	154	31	1.19	0.17	0.48
C 2	0.23	0.04	8.56	0.44	1.18	0.05	150	31	1.20	0.18	0.48
C 3	0.24	0.04	8.70	0.43	1.16	0.05	148	29	1.16	0.16	0.48
average of C:	0.24		8.65		1.17		150		1.18		

To be continued.

Continue:

Sample	Re		Os		^{187}Os						
	(ng g^{-1})	±	(pg g^{-1})	±	(pg g^{-1})	±	^{187}Re/^{188}Os	±	^{187}Os/^{188}Os	±	rho
D 1	0.22	0.04	8.16	0.43	1.03	0.02	149	32	1.09	0.16	0.47
D 2	0.25	0.04	8.71	0.45	1.21	0.05	158	33	1.22	0.18	0.49
D 3	0.24	0.04	8.50	0.43	1.15	0.05	152	31	1.18	0.17	0.48
average of D:	0.24		8.46		1.13		153		1.16		
E 1	0.24	0.04	7.99	0.42	1.11	0.05	162	33	1.22	0.18	0.50
E 2	0.24	0.04	8.89	0.44	1.22	0.05	148	30	1.20	0.17	0.48
E 3	0.27	0.04	8.81	0.44	1.19	0.03	167	31	1.18	0.17	0.51
average of E:	0.25		8.56		1.17		159		1.20		
median of all	0.24		8.46		1.16		157		1.21		
average of all	0.25		8.41		1.15		161		1.20		
SD of all	0.02		0.33		0.05		12		0.04		
RSD of all	6.75%		3.92%		4.54%		7.71%		3.69%		

Table 2.5 Rhenium and osmium abundances and isotopic ratios of the homogenized asphaltene samples.

Sample	Re		Os		$^{187}Re/^{188}Os$		$^{187}Os/^{188}Os$		
	(ng g^{-1})	±	(pg g^{-1})	±		±		±	rho
A1	16.73	0.06	166.9	1.6	578.3	7.7	1.64	0.03	0.71
A1'	16.67	0.06	167.3	1.5	576.3	7.0	1.66	0.03	0.71
A2	16.88	0.06	167.3	1.6	581.7	7.7	1.64	0.03	0.71
A2'	16.33	0.06	165.2	1.4	570.8	6.9	1.65	0.03	0.71
A3	16.33	0.06	161.2	1.5	584.8	7.8	1.65	0.03	0.71
A3'	16.18	0.06	162.6	1.4	574.1	7.0	1.64	0.03	0.71
A4	16.28	0.06	162.8	1.5	576.9	7.7	1.64	0.03	0.71
A4'	16.46	0.08	168.0	1.6	566.0	7.8	1.65	0.03	0.72
A5	16.30	0.06	165.0	1.5	570.3	7.6	1.65	0.03	0.71
A5'	16.45	0.06	166.6	1.5	570.3	6.9	1.65	0.03	0.71
A6	16.72	0.06	166.8	1.6	576.7	7.7	1.62	0.03	0.71
A6'	16.40	0.06	165.6	1.4	571.8	6.9	1.64	0.03	0.71
A7	16.32	0.06	167.6	1.6	560.5	7.4	1.62	0.03	0.71
A7'	17.00	0.06	165.8	1.4	591.7	7.1	1.64	0.03	0.71
A8	16.75	0.06	166.1	1.6	582.2	7.8	1.64	0.03	0.71
A8'	16.50	0.06	169.0	1.5	562.9	6.8	1.63	0.03	0.71
A9	16.52	0.06	167.1	1.6	570.9	7.6	1.65	0.03	0.71
A9'	17.01	0.06	169.6	1.5	578.5	7.0	1.64	0.03	0.71
A10	16.37	0.06	165.9	1.6	569.0	7.6	1.64	0.03	0.71
A10'	16.52	0.06	166.0	1.4	574.7	7.0	1.65	0.03	0.71
A11	16.40	0.06	164.9	1.5	573.8	7.6	1.64	0.03	0.71
A11'	16.67	0.06	163.7	1.4	588.1	7.1	1.65	0.03	0.71
A12	16.32	0.06	163.8	1.5	574.4	7.7	1.63	0.03	0.71
A12'	16.44	0.06	169.5	1.5	558.0	6.9	1.61	0.03	0.70
median	16.46		166.1		574.2		1.64		
average	16.52		166.0		574.3		1.64		
SD	0.23		2.1		8.1		0.01		
RSD	1.39%		1.29%		1.41%		0.74%		

Table 2.6 Asphaltene and maltene mass percentage and proportion of their total Re and Os, i.e. those of the whole oil regardless of lost fractions

Sample	mass fractions (%)			total of asphaltene and maltene			asphaltene portion		maltene portion	
	asphaltene	maltene	loss	Re (ng g^{-1})	Os (pg g^{-1})	^{187}Os (pg g^{-1})	Re (%)	Os (%)	Re (%)	Os (%)
A 1	12.2	79.8	8.0	1.87	23.52	3.95	89.2	72.6	10.8	27.4
A 2	12.5	77.6	9.9	1.89	24.08	4.02	89.5	72.0	10.5	28.0
A 3	12.3	79.3	8.4	1.86	23.10	3.88	89.2	73.3	10.8	26.7
A 4	12.1	79.6	8.2	1.87	23.78	3.98	88.4	70.9	11.6	29.1
A 5	12.1	80.0	7.9	1.88	23.44	3.97	88.5	72.2	11.5	27.8
A 6	11.2	82.3	6.5	1.86	23.32	3.92	87.9	70.9	12.1	29.1
	the range of A whole oil values:			1.69 - 1.94	20.96 - 24.29	3.54 - 4.08				
B 1	13.3	78.4	8.3	2.11	26.75	4.45	91.4	76.1	8.6	23.9
B 2	13.4	79.2	7.4	2.02	25.61	4.22	91.1	75.0	8.9	25.0
B 3	12.9	83.8	3.3	1.99	25.77	4.22	90.4	72.6	9.6	27.4
	the range of B whole oil values:			2.06 - 2.15	25.97 - 27.02	4.28 - 4.51				
C 1	13.5	78.8	7.7	2.10	26.73	4.41	90.9	74.4	9.1	25.6
C 2	13.1	77.7	9.3	2.05	26.05	4.27	91.2	74.5	8.8	25.5
C 3	13.3	77.7	9.0	2.04	26.42	4.36	91.0	74.4	9.0	25.6
	the range of C whole oil values:			1.88 - 1.94	23.61 - 25.03	3.95 - 4.18				

To be continued.

Continue:

Sample	mass fractions (%)			total of asphaltene and maltene			asphaltene portion		maltene portion	
	asphaltene	maltene	loss	Re (ng g^{-1})	Os (pg g^{-1})	^{187}Os (pg g^{-1})	Re (%)	Os (%)	Re (%)	Os (%)
D 1	13.3	76.6	10.1	2.06	26.10	4.26	91.7	76.1	8.3	23.9
D 2	13.0	78.6	8.4	2.09	26.69	4.41	90.6	74.3	9.4	25.7
D 3	13.4	79.2	7.4	2.03	25.92	4.27	90.8	74.0	9.2	26.0
	the range of D whole oil values:			1.94 - 2.03	24.40 - 26.29	4.12 - 4.33				
E 1	12.9	81.1	6.0	2.03	25.55	4.22	90.6	74.6	9.4	25.4
E 2	13.2	79.4	7.4	2.07	26.54	4.37	90.8	73.4	9.2	26.6
E 3	13.0	77.9	9.1	2.09	26.00	4.28	90.0	73.6	10.0	26.4
	the range of E whole oil values:			2.01 - 2.06	24.81 - 25.38	4.10 - 4.29				
	the range of all whole oil values:			1.69 - 2.15	20.96 - 27.02	3.54 - 4.51				
median	13.0	79.2	8.1	2.03	25.85	4.24	90.6	73.8	9.4	26.2
average	12.8	79.3	7.9	1.99	25.30	4.19	90.2	73.6	9.8	26.4
SD	0.006	0.017	0.016	0.09	1.34	0.19	0.011	0.015	0.011	0.015
RSD	4.7%	2.2%	19.7%	4.8%	5.3%	4.5%	1.2%	2.1%	11.5%	5.8%

Figure 2.1 Linearized probability plots (top) and histograms and probability density curves (bottom) of RM8505 whole oil Re-Os data. The linearized probability data points are plotted using 1σ level uncertainties. Two whole oil sample Re-Os results from Georgiev et al. (2016) are also plotted (in the dashed boxes) except the Os data as the values exceed the range of the plot.

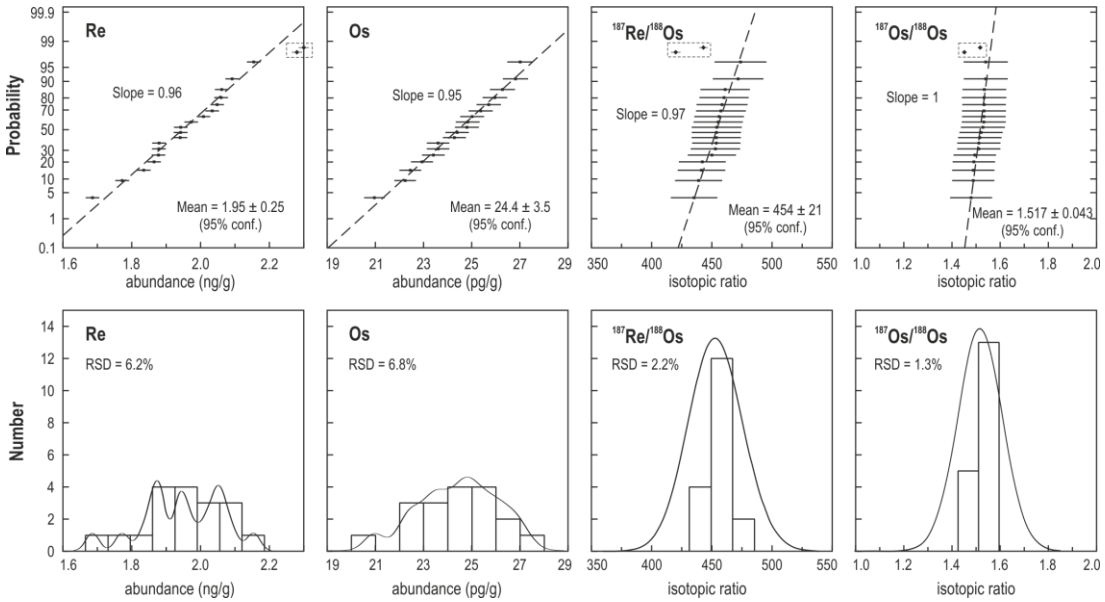
Probability
Re
Slope = 0.96
Mean = 1.95 ± 0.25
(95% conf.)
abundance (ng/g)
Os
Slope = 0.95
Mean = 24.4 ± 3.5
(95% conf.)
abundance (pg/g)
187Re/188Os
Slope = 0.97
Mean = 454 ± 21
(95% conf.)
isotopic ratio
187Os/188Os
Slope = 1
Mean = 1.517 ± 0.043
(95% conf.)
isotopic ratio
Number
Re
RSD = 6.2%
abundance (ng/g)
Os
RSD = 6.8%
abundance (pg/g)
187Re/188Os
RSD = 2.2%
isotopic ratio
187Os/188Os
RSD = 1.3%
isotopic ratio

Figure 2.2 Linearized probability plots (top) and histograms and probability density curves (bottom) for individually separated asphaltene Re-Os data. The linearized probability data points are plotted using 1σ level uncertainties.

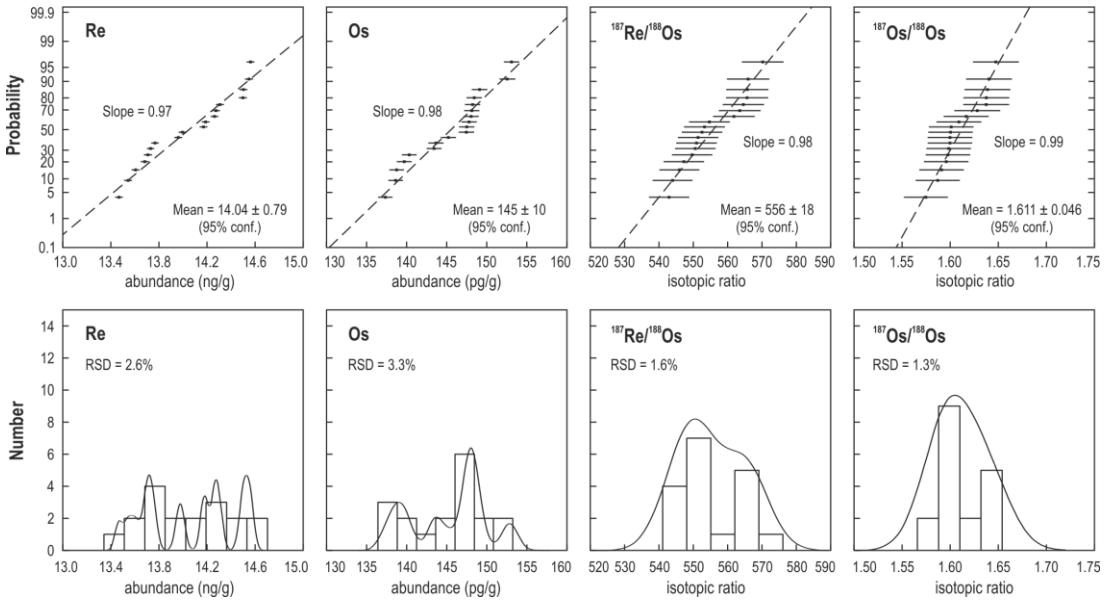
Probability
Re
Slope = 0.97
Mean = 14.04 ± 0.79
(95% conf.)
abundance (ng/g)
Os
Slope = 0.98
Mean = 145 ± 10
(95% conf.)
abundance (pg/g)
187Re/188Os
Slope = 0.98
Mean = 556 ± 18
(95% conf.)
isotopic ratio
187Os/188Os
Slope = 0.99
Mean = 1.611 ± 0.046
(95% conf.)
isotopic ratio
Number
Re
RSD = 2.6%
abundance (ng/g)
Os
RSD = 3.3%
abundance (pg/g)
187Re/188Os
RSD = 1.6%
isotopic ratio
187Os/188Os
RSD = 1.3%
isotopic ratio

Figure 2.3 Linearized probability plots (top) and histograms and probability density curves (bottom) of separated maltene Re-Os data. The linearized probability data points are plotted using 1σ level uncertainties.

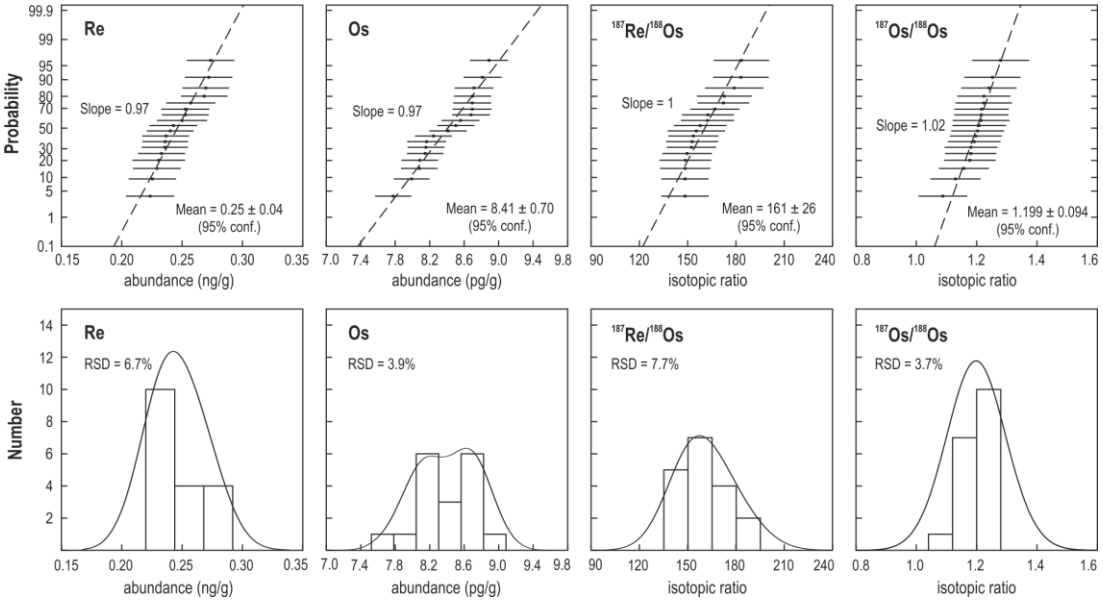
Probability
Re
Slope = 0.97
Mean = 0.25 ± 0.04
(95% conf.)
abundance (ng/g)
Os
Slope = 0.97
Mean = 8.41 ± 0.70
(95% conf.)
abundance (pg/g)
187Re/188Os
Slope = 1
Mean = 161 ± 26
(95% conf.)
isotopic ratio
187Os/188Os
Slope = 1.02
Mean = 1.199 ± 0.094
(95% conf.)
isotopic ratio
Number
Re
RSD = 6.7%
abundance (ng/g)
Os
RSD = 3.9%
abundance (pg/g)
187Re/188Os
RSD = 7.7%
isotopic ratio
187Os/188Os
RSD = 3.7%
isotopic ratio

Figure 2.4 Comparison of the Re and Os abundances of RM8505 whole oil, asphaltene and maltene. Data-point error ellipses are 2σ.

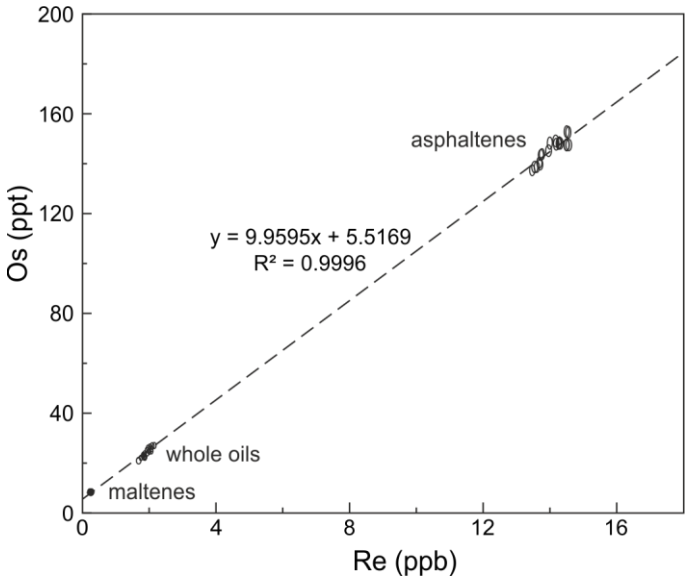
200
160
120
80
40
0
Os (ppt)
0
4
8
12
16
Re (ppb)
asphaltenes
y = 9.9595x + 5.5169
R² = 0.9996
whole oils
maltenes

Figure 2.5 Comparison of the Re-Os isotopic compositions of the RM8505 whole oil, asphaltene and maltene. Data-point error ellipses are 2σ. Regression of the Re-Os data of the whole oil, asphaltene and maltene fractions yields a date of 62.7 ± 5.7 Ma (initial $^{187}Os/^{188}Os$ = 1.030 ± 0.051, MSWD = 0.31). It is noted that this date value likely does not bear any geological meaning in regard to the timing of oil generation of Venezuelan petroleum systems (see text for discussion).

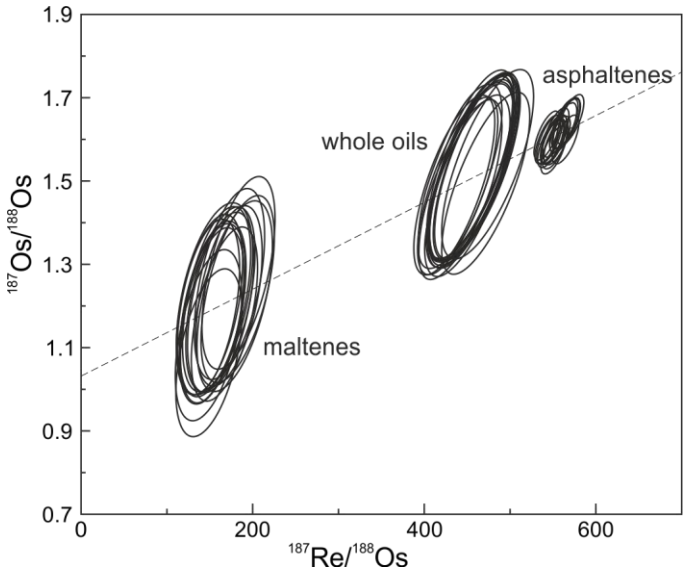
1.9
1.7
1.5
1.3
1.1
0.9
0.7
0
200
400
600
$^{187}Os/^{188}Os$
$^{187}Re/^{188}Os$
asphaltenes
whole oils
maltenes

Figure 2.6 Mass balance of asphaltene-maltene separation and Re-Os budget of RM8505 oil: a) mass percentages of asphaltene and maltene; b) Re budget of RM8505 oil separated asphaltene and maltene fractions, i.e. $Total\ Re = asphaltene\ Re\ abundances \times asphaltene\ mass\ fraction + maltene\ Re\ abundances \times maltene\ mass\ fraction$; c) Os budget of RM8505 oil separated asphaltene and maltene fractions, i.e. $Total\ Os = asphaltene\ Os\ abundances \times asphaltene\ mass\ fraction + maltene\ Os\ abundances \times maltene\ mass\ fraction$; d) Re percentages of asphaltene and maltene within oil, e.g. $maltene\ Re\ abundances \times maltene\ mass\ fraction/Total\ Re$ and e) Os percentages of asphaltene and maltene within oil, e.g. $maltene\ Os\ abundances \times maltene\ mass\ fraction/Total\ Os$. See text for discussion.

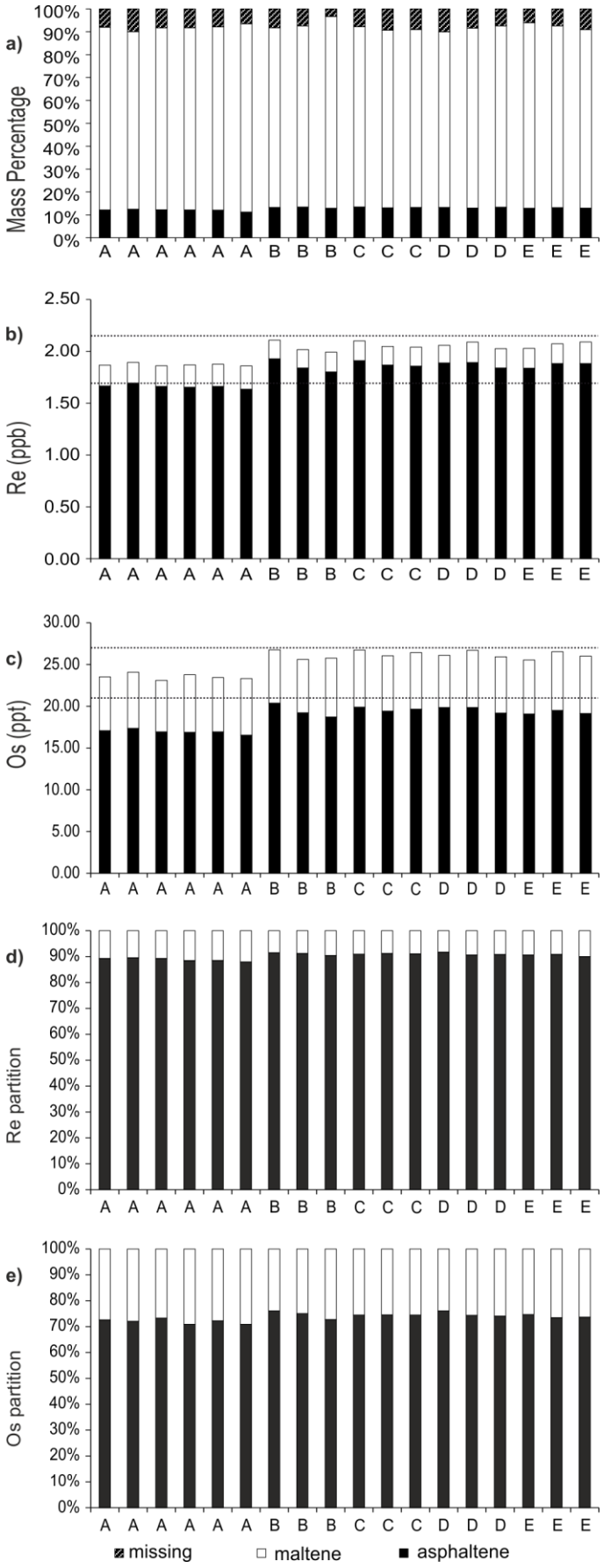
a)
Mass Percentage
100%
90%
80%
70%
60%
50%
40%
30%
20%
10%
0%
A A A A A A B B B C C C D D D E E E
b)
Re (ppb)
2.50
2.00
1.50
1.00
0.50
0.00
A A A A A A B B B C C C D D D E E E
c)
Os (ppt)
30.00
25.00
20.00
15.00
10.00
5.00
0.00
A A A A A A B B B C C C D D D E E E
d)
Re partition
100%
90%
80%
70%
60%
50%
40%
30%
20%
10%
0%
A A A A A A B B B C C C D D D E E E
e)
Os partition
100%
90%
80%
70%
60%
50%
40%
30%
20%
10%
0%
A A A A A A B B B C C C D D D E E E
missing
maltene
asphaltene

Figure 2.7 Comparison of the Re-Os isotopic compositions of asphaltene, crude oil and maltene of previously studied oils: a) seven oils from Selby *et al*. (2007) and b) selected data of three oils from Georgiev *et al*. (2016). Both studies utilized *n*-heptane for the separation although with slightly different protocols. See text for discussion.

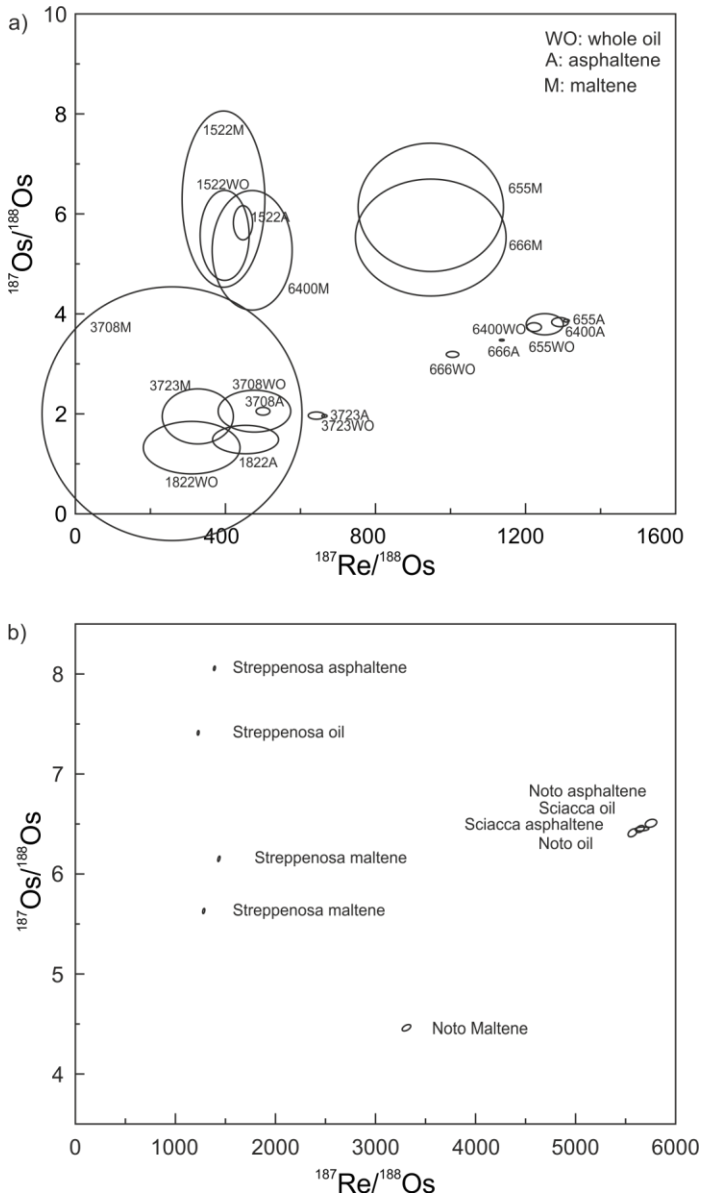
a)
WO: whole oil
A: asphaltene
M: maltene
1522M
1522WO
1522A
6400M
655M
666M
3708M
6400WO
655A
6400A
666A
655WO
666WO
3723M
3708WO
3708A
3723A
3723WO
1822A
1822WO
$^{187}Os/^{188}Os$
$^{187}Re/^{188}Os$
b)
Streppenosa asphaltene
Streppenosa oil
Noto asphaltene
Sciacca oil
Sciacca asphaltene
Noto oil
Streppenosa maltene
Streppenosa maltene
Noto Maltene
$^{187}Os/^{188}Os$
$^{187}Re/^{188}Os$

Figure 2.8 Linearized probability plots (top) and histograms and probability density curves (bottom) of the homogenized asphaltene Re-Os data. The linearized probability data points are plotted using 1σ level uncertainties.

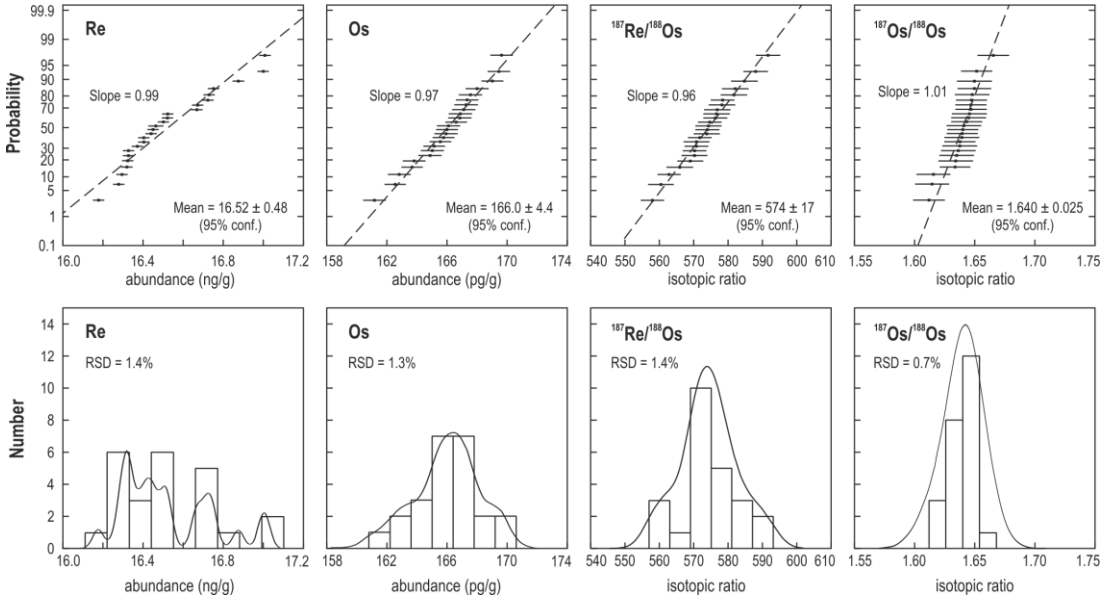
Probability
Re
Slope = 0.99
Mean = 16.52 ± 0.48
(95% conf.)
abundance (ng/g)
Os
Slope = 0.97
Mean = 166.0 ± 4.4
(95% conf.)
abundance (pg/g)
187Re/188Os
Slope = 0.96
Mean = 574 ± 17
(95% conf.)
isotopic ratio
187Os/188Os
Slope = 1.01
Mean = 1.640 ± 0.025
(95% conf.)
isotopic ratio
Number
Re
RSD = 1.4%
abundance (ng/g)
Os
RSD = 1.3%
abundance (pg/g)
187Re/188Os
RSD = 1.4%
isotopic ratio
187Os/188Os
RSD = 0.7%
isotopic ratio

Chapter 3 Re-Os geochronology and oil-source correlation of the Duvernay petroleum system, Western Canada sedimentary basin: Implications for the application of the Re-Os geochronometer to petroleum systems

A version of this chapter is accepted, revised and resubmitted to AAPG Bulletin co-authored by David Selby, Mark Obermajer, and Andy Mort.

3.1 Introduction

Establishing an accurate and precise age of hydrocarbon generation is crucial for understanding the evolution of a petroleum system. Timing constraints for hydrocarbon generation can be achieved through many techniques, for example, basin modelling with paleotemperature and petroleum generation kinetics; or the timing of oil generation can be inferred by constraining the earliest migration of oil using radiometric dating ($^{40}Ar/^{39}Ar$) of fluid inclusions and diagenetic minerals, e.g., authigenic illite and K-feldspar (Eadington et al., 1991; Kelly, 2002; Mark et al., 2005; Mark et al., 2010; Welte et al., 2012). Despite the contribution of these methods to the understanding of petroleum system evolution, they are limited by poorly constrained parameters (e.g., paleogeothermal gradient) or difficulties associated with sampling and analyzing (e.g., grain size versus purity of authigenic minerals for radiometric dating). During the past decade, the rhenium-osmium (Re-Os) chronometer has been demonstrated to be a promising radiometric tool to directly date petroleum samples and for oil-source correlation (Selby and Creaser, 2005b; Selby and Creaser, 2005a; Selby et al., 2007; Finlay et al., 2011; Finlay et al., 2012; Rooney et al., 2012; Lillis and Selby, 2013; Cumming et al., 2014; Ge et al., 2017).

Rhenium-Os analysis demonstrating chronologic information in petroleum systems was first shown by Selby et al. (2005), who derived a Re-Os date of 374.2 ± 8.6 Ma (MSWD = 11.7, Model 3) for bitumen formation in the Polaris Mississippi Valley Type deposit, which is in agreement with contemporaneous Pb-Zn mineralization dated at 366 ± 15 Ma (Rb-Sr sphalerite methodology). In addition, Re-Os data derived from highly biodegraded oil from the Oil Sand deposits of Alberta, Canada,

give an age of 111.6 ± 5.3 Ma (MSWD = 2.2, Model 3) (Selby and Creaser, 2005a), which is in agreement with the basin model of Riediger et al. (2001). Consequently, the Re-Os date is taken to record the timing of oil generation/migration in the world's largest oil sand system. However, the Re-Os age for the oil sands is inconsistent with some other basin models proposed for this complex oil system, e.g. Higley et al. (2009), Berbesi et al. (2012), and a recent study on trap restoration and the bitumen present in kimberlites (Tozer et al., 2014) which could relate to secondary migration of oil in the Alberta basin.

Oil Re-Os dates from the UK Atlantic Margin (UKAM) petroleum system (Finlay et al., 2011) also correspond to the age of petroleum generation determined through basin modelling and K-feldspar cement $^{40}Ar/^{39}Ar$ dating (Lamers and Carmichael, 1999; Mark et al., 2005; Finlay et al., 2011). A Re-Os study of oils from the Phosphoria petroleum system, Bighorn basin, USA produced an age of 211 ± 21 Ma, corresponding to the start of petroleum generation according to basin modelling rather than the re-migration of oil (during the Laramide orogeny, 80~35 Ma) or the deposition of the source rock (during the Permian, ~270 Ma) (Lillis and Selby, 2013). Although the UKAM and Phosphoria oils are variably biodegraded, the process has not appreciably disturbed the Re-Os systematics from recording the timing of generation of oil. This is supported by the fact that Re and Os in oil are hosted predominantly by the asphaltene fraction (Selby et al., 2007), which is the most resistant phase to biodegradation (Wenger et al., 2001; Peters et al., 2005). More recently, Re-Os bitumen data has provided insights into the temporal hydrocarbon evolution in the Longmen Shan Thrust Belt, southwest China and its relationship to tectonism, and additionally discussed implications for future exploration of the adjacent petroliferous Sichuan Basin (Ge et al., 2017). Furthermore, a study of the Green River petroleum system in the Uinta basin, USA, demonstrated the capacity of the Re-Os chronometer to yield the timing of oil generation (19 ± 14 Ma) in lacustrine petroleum systems in addition to marine petroleum systems (Cumming et al., 2014).

Unlike previous studies using multiple oil/bitumen samples to establish a Re-Os date, a study focusing on two oil families of the Gela oil field, southern Sicily, Italy, promotes the establishment of Re-Os dates using fractions of one single oil sample,

in order to negate possible disadvantages of using multiple oil samples from a wide geographic region (Georgiev et al., 2016). The authors analysed the asphaltene and maltene fractions, which were separated using a series of solvents (*n*-pentane, *n*-hexane, *n*-heptane and *n*-decane). The best-fit of the Re-Os data for asphaltenes from one oil family and for maltenes from the other oil family yields reasonable oil generation ages for each family. However, this approach of obtaining a Re-Os oil generation age from one single oil sample is potentially confined to oils with high asphaltene contents and Re and Os abundances. It also depends on the difference of asphaltenes and maltenes separated by different *n*-alkanes from the same oil to obtain a range in Re-Os isotopic compositions sufficient to obtain an isochron. As such, oils with low Re and Os abundances will be too analytically challenging to obtain precise data to distinguish these differences.

Hydrous pyrolysis experiments on organic-rich sedimentary rocks (Rooney et al., 2012; Cumming et al., 2014) have shown that during thermal maturation, Re and Os will be transferred to the generated oil, although the majority of the Re and Os remains in the source rock. The $^{187}Re/^{188}Os$ values show no consistent relationship between the source rock and the generated oil, but the $^{187}Os/^{188}Os$ composition of a source rock is inherited by the generated oil (Selby et al., 2005; Finlay et al., 2011; Rooney et al., 2012; Cumming et al., 2014). The relationship between the $^{187}Os/^{188}Os$ composition of a source rock and the $^{187}Os/^{188}Os$ composition of the generated oil (at the time of generation) is employed in the aforementioned studies for oil-source correlation. In addition, the coupling of Pt/Pd values with $^{187}Os/^{188}Os$ compositions has been employed as a viable inorganic oil-source correlation tool in recognizing the Lower Jurassic Gordondale Member as the predominant source of the Canadian oil sands (Finlay et al., 2012), which is supported by basin and migration modelling studies (Higley et al., 2009; Berbesi et al., 2012).

Although present studies show that biodegradation has little influence on the Re-Os systematics of asphaltene (Selby and Creaser, 2005a; Selby et al., 2005; Finlay et al., 2012; 2014), they can be vulnerable to other secondary alteration processes of petroleum. For example, disturbance of the Re-Os systematics has been shown for oils spatially associated with the main basin-bounding faults of the Viking Graben and East Shetland basin of the North Sea, United Kingdom (Finlay et al., 2010).

Here, oils are suggested to have been contaminated by fault-charged mantle-fluids that contain Os with a non-radiogenic $^{187}Os/^{188}Os$ composition. As a result, the Re-Os systematics of the oil fail to yield a generation age, but instead trace the crustal-scale fluid dynamics and migration. Such processes have also been demonstrated in the laboratory, where experiments have shown that Re and Os in aqueous phase can transfer into oil during oil-water contact under various conditions (Mahdaoui et al., 2015). Thermal cracking may also reset the Re–Os isotope systematics in petroleum and result in only the timing of thermal cracking and generation of dry gas and pyrobitumen being recorded (Lillis and Selby, 2013; Ge et al., 2016). Similarly, thermochemical sulphate reduction (TSR) of oil may also disturb/reset the Re-Os systematics in oil. For example, the Re-Os data from oils affected by TSR in the Big Horn basin yield a Re-Os date of 9.24 ± 0.39 Ma, which is in agreement with the proposed end of TSR as a result of reservoir cooling due to the major uplift and erosion at ~10 Ma (Lillis and Selby, 2013).

The previous attempts and achievements of using Re-Os as petroleum generation geochronometer and oil-source tracer are often compromised by the lack of understanding, or intrinsic complex geological characteristics, of the petroleum systems. The source units of some petroleum systems are often debated or represent mixed sources. For example: 1) the Phosphoria system records a mixed oil generated from two separate members of the Permian Phosphoria Formation that were deposited over 5 million years; 2) the Eocene Green River Formation is over 3000 m (9843 ft) thick, within which many members are considered as possible oil sources (Anders et al., 1992; Ruble et al., 2001); 3) the Canadian Oil Sands may have a mixed source, although the main contributor is highly debated (Riediger et al., 2001; Higley et al., 2009; Berbesi et al., 2012; Finlay et al., 2012; Adams et al., 2013). Inconsistent thermal maturation timings, multiple stages of oil generation and remigration are also often proposed by geological models. Both multiple sources and multiple stages, or prolonged oil generation, are likely to yield a large range of initial $^{187}Os/^{188}Os$ compositions of generated oil. Some oil samples are also altered (e.g., biodegradation, thermal cracking, and thermochemical sulphate reduction), for which the possibility and degree of disturbance to the oil Re-Os systematics has been discussed, but not yet fully understood. Further, the application of the $^{187}Os/^{188}Os$ composition as an oil-source correlation tool suffers from the lack of source rock Re-

Os data in many cases. For example, the Green River Formation is over 3000 m (9843 ft) thick, but the shale samples for Re-Os dating were collected from three intervals with most of the samples spanning only 1 to 3 m (3.28 to 9.84 ft) (Cumming et al., 2014).

Here, as an examination of the usefulness of the application of the Re-Os chronometer in petroleum systems, we present the study on the simple and well-characterized Duvernay petroleum system of the Western Canada sedimentary basin (WCSB). The oil in this petroleum system is sourced from the Late Devonian Duvernay carbonaceous shale (Stoakes and Creaney, 1984; Li et al., 1998; Fowler et al., 2001). Oil generation from the Late Devonian Duvernay carbonaceous shale occurred during the Late Cretaceous to Eocene, associated with the Laramide orogeny (Deroo et al., 1977; Creaney and Allan, 1990). The generated oil migrated into the adjacent Leduc reef build-ups in the Rimbey-Meadowbrook reef chain and Bashaw reef complex area, and then into the overlying Winterburn Group Nisku Formation (Creaney et al., 1994; Rostron, 1997). Biomarker analyses indicate that the Duvernay Formation is the only source of this petroleum system and that crude oil has experienced limited secondary alteration (Li et al., 1998; Fowler et al., 2001). We present Re-Os data from oil and source units, coupled with organic geochemistry, and discuss the geochronology and oil-source correlation of the Duvernay petroleum system and the implications for the application of the Re-Os geochronometer to petroleum systems.

3.2 Geological setting

The Duvernay petroleum system is located in south-central Alberta within the Western Canada sedimentary basin (Figure 3.1). The Late Devonian Woodbend and Winterburn strata in the basin represent a thick and lithologically complex accumulation of shales and carbonates (Figure 3.2). The two salient features of the Woodbend and Winterburn strata are the high quality source rocks and reservoirs they encompass, for example, the proliferous Duvernay Formation and the porous carbonates of the Leduc and Nisku Formations.

The Late Devonian Duvernay Formation of the Woodbend Group was deposited as marine basin-filling laminated carbonates and shales (Stoakes and Creaney, 1984;

Switzer et al., 1994; Chow et al., 1995; Fowler et al., 2001; Fothergill, 2014). The Duvernay Formation correlates with the Muskwa Formation to the north, and the Horn River and Canol Formations in the Northwest Territories. The formation also overlies the platform carbonates of the Cooking Lake Formation and is in turn overlain by the basin-filling calcareous shales of the Ireton Formation. The thickness varies depending on proximity to Devonian reef build-ups and is predominantly 20 - 60 m (66 to 197 ft) (Figure 17, Switzer et al., 1994; Fothergill, 2014), but is up to 90 m (295 ft) within some carbonate embayments adjacent to the Killam Barrier reef-edge (Switzer et al., 1994; Fowler et al., 2001). The organic matter is concentrated in thin (typically a few mm) alternating laminae within the Duvernay Formation, which are separated by an organic-poor mudstone. Petrographically, the laminates of the Duvernay Formation contain abundant alganite macerals and some bituminite, often within an amorphous organic matrix, indicating that they represent periods of significant accumulation and preservation of oil-prone Type II marine organic matter (Fowler et al., 2001). This organic-poor mudstone becomes thinner (30 m (98 ft)) in the center of the basin (Switzer et al., 1994) to the west and reduces the separation between the two organic-rich intervals (Chow et al., 1995). The average TOC content ranges from 4 wt.% to 6 wt.%, although occasionally it is as high as 17 wt. % (Stoakes and Creaney, 1984; Chow et al., 1995; Higley et al., 2009; Dunn et al., 2012).

The numerous isolated Leduc reef build-ups (e.g., Rimbey-Leduc-Meadowbrook chain, Redwater, Bashaw) sit stratigraphically above the Cooking Lake Formation and partially interfinger with the Duvernay Formation (Figures 3.1 - 3.2). The Leduc reefs are up to 275 m (902 ft) thick (Switzer et al., 1994; Chow et al., 1995; Rostron, 1997) and are highly porous and permeable (Amthor et al., 1994). A broad Leduc carbonate shelf also developed on the Cooking Lake Formation to the southeast of the basin. The Winterburn Nisku Formation is dominated by an extensive carbonate shelf in the East Shale basin to the east of the Rimbey-Meadowbrook Leduc reef trend. Its thickness decreases from 60 m (197 ft) near the underlying Leduc reef trend to about 20 m (66 ft) in the east, with its lithology changing stratigraphically from interbedded shale and limestone to relatively pure carbonates (Switzer et al., 1994).

The hydrocarbon maturation of the majority of the Phanerozoic strata of the WCSB did not occur until the Laramide orogeny (Late Cretaceous-Eocene) and was terminated by subsequent uplift and erosion (Deroo et al., 1977; Creaney and Allan, 1990; Bustin, 1991). As a result of the eastward propagation of crustal down-warping and foreland basin development, deep burial and thermal maturation progressed from the foreland belt northeastward across the plain. Present day isomaturity maps of Jurassic and younger source rocks (Bustin, 1991) display a decrease in thermal maturity from the foredeep to the shallower part of the basin in the northeast, where significant hydrocarbon generation occurred until the Eocene. Also estimated by apatite fission track studies (Issler et al., 1999), the peak paleo-temperature and inferred maximum burial depth is estimated from apatite fission track dating to have occurred at ~ 60 Ma.

It is generally accepted that the Duvernay source rocks have generated large amounts of hydrocarbons, with volume estimations ranging up to 100 million barrels (MMbbl) per square mile (Jenden and Monnier, 1997). The generated oil migrated extensively both laterally and stratigraphically within the basin, including in the older Beaverhill Lake and Elk Point reservoirs. But migration of oils was largely confined to the Cooking Lake-Leduc and Nisku Formations by the low permeability shales, dolomitic carbonates and anhydrites of the Devonian Waterways Formation, Ireton Formation and Wabamun Group (Figure 3.3; Stoakes and Creaney, 1985; Creaney and Allan, 1990; Rostron, 1997) over most of central and northern Alberta. The generated oil migrated locally into the Cooking Lake platform margins and Leduc reefs (Rimbey-Meadowbrook trend and Bashaw Reefs), and the stratigraphically older Beaverhill Lake platform present in an updip position due to the regional tilt of the strata (Figure 31, Creaney and Allan, 1992; Creaney et al., 1994; Figure 5, Rostron, 1997. The Cooking Lake Formation also provided a migration pathway for the isolated Leduc reef as a "leaky pipeline" dependent on the local presence or absence of permeability barriers (Stoakes and Creaney, 1984). The Ireton shale serves as the seal to the Duvernay petroleum system. However, due to the absence or the thin nature of the Ireton shale in some places, oil also leaked into the overlying Nisku carbonates in the Bashaw area (Rostron, 1997; Li et al., 1998). Geochemical studies (Creaney et al., 1994; Li et al., 1998; Fowler et al, 2001) documented that the organic geochemical composition of the Duvernay Formation extracts is quite

similar to most of the crude oils found within the Leduc-Nisku intervals along the Rimbey-Meadowbrook and Bashaw reef trends. In fact, geochemical oil-source correlations have demonstrated that the Leduc and Nisku oils are almost all sourced from the Duvernay Formation with probably only a very small contribution of the Nisku source to the Nisku oils (Rostron, 1997; Li et al., 1998; Harris et al., 2003).

Gas chromatography and biomarker data show that there is no or limited alteration of the Leduc and Nisku oils by biodegradation or water washing. Thermal cracking and thermochemical sulphate reduction of crude oil occurred only in the foredeep (Evans et al., 1971; Rogers et al., 1974; Creaney and Allan, 1992; Marquez, 1994; Stasiuk, 1997; Fowler et al., 2001). The generated gas migrated up-dip and may have resulted in deasphalting, which is considered responsible for the high H_2S content of some of the stratigraphically-higher crude oil (Simpson, 1999; Fowler et al., 2001).

3.3 Sample preparation and analysis methodology

3.3.1 Oil samples

All oil samples analysed in this study were taken from the oil library of the Geological Survey of Canada (GSC), Calgary. The selected oils are from both the Leduc and Nisku reservoirs in the area of the Rimbey-Meadowbrook Leduc reef trend and the Bashaw reef complex between Edmonton and Calgary (Figure 3.1; Table 3.1). Prior to sampling, the archived oil was thoroughly mixed to remove any density separation of oil fractions that had occurred during storage.

The selected Duvernay oil samples typically have low asphaltene contents. Given that Re and Os are both predominantly present in the asphaltene fraction, and that the Re–Os isotopic composition of an asphaltene can be used as an approximation for that of the bulk oil (Selby et al., 2007), the asphaltene fractions were separated from the oils to permit more precise determinations of the Re and Os isotope compositions. The separation of asphaltene from the bulk oil follows the principles and steps outlined by Speight (2004) and Selby et al. (2007). For each gram of crude oil, 40 ml of *n*-heptane (or *n*-pentane) was added, and the mixture was agitated on a rocker overnight (~ 20 h) at room temperature. Asphaltene is the insoluble fraction of oil in *n*-heptane (and *n*-pentane) and was isolated from the maltene-bearing *n*-heptane / *n*-pentane fraction by centrifuging at 3500 rpm for 15 minutes. Following the removal

of the *n*-heptane / *n*-pentane, the asphaltene was extracted using chloroform and dried at 60 °C.

3.3.2 Source rock

In addition to the Duvernay oil asphaltene, the organic-rich Duvernay Formation was also analysed for its Re and Os abundances and Re-Os isotopic composition. The shale/carbonaceous shale samples of the Duvernay Formation were collected from the cores of wells 16-18-52-5W5, 14-29-48-6W5, 2-6-47-4W5 and 10-27-57-21W4 (Figure 3.1; Table 3.2). The Re-Os data from these samples were compiled with previously published Re-Os data from the Duvernay Formation from wells 2-12-50-26W4, 8-35-31-25W4 and 1-28-36-3W5 (Selby et al., 2007; Finlay et al., 2012). The entire sample set covers a large geographical area of 300 × 150 km^2 (1866 × 93 sq mi). As a result, the sample set, with respect to hydrocarbon maturation, ranges from immature to overmature with an average R_o from 0.5 % of 10-27-57-21W4 to 1.25 % of 2-6-47-4W5 and 1.45 % of 1-28-36-3W5 (Stasiuk and Fowler, 2002), and possesses highly variable TOC contents (from less than 1 wt.% to over 10 wt.%).

Depending on the thickness of the Duvernay Formation interval of each well, most samples were taken equally from each well at 0.5 m (16-18-52-5W5, ~1.5 m) and 2 m (14-29-48-6W5, ~8 m; 2-6-47-4W5, ~20 m) or as equal as possible depending on availability (10-27-57-21W4) in order to obtain a Re-Os data set that was representative of the entire Duvernay Formation organic-rich interval (Table 3.2). The collected core samples were cut and polished to remove any drilling marks and materials, and dried at 60˚C. Approximately 30 g of rock for each sample was crushed to a fine homogeneous powder using a Zr dish.

3.3.3 Gas chromatography and biomarker analyses of crude oil and source rock extracts

Geochemical analyses were performed on low- to high-maturity Duvernay sourced oil samples and source rock solvent extracts. Soluble organic matter was extracted from powered rock samples of the Duvernay Formation for 24 hours using a chloroform:methanol (87:13) mixture. The extracts and crude oils were treated with approximately 40 volumes of *n*-pentane to precipitate the asphaltenes. The deasphalted extracts and oils were fractionated using open column chromatography.

Saturates were recovered by eluting with pentane, aromatics by eluting with a 50:50 mixture of pentane-dichloromethane, and resins were recovered with methanol.

The gasoline range fractions (*i*-C_5-*n*-C_8) of the crude oils were analysed on a HP5890 Gas Chromatograph (50m HP-1 column, siloxane gum used as a fixed phase) connected to an OI Analytical 4460 Sample Concentrator. A small amount of the whole crude oil was mixed with deactivated alumina and transferred to the Sample Concentrator. The temperature was initially held at 30 °C for 10 minutes, then increased at a rate of 1 °C/min to 45 °C and held for 25 minutes. The eluting hydrocarbons were detected using a flame ionization detector.

Saturate fractions were analysed using a Varian 3700 FID gas chromatograph equipped with a 30m DB-1 column. The temperature was programmed from 60 °C to 300 °C at a rate of 6 °C/min and then held for 30 min at 300 °C. Gas chromatography-mass spectrometry (GCMS) was performed on a VG 7070 mass spectrometer with a gas chromatograph attached directly to the ion source (30 m DB-5 fused silica column used for GC separation). The temperature was initially held at 100 °C for 2 min and then programmed at 40 °C/min to 180 °C and at 4 °C/min to 320 °C. After reaching 320 °C, the temperature was held for 15 min. The mass spectrometer was operated with a 70 eV ionization voltage, 100 mA filament emission current, and interface temperature of 280 °C.

3.3.4 Re-Os analyses

The measurement of asphaltene and shale Re and Os abundances, and Re and Os isotopic compositions were undertaken at Durham University in the Laboratory for Source Rock and Sulphide Geochronology and Geochemistry (a member of the Durham Geochemistry Centre) by isotope dilution - negative thermal ionization mass spectrometry (ID-NTIMS). The chemical processing of samples to isolate and purify Re and Os and the measurement by NTIMS follow previously published protocols (Selby and Creaser, 2001; Selby and Creaser, 2003; Selby, 2007; Rooney et al., 2011; Cumming et al., 2014). In brief, a known amount of shale (~0.1 to 1 g) and asphaltene (~0.15 g), together with a known amount of mixed spike containing ^{185}Re and ^{190}Os, was digested by a Cr^{VI}-H_2SO_4 solution for shale and inverse *aqua-regia* (2:1 16 N HNO_3 and 12 N HCl, 9 ml) for asphaltene in carius tubes at 220˚C for 48

hours. For some of the samples, the amount of asphaltene digested is limited by the amount of asphaltene obtained from the oil. The Os was extracted from the digested samples using chloroform, and then back-extracted from the chloroform using 9N HBr, before being purified by micro-distillation. Following the Os extraction, for shale samples, a 1 ml aliquot of the Cr^{VI}-H_2SO_4 solution was evaporated to dryness, and the Re fraction was isolated using sodium hydroxide-acetone solvent extraction, before being further purified by anion chromatography. For the asphaltene samples, the *aqua-regia* was evaporated to dryness and the Re fraction purified by anion chromatography. The purified Re and Os were loaded onto Ni and Pt filaments, respectively (Selby et al. 2007). Isotopic measurements were conducted using negative thermal ionization mass spectrometry (Creaser et al. 1991; Völkening et al., 1991) on a Thermo Scientific TRITON mass spectrometer via ion-counting, using a secondary electron multiplier in peak-hopping mode for Os, and static Faraday collection for Re. In-house solution standards are 0.1611 ± 0.0004 (1SD, n = 126) for DROsS and 0.5989 ± 0.0019 (1SD, n = 116) for Re Standard solution, which are in agreement with those previously reported (Nowell et al., 2008; Cumming et al., 2012 and references therein).

The measured difference in $^{185}Re/^{187}Re$ values for the Re standard solution and the accepted $^{185}Re/^{187}Re$ value (0.5974; Gramlich et al., 1973) is used for mass fractionation correction of the Re sample data. All Re and Os data are oxide and blank corrected. The total procedural blanks of inverse *aqua-regia* are ~ 1.6 pg Re and 0.04 ~ 0.1 pg Os, with an average $^{187}Os/^{188}Os$ of 0.24 ± 0.06 (n = 3). The total procedural blanks of Cr^{VI}-H_2SO_4 digested samples are ~12 pg Re and 0.02 ~ 0.05 pg Os, with average $^{187}Os/^{188}Os$ of 0.22 ± 0.06 (n = 4). All uncertainties are determined by error propagation of uncertainties in Re and Os mass spectrometer measurements, weighing, blank abundances and isotopic compositions, spike calibrations, and the reproducibility of standard Re and Os isotopic values. The Re-Os data are regressed using *Isoplot* (V. 4.15; Ludwig, 2012) with the ^{187}Re decay constant value of 1.666×10^{-11} a^{-1} (Smoliar et al., 1996). This decay constant is also used for the calculation of the $^{187}Os/^{188}Os$ values of the shales at the time of deposition and oil generation, and the $^{187}Os/^{188}Os$ values of the asphaltene at oil generation.

3.4 Results

3.4.1 Asphaltene Re-Os data

The asphaltene contents and Re-Os data of asphaltene fractions of this study, and one analysis reported by Selby et al. (2007), are shown in Table 3.3. The asphaltene abundance of the sampled Duvernay oils is between 0.23 and 14.10 %. Coupled with low asphaltene contents are low Re and Os abundances of the asphaltene fractions, which range from 0.01 to 3.78 ppb Re and 0.6 to 41.2 ppt Os (^{192}Os 0.2 to 14.9), respectively. Oil samples possessing asphaltene abundances up to ~4 % show a positive correlation with both Re and ^{192}Os abundance (Figure 3.4). However, this relationship does not hold for the remaining oil samples that possess higher asphaltene content (6 – 8% and ~15%) (Figure 3.4). Though, in general, oil samples possessing higher asphaltene contents have higher Re and ^{192}Os abundances (Figure 3.4). The low Re and Os abundances, coupled with the limited asphaltene obtained for Re-Os analyses, make precise measurements very challenging. The majority of the samples possess blank corrections between 0.3 – 3.3 % for Re and 1 - 10 % for Os (L02221 to L02155), although a few samples (e.g., L01810) have significant Re and Os corrections (40% Re and 50% Os). The samples with such large blank corrections also possess large uncertainties. Samples with uncertainty greater than 55% for ^{187}Re/^{188}Os and 30% for ^{187}Os/^{188}Os are excluded when determining a Re-Os age and are not further discussed. The ^{187}Re/^{188}Os and ^{187}Os/^{188}Os values of the asphaltene used for isochron construction range between ~67 and 642, and 0.78 and 1.62, respectively (Table 3.3). Together with the sample of Selby et al. (2007), the Re-Os data yield a Model 3 date (a model assuming variable initial ^{187}Os/^{188}Os values for samples) of 66 ± 31 Ma (n = 14, MSWD = 6.7, initial ^{187}Os/^{188}Os = 0.77 ± 0.20; Figures 3.5 - 3.6).

3.4.2 Re-Os data for organic-rich intervals of the Duvernay Formation

The Re and Os abundances and isotope data for the Duvernay source rock analysed from four wells of this study, plus those of previous studies (Selby et al., 2007; Finlay et al., 2012) are reported in Table 3.2. The Re and Os abundances for the Duvernay source range between 0.3 and 68 ppb Re, and 29 and 1965 ppt Os. The more Re- and Os- (^{192}Os) enriched sectors of the Duvernay source rock broadly correlate with intervals possessing higher TOC abundances (Figure 3.7). The

$^{187}Re/^{188}Os$ and $^{187}Os/^{188}Os$ ratios range from ~26 to 229 and 0.49 to 1.74, respectively.

We have calculated the $^{187}Os/^{188}Os$ composition of the Duvernay Formation at the time of deposition (initial $^{187}Os/^{188}Os$ (Os_i)), a value that is equal to the $^{187}Os/^{188}Os$ composition of the contemporaneous seawater (Cohen et al., 1999). The biostratigraphy of the Duvernay Formation shows mainly the occurrence of *Palmatolepis punctata* and *Palmatolepis hassi* (Ziegler and Sandberg, 1990; McLean and Klapper, 1998; Whalen et al., 2000), which constrains the deposition age to be between 376.5 and 380.5 Ma based on the Geologic Timescale 2016 (Ogg et al., 2016). The Os_i values for the shale samples are calculated at 378.5 Ma. The Os_i values range between 0.28 and 0.38, with a Tukey's Biweight average of 0.330 ± 0.008 (n = 33; Table 3.2; Figure 3.7).

3.4.3 Organic geochemistry of crude oil and source rock

The Leduc-Nisku oils, although typically not altered by biodegradation or water-washing, show a wide range of thermal maturities, often resulting in variable geochemical characteristics, and have been classified into three main subgroups that include low-, normal- and high-maturity oils (Figure 3.8). These hydrocarbons, however, represent a continuum that can be easily documented by examples of crude oils having maturities intermediate between the three subgroups. The following overview pertains mostly to the saturated hydrocarbon fractions of the three oil sub-types resulting from differences in thermal maturity (although similar compositional variations have also been observed in the aromatic fraction by Li et al., 1998). Main compositional characteristics of the organic extracts and a brief oil-source correlation summary are also included.

The least mature Duvernay sourced oils are found in the Leduc and Nisku reservoirs in central eastern Alberta, to the south of the Bashaw Reef Complex. These oils are characterized by low saturate/aromatic ratio, relatively high amounts of NSO compounds, and relatively high sulphur content (1-1.5%). Gasoline range chromatograms show high *n*-heptane and methylcyclohexane peaks (n-C_7>MCH), with toluene often in relatively high abundance compared to most other oils sourced from Devonian units. Saturate fraction gas chromatograms display smooth

distribution of n-alkanes with slight odd carbon number preference of *n*-C_{15} – *n*-C_{19} members, high abundance of acyclic isoprenoids relative to n-alkanes, low pristane/phytane ratio (~0.80), and evident biomarkers.

Biomarker distributions show a smooth homohopane (C_{31}–C_{35}) profile, gammacerane present in moderate abundance, low amounts of rearranged hopanes (i.e. low Ts/Tm) and tricyclic and tetracyclic terpanes relative to 17α(H)-hopane, C_{24} tetracyclic terpane in similar abundance to the two C_{26} tricyclic terpane isomers, relatively low abundances of diasteranes and short-chain steranes relative to regular steranes, and a C_{27}-C_{29} sterane abundance of C_{29}>C_{27}>>C_{28}.

The majority of the oil pools along the Rimbey-Meadowbrook trend contain normal-maturity Duvernay Formation sourced oils. Compared to low maturity oils, these oils have higher saturate/aromatic ratios, lower amounts of NSO compounds and lower sulphur content.

Gasoline range and saturate fraction gas chromatograms are generally similar in both subgroups, with notably lower abundance of acyclic isoprenoids relative to *n*-alkanes and some biomarker peaks in more mature oils.

Furthermore, normal maturity oils contain higher amounts of rearranged hopanes (hence higher Ts/Tm), tricyclic and tetracyclic terpanes compared to the hopanes, C_{24} tetracyclic terpane slightly greater than C_{26} tricyclic terpanes, very low abundance of gammacerane, higher abundances of diasteranes and short-chain steranes, and similar carbon number distributions for C_{27}-C_{29} regular steranes.

The high maturity Duvernay sourced oils/condensates tend to be those from the deeper, westerly pools with higher API gravities, typically occurring in the southern half of the province. Compared with other Duvernay sourced oils, they have higher saturate/aromatic ratios and lower amounts of NSO compounds. Although these oil can still be correlated to oils from the other two subgroups by gasoline range and saturate fraction gas chromatography data (though maturation parameters indicate higher maturity and *n*-alkane profiles shows more bias towards lower molecular weight homologues), they are quite easily distinguished based on the lack of or very low abundance of biomarkers such as hopanes and steranes. The visible peaks in the m/z 191 and m/z 217 chromatograms are typically tricyclic terpanes, Ts and C_{29} Ts,

low molecular weight steranes, high diasteranes and secosteranes with an extremely low abundance of regular steranes.

The organic extracts of the Duvernay Formation typically show *n*-alkane distributions dominated by shorter-chain homologues (*n*-C_{15} – *n*-C_{20}) (Figure 3.9). Amounts of acyclic isoprenoids relative to *n*-alkanes are high in low maturity samples and decrease with increasing level of thermal maturity. Pristane/phytane ratios generally fall within 1-2 range. Saturate biomarker signatures of mature extracts show relatively high amounts of rearranged hopanes and steranes with no homohopane prominence, low tricyclic terpanes, Ts/Tm ratios greater than 1.0 and high diasteranes. The geochemical character of the Duvernay Formation extracts is different compared with other Devonian units in Alberta that show petroleum source potential (Creaney et al., 1994).

Correlation of biomarker data indicates that organic geochemical composition of the thermally mature Duvernay Formation solvent extracts is very similar to that of the normal naturity crude oils found within the Leduc-Nisku intervals along the Rimbey-Meadowbrook and Bashaw reef trends (Figure 3.10). Both extracts and oils have higher concentrations of *n*-C_{17} and *n*-C_{18} relative to pristane and phytane, and average Pr/Ph ratios typical of suboxic depositional conditions (average of 1.66 and 1.38 for extracts and oils, respectively), show predominace of Ts over Tm, a smooth homohopane distributions without C_{34} or C_{35} prominence, relatively high amounts of rearranged steranes and common C_{29}>C_{27}>C_{28} regular sterane profile. Their overall similarity and genetic relationship are further supported by regional geology and stratigraphic data. As noted previously (Stoakes and Creaney, 1984 and 1985; Li et al., 1998), the Duvernay strata is the only prolific source rock interval that occurs in close stratigraphic proximity to the Leduc reefs to account for the large volume of oil found in the Leduc reservoirs and, therefore, is considered as the main source of these oils.

3.5 Discussion

3.5.1 Petroleum Re-Os geochronology

The burial history of the Albertan part of the Western Canada sedimentary basin has been constructed with isopach maps of the stratigraphic formations (Deroo et al.,

1977; Higley et al., 2005) and basin modelling based on oil generation kinetic parameters (Higley et al., 2009; Berbesi et al., 2012), which indicate that the Duvernay Formation started to generate oil at the onset of the Laramide orogeny, i.e., around 80 Ma. According to the most recent basin models (Higley et al., 2009; Berbesi et al., 2012), the majority of the oil generation occurred between ~70 and ~58 Ma, with a significant kerogen transformation ratio (>50%) of the Duvernay Formation being reached by ~65 Ma, and cessation of oil generation by ~50 Ma due to basin uplift.

The Re-Os oil date (66 ± 31 Ma, n = 14, MSWD = 6.7; Figure 3.5) obtained from the asphaltene fraction Re-Os data, although possessing a large uncertainty, is in good agreement with the timing of peak oil generation indicated by geological modelling. We note that the Re-Os oil date does not in any way reflect the age of the Duvernay oil source, the Duvernay Formation (this study; Deroo et al., 1977; Creaney et al., 1994; Li et al., 1998), which is early Late Devonian (Frasnian) (this study as discussed in Section 5.3; Switzer et al., 1994).

The Re-Os date is derived from a Model 3 *Isoplot* solution (Ludwig, 2012), which means that the scatter about the best-fit line (the isochron), as represented by the MSWD (mean square weighted deviation) value, is due to a combination of the calculated uncertainties for the $^{187}Re/^{188}Os$ and $^{187}Os/^{188}Os$ values and the error correlation, rho, plus an unknown but normally distributed variation in the initial $^{187}Os/^{188}Os$ (Os_i) values. The uncertainty in the Re-Os date spans the entire duration of oil generation; however, it is not to say that the uncertainty of the Re-Os oil age will necessarily be indicative of the duration of oil generation. The MSWD value (6.7) being >1 for the best-fit line suggests that the scatter about the best-fit line is controlled by geological factors rather than purely analytical uncertainties (Ludwig, 2012). The ~25% uncertainty in the calculated initial Os_i composition (0.77 ± 0.20; Figures 3.5 - 3.6; Table 3.3) suggests that the primary factor causing the degree of scatter about the best-fit of the Re-Os data is the variation in the Os_i composition of the oil sample set. The geological cause of the variation in the Os_i composition of the Duvernay oil is discussed below (Section 5.2).

3.5.2 $^{187}Os/^{188}Os$ composition oil-source fingerprinting

Previous research has proposed that at the time of oil generation, an oil inherits the $^{187}Os/^{188}Os$ composition of the source rock (Selby et al., 2005; Selby and Creaser, 2005; Finlay et al., 2011; Finlay et al., 2012; Rooney et al., 2012; Cumming et al., 2014). Compared to the previous attempts to apply the $^{187}Os/^{188}Os$ composition of oil and source rock as an absolute fingerprinting tool, the Duvernay petroleum system benefits from its single source and simple thermal maturation history. Here we have also obtained source rock Re-Os data for the entire stratigraphic interval of the Duvernay Formation over a large geographical area, to reflect the source rock Re-Os systematics as completely as possible.

Although not sampled for shale geochronology, for which an intensive sampling strategy should be adopted to minimize the time span of samples and limit any possible variability in the initial $^{187}Os/^{188}Os$ value, the Duvernay Formation source rock $^{187}Re/^{188}Os$ and $^{187}Os/^{188}Os$ data do display a positive correlation and yield Late Devonian ages (well 10-27-57-21W4, 10 samples over 55 m, Re-Os data yield 371 ± 22 Ma, initial $^{187}Os/^{188}Os$ = 0.33 ± 0.03, MWSD = 66; well 16-18-52-5W5, 4 samples over 1.5 m, Re-Os data yield 372 ± 13 Ma, initial $^{187}Os/^{188}Os$ = 0.33 ± 0.02, MWSD = 0.06; well 14-29-48-6W5, 5 samples over 6 m, Re-Os data yield 377 ± 62 Ma, initial $^{187}Os/^{188}Os$ = 0.33 ± 0.14, MWSD = 84; well 2-6-47-4W5, 11 samples over 20 m, Re-Os data yield 360 ± 15 Ma, initial $^{187}Os/^{188}Os$ = 0.38 ± 0.03, MWSD = 33; Figure 3.11). Further, given that the samples analysed are considered broadly the same geological age (Figure 3.11A-D), we also present a calculated Re-Os date from all 33 samples. The Re-Os data for the entire sample set yield 373.9 ± 9.4 Ma, with an initial $^{187}Os/^{188}Os$ = 0.34 ± 0.02 (MWSD = 82; Figure 3.11E). The uncertainties of the ages are due to the variation in the Os_i compositions (Table 3.2, Figure 3.7), which range from 0.28 to 0.38, and the limited spread in the $^{187}Re/^{188}Os$ values (≤160 $^{187}Re/^{188}Os$ units; Table 3.2 and Figure 3.11). Although the Re-Os dates are imprecise, they are nominally in agreement with the Late Devonian biostratigraphic age constraints for the Duvernay Formation.

To evaluate the relationship between the oil Os_i (Figures 3.5 - 3.6) composition and that of the source rock at the time of oil generation, the Duvernay source rock $^{187}Os/^{188}Os$ compositions at 66 Ma (Os_g) are calculated from the present day Re-Os data of shale samples. The Duvernay Formation Os_g values range between 0.46 and

1.48 (n = 33 from 7 wells), and yield a Tukey's Biweight average of 0.83 ± 0.01 (Table 3.2; Figure 3.7). The oil Os_i defined by the Re-Os isochron is 0.77 ± 0.20 (Figure 3.5). The range of the individual oil Os_i values is between 0.55 and 1.06 (Figure 3.6). Seventy-nine percent (26 of the 33 samples) of the shale Os_g values are indistinguishable from the individual oil Os_i values (Figure 3.7). The evidence from organic geochemistry of the Duvernay petroleum system indicates that the Duvernay Formation is the principal source of the Duvernay oils. As such, the similarity of the oil Os_i and Duvernay Formation Os_g compositions supports the research hypothesis that the oil Os_i is inherited from the source at the time of oil generation, and therefore oil Os_i and source Os_g values can be used as an oil-source correlation tool.

An oil-source correlation based on Os isotopic compositions is supported by the comparison of Duvernay petroleum system oil Os_i and shale Os_g values with the Os_g values of other oil-prone strata of the WCSB. As most of the oil-prone Phanerozoic strata of the WCSB underwent hydrocarbon maturation during the Laramide orogeny (Bustin, 1991; Higley et al., 2009), the Os_g values of these strata with available Re-Os data are also calculated at 66 Ma (Table 3.5; Figure 3.12). However, in contrast to the Duvernay petroleum system oil Os_i and shale Os_g values, the Os_g values of the other oil-prone strata of the WCSB are distinctly more radiogenic (e.g., the Gordondale Member of the Early Jurassic Fernie Formation (Selby et al., 2007; Finlay et al., 2012) has Os_g values are between 0.99 and 4.06, with an arithmetic average and median of 2.04 and 1.51; the Devonian-Mississippian Exshaw Formation (Creaser et al., 2002; Selby and Creaser, 2003; Finlay et al., 2012) has Os_g values between 1.35 and 4.96 with an arithmetic average and median of 2.22 and 1.93; the Middle Devonian Keg River Formation (Miller, 2004) laminates of La Crete basin have Os_g values between 1.34 and 4.25, with an arithmetic average and median of 1.97 and 1.64). The exceptions to the latter are the Os_g values of the kukersites of the Ordovician Yeoman Formation, Williston basin (Miller, 2004), which are between 0.46 and 5.36, with an arithmetic average and median of 1.21 and 0.84. The Ordovician kukersites Os_g values are only slightly more radiogenic than the Duvernay petroleum system oil Os_i and shale Os_g values, however, it can be spatially (eastern Montana - western North Dakota and southern Saskatchewan versus south-central Alberta) excluded as the source of the Duvernay oils (Creaney et al., 1994). The Os_i and Os_g data, coupled with the organic geochemistry, support

the Duvernay Formation as the key source unit of the Duvernay oils, and eliminate the other oil-prone Phanerozoic strata of the WCSB as sources of the Duvernay petroleum system.

Although we show a strong similarity between the Os_i and Os_g values for the Duvernay oils and Formation, we observe that the Os_g values in the cores studied here and the oil Os_i values show some heterogeneity (Figures 3.5 - 3.7). If we consider each core separately, the average Os_g values are nominally skewed either positively or negatively to the overall average of the Os_g values (0.83 ± 0.01; Figure 3.11; Table 3.2). For example, the Tukey's Biweight average of Os_g values for core 10-27-57-21W4 is 0.72 ± 0.12, for core 12-6-47-4W5 it is 0.90 ± 0.17, for core 14-29-48-6W5 it is 0.96 ± 0.07, and for core 16-18-52-5W5 the arithmetic average is 0.66 ± 0.22 (2 SD; weighted by assigned/internal errors only as Tukey's Biweight average is not suitable for its small sample set).

The change in the $^{187}Os/^{188}Os$ composition from the time of source rock deposition to the time of oil generation is dependent on the duration between deposition and hydrocarbon maturation, and the Re abundance in the source rock. Variability in the Re abundance stratigraphically, plus the variations in local seawater $^{187}Os/^{188}Os$ values inherited by the organic-rich rock, such as that shown by the Duvernay Formation (Table 3.2), results in heterogeneous $^{187}Os/^{188}Os$ values with ^{187}Re decay (Table 3.2; Figures 3.7 and 3.11).

As such, if the heterogeneous Os_g is inherited by the generated oils then our data propose that the oil generated from different geographical sections of the same source interval could lead to reservoired oils possessing variable Os_i. The primary migration and expulsion of oil within and from a source rock, which is often broadly contemporaneous with or occurs shortly after oil generation, could result in the homogenization of the $^{187}Os/^{188}Os$ values of oil. Although, the extent of homogenization should depend on many factors (e.g. permeability of source rock and carrier beds). In the case of the Duvernay Formation, the oils generated could possess a range in Os_i from 0.46 to 1.48, which is similar to what is observed in this study with the Duvernay oil Os_i values, ranging from ~0.55 to 1.06 (Tables 3.2 - 3.3; Figures 3.5 - 3.7). The variability in the Os_i values makes it analytically challenging to obtain a precise isochron (66 ± 31 Ma). The determined Os_i by the isochron (0.77

± 0.20) demonstrates the variability in the Os_i values. As such, if we select the samples with the most similar Os_i (e.g., L00864, L00873, L02196, L02220 and L02221), a Re-Os date of 56 ± 18 Ma is obtained, with an Os_i of 0.74 ± 0.10 and MSWD of 0.33. The Re-Os date still coincides with the timing of hydrocarbon maturation associated with the Laramide orogeny, but is almost 50% more precise.

3.5.3 Oil Re-Os systematics: effect of oil-water contact

Although we propose that the Re and Os in oil are inherited from a source rock, based on the similarity of the Os_i values of the asphaltene fractions and the Os_g values of the Duvernay Formation shales, an experimental study has suggested that Re and Os in oil can also be derived from contact with formation water (Mahdaoui et al., 2015). The outcome of this experimental work has recently been questioned (Wu et al., 2016), particularly based on the several orders of magnitude higher Re and Os concentrations applied in the experiment (1 ng/g to 100 ug/g Re and 1 or 10 ng/g) compared with the known low Re and Os concentrations of basin fluids (typically 4 pg/g Re and 70 fg/g Os; Mahdaoui et al. (2015) and references therein) in most oil-bearing sedimentary basins. Nevertheless, we consider here if the oil Re-Os systematics may have been affected by or originated from the basin fluids in the Leduc reef trend and Nisku Formation. There are very limited Re and Os data for basin fluids available at present and if we also use the typical formation water Re and Os abundances of 4 pg/g and 70 fg/g, respectively (Mahdaoui et al., 2015), approximately 2 to 40 g of such water contains equivalent Re and Os in 1 gram of Duvernay oil (Table 3.3). Such oil-water contact ratios are highly probable in a petroleum system (Magoon and Dow, 1991). As such, based on the experiments of Mahdaoui et al. (2015), the Re-Os systematics of the low Re- and Os-bearing Duvernay oils could have been easily influenced by oil-basin fluid interaction and reflect the Os isotopic composition of the basin fluid. However, comparing the $^{87}Sr/^{86}Sr$ values of Late Devonian seawater of 0.7080 - 0.7084 (Burke et al., 1982) with the $^{87}Sr/^{86}Sr$ values of calcites and dolomite cements (0.7088 - 0.7108) of the Leduc Rimbey-Meadowbrook reef trend (Stasiuk, 1997), and that of the brines of Nisku Formation (0.70998-0.71206) and Leduc Formation (0.70872 - 0.70981) (Connolly et al., 1990), it is suggested that the basin fluids could have interacted with the radiogenic crystalline basement and/or Proterozoic/Lower Cambrian clastics

(Mountjoy et al., 1999). As such, the $^{187}Os/^{188}Os$ compositions of the basin fluids should be radiogenic, considering the high $^{187}Os/^{188}Os$ initial values of these strata (Kendall et al., 2009) and the long duration between the depositional age and the timing of oil generation. For example, the Neoproterozoic Old Fort Point Formation has an initial $^{187}Os/^{188}Os$ value of ~ 0.62 at deposition of 608 Ma (Kendall et al., 2004), which will have radiogenically evolved to $^{187}Os/^{188}Os$ values >3 at 66 Ma (Table 3.5). Further, considering a lower end member $^{187}Re/^{188}Os$ value of 100 for the crystalline basement/Proterozoic/Lower Cambrian strata and an initial $^{187}Os/^{188}Os$ composition of 0.5, the decay of ^{187}Re over ≥450 million years will yield a $^{187}Os/^{188}Os$ value > 1.25 at the time that the Duvernay Formation underwent thermal maturation. These $^{187}Os/^{188}Os$ values are, even at this very low estimate, more radiogenic compared to the Duvernay oil Os_i values (0.77 ± 0.20). As a result, we propose that the predominant Re and Os budget and the isotope systematics of the Duvernay oil represent that inherited from the Duvernay Formation source rocks during thermal maturation, and not Re and Os sequestered from basin fluids. And therefore the Os_i values are inherited at the time of oil generation, and are ultimately linked to the source rock rather than formation fluids.

3.6 Conclusions

Despite the uncertainty of Re-Os asphaltene isotopic data of the Duvernay oils, which is a direct result of the low Re and Os abundance, limited range in the $^{187}Re/^{188}Os$ values, and variation in the Os_i values of the asphaltene, the Re-Os age derived from asphaltene fractions agrees well with the widely accepted burial and hydrocarbon maturation models that indicate that hydrocarbon generation occurred long after source rock deposition during the Laramide orogeny. Further, the similarity between the oil Os_i values and the Duvernay Formation Os_g values, and their difference to other oil-prone strata of the WCSB, coupled with the evidence from organic geochemistry, confirms the Duvernay Formation as the source and the ability of the $^{187}Os/^{188}Os$ composition as an oil-source correlation tool. Moreover, the Duvernay-sourced oils Re-Os systematics are not considered to have been significantly affected by basin fluids, indicating that the majority of Re-Os systematics in the oil (asphaltene fraction) is inherited from its source.

We suggest that one of the major factors controlling the precision of a Re-Os date for oil relates to the variation in Os_i values inherited by an oil from its source at the time of oil generation, which is independent of the radiogenic evolution of the $^{187}Os/^{188}Os$ composition in the source rock. For example, the relative homogeneous $^{187}Os/^{188}Os$ of Duvernay Formation at the time of deposition (Os_i = ~0.33) evolved with time to a heterogeneous $^{187}Os/^{188}Os$ composition due to the variable Re abundance in the source unit. The heterogeneous $^{187}Os/^{188}Os$ composition of the Duvernay Formation was inherited by the generated oil. Our data suggests that basin wide homogenization of the Os isotopic composition did not occur during migration.

The agreement of the Re-Os asphaltene date, coupled with the similarity of the Os_i and Os_g values of the asphaltene and Duvernay Formation, respectively, of the relatively simple Duvernay petroleum system of Western Canada sedimentary basin with basin models and organic geochemistry confirms the potential ability of the Re-Os oil (asphaltene fraction) systematics to record the timing of hydrocarbon generation, and to serve as an effective oil-source correlation tool.

3.7 References

Adams, J., S. Larter, B. Bennett, H. Huang, J. Westrich, and C. van Kruisdijk, 2013, The dynamic interplay of oil mixing, charge timing, and biodegradation in forming the Alberta oil sands: Insights from geologic modeling and biogeochemistry, in F. J. Hein, D. Leckie, S. Larter, and J. R. Suter, eds., Heavy-oil and oil-sand petroleum systems in Alberta and beyond: AAPG Studies in Geology 64, p. 23–102.

Amthor, J. E., E. W. Mountjoy, and H. G. Machel, 1994, Regional-scale porosity and permeability variations in Upper Devonian Leduc buildups: Implications for reservoir development and prediction in carbonates: AAPG Bulletin, v. 78, no. 10, p. 1541-1558

Anders, D. E., J. G. Palacas, and R. C. Johnson, 1992, Thermal maturity of rocks and 944 hydrocarbon deposits, Uinta Basin, Utah, in Thomas D. Fouch, Vito F. Nuccio, Thomas C. Chidsey, Jr., eds., Hydrocarbon and mineral resources of the Uinta Basin, Utah and Colorado: Utah Geological Association Guidebook, no. 20, p. 53-74.

Berbesi, L. A., R. di Primio, Z. Anka, B. Horsfield, and D. K. Higley, 2012, Source rock contributions to the Lower Cretaceous heavy oil accumulations in Alberta: A basin modeling study: AAPG Bulletin, v. 96, no. 7, p. 1211-1234.

Burke, W., R. Denison, E. Hetherington, R. Koepnick, H. Nelson, and J. Otto, 1982, Variation of seawater $^{87}Sr/^{86}Sr$ throughout Phanerozoic time: Geology, v. 10, no. 10, p. 516-519.

Bustin, R., 1991, Organic maturity in the Western Canada sedimentary basin: International Journal of Coal Geology, v. 19, no. 1, p. 319-358.

Chow, N., J. Wendte, and L. D. Stasiuk, 1995, Productivity versus preservation controls on two organic-rich carbonate facies in the Devonian of Alberta: Sedimentological and organic petrological evidence: Bulletin of Canadian Petroleum Geology, v. 43, no. 4, p. 433-460.

Cohen, A. S., A. L. Coe, J. M. Bartlett, and C. J. Hawkesworth, 1999, Precise Re–Os ages of organic-rich mudrocks and the Os isotope composition of Jurassic seawater: Earth and Planetary Science Letters, v. 167, no. 3-4, p. 159-173.

Connolly, C. A., L. M. Walter, H. Baadsgaard, and F. J. Longstaffe, 1990, Origin and evolution of formation waters, Alberta basin, Western Canada sedimentary basin. II. Isotope systematics and water mixing: Applied Geochemistry, v. 5, no. 4, p. 397-413.

Creaney, S., and J. Allan, 1990, Hydrocarbon generation and migration in the Western Canada sedimentary basin: Geological Society, London, Special Publications, v. 50, no. 1, p. 189-202.

Creaney, S., 1992, Petroleum Systems in the foreland basin of Western Canada, in R. Macqueen and D. Leckie, eds., Foreland basins and fold belts: AAPG Memoir 55, p. 279-308.

Creaney, S., J. Allan, K. Cole, M. Fowler, P. Brooks, K. Osadetz, R. Macqueen, L. Snowdon, and C. Riediger, 1994, Petroleum generation and migration in the Western Canada sedimentary basin, in G. D. Mossop and I. Shetson, eds., Geological Atlas of the Western Canada sedimentary basin, p. 455-468.

Creaser, R. A., P. Sannigrahi, T. Chacko, and D. Selby, 2002, Further evaluation of the Re-Os geochronometer in organic-rich sedimentary rocks: A test of hydrocarbon maturation effects in the Exshaw Formation, Western Canada

sedimentary basin: Geochimica et Cosmochimica Acta, v. 66, no. 19, p. 3441-3452.

Cumming, V. M., D. Selby, and P. G. Lillis, 2012, Re–Os geochronology of the lacustrine Green River Formation: Insights into direct depositional dating of lacustrine successions, Re–Os systematics and paleocontinental weathering: Earth and Planetary Science Letters, v. 359-360, p. 194-205.

Cumming, V. M., D. Selby, P. G. Lillis, and M. D. Lewan, 2014, Re–Os geochronology and Os isotope fingerprinting of petroleum sourced from a Type I lacustrine kerogen: Insights from the natural Green River petroleum system in the Uinta basin and hydrous pyrolysis experiments: Geochimica et Cosmochimica Acta, v. 138, p. 32-56.

Deroo, G., T. G. Powell, B. Tissot, and R. G. McCrossan, 1977, The origin and migration of petroleum in the Western Canadian sedimentary basin, Alberta - A geochemical and thermal maturation study: Geological Survey of Canada Bulletin 262, 136 p.

Dunn, L., G. Schmidt, K. Hammermaster, M. Brown, R. Bernard, E. Wen, R. Befus, and S. Gardiner, 2012, The Duvernay Formation (Devonian): Sedimentology and reservoir characterization of a shale gas/liquids play in Alberta, Canada (abs.), in Proceedings Canadian Society of Petroleum Geologists: Annual Convention, Calgary.

Eadington, P., P. Hamilton, and G. Bai, 1991, Fluid history analysis - A new concept for prospect evaluation: Australian Petroleum Exploration Association Journal, v. 31, no. 1, p. 282-294.

Evans, C. R., M. A. Rogers, and N. J. L. Bailey, 1971, Evolution and alteration of petroleum in Western Canada: Chemical Geology, v. 8, no. 3, p. 147-170.

Finlay, A. J., D. Selby, M. J. Osborne, and D. Finucane, 2010, Fault-charged mantle-fluid contamination of United Kingdom North Sea oils: Insights from Re-Os isotopes: Geology, v. 38, no. 11, p. 979-982.

Finlay, A. J., D. Selby, and M. J. Osborne, 2011, Re-Os geochronology and fingerprinting of United Kingdom Atlantic Margin oil: Temporal implications for regional petroleum systems: Geology, v. 39, no. 5, p. 475-478.

Finlay, A. J., D. Selby, and M. J. Osborne, 2012, Petroleum source rock identification of United Kingdom Atlantic Margin oil fields and the Western Canadian Oil Sands using Platinum, Palladium, Osmium and Rhenium: Implications for global petroleum systems: Earth and Planetary Science Letters, v. 313-314, p. 95-104.

Fothergill, P. A., D. Boskovic, P. Murphy, M. Mukati, and N. Schoellkopf, 2014, Regional Modelling of the Late Devonian Duvernay Formation, Western Alberta, Canada: Unconventional Resources Technology Conference (URTEC), p. 95-102.

Fowler, M. G., L. D. Stasiuk, M. Hearn, and M. Obermajer, 2001, Devonian hydrocarbon source rocks and their derived oils in the Western Canada sedimentary basin: Bulletin of Canadian Petroleum Geology, v. 49, no. 1, p. 117-148.

Fowler, M. G., M. Obermajer, and L. D. Stasiuk, 2003, Rock-Eval/TOC data for Devonian potential source rocks, Western Canada sedimentary basin: Geological Survey of Canada Open File 1579.

Ge, X., C. Shen, D. Selby, D. Deng, and L. Mei, 2016, Apatite fission-track and Re-Os geochronology of the Xuefeng uplift, China: Temporal implications for dry gas associated hydrocarbon systems: Geology, v. 44, no. 6, p. 491-494.

Ge, X., C. Shen, D. Selby, J. Wang, L. Ma, X. Ruan, S. Hu, L. Mei, 2017, Petroleum generation timing and source in the Northern Longmen Shan Thrust Belt, Southwest China: Implications for multiple oil generation episodes and sources: AAPG Bulletin, in press

Georgiev, S. V., H. J. Stein, J. L. Hannah, R. Galimberti, M. Nali, G. Yang, and A. Zimmerman, 2016, Re-Os dating of maltenes and asphaltenes within single samples of crude oil: Geochimica et Cosmochimica Acta, v. 179, p. 53-75.

Gramlich, J. W., T. J. Murphy, E. L. Garner, and W. R. Shields, 1973, Absolute isotopic abundance ratio and atomic weight of a reference sample of rhenium: Journal of Research of the National Bureau of Standards – A. Physics and Chemistry, v. 77A, no. 6, p. 691–698.

Harris, S. A., M. J. Whiticar, and M. G. Fowler, 2003, Classification of Duvernay sourced oils from central and southern Alberta using Compound Specific Isotope Correlation (CSIC): Bulletin of Canadian Petroleum Geology, v. 51, no. 2, p. 99-125.

Higley, D. K., M. Henry, L. N. R. Roberts, and D. W. Steinshouer, 2005, 1-D/3-D geologic model of the Western Canada sedimentary basin: The Mountain Geologist, v. 42, no. 2, p. 53-66.

Higley, D. K., M. D. Lewan, L. N. R. Roberts, and M. Henry, 2009, Timing and petroleum sources for the Lower Cretaceous Mannville Group oil sands of northern Alberta based on 4-D modeling: AAPG Bulletin, v. 93, no. 2, p. 203-230.

Issler, D. R., S. D. Willett, C. Beaumont, R. A. Donelick, and A. M. Grist, 1999, Paleotemperature history of two transects across the Western Canada sedimentary basin: Constraints from apatite fission track analysis: Bulletin of Canadian Petroleum Geology, v. 47, no. 4, p. 475-486.

Jenden, P. D., and F. Monnier, 1997, Regional variations in initial petroleum potential of the Upper Devonian Duvernay and Muskwa formations, Central Alberta (abs.): Canadian Society of Petroleum Geologists - SEPM Joint Convention: Program with Abstracts, Calgary, p. 146

Kelley, S., 2002, K-Ar and Ar-Ar dating: Reviews in Mineralogy and Geochemistry, v. 47, no. 1, p. 785-818.

Kendall, B. S., R. A. Creaser, G. M. Ross, and D. Selby, 2004, Constraints on the timing of Marinoan "Snowball Earth" glaciation by ^{187}Re–^{187}Os dating of a Neoproterozoic, post-glacial black shale in Western Canada: Earth and Planetary Science Letters, v. 222, no. 3-4, p. 729-740.

Kendall, B., R. A. Creaser, and D. Selby, 2009, ^{187}Re-^{187}Os geochronology of Precambrian organic-rich sedimentary rocks: Geological Society, London, Special Publications, v. 326, no. 1, p. 85-107.

Lamers, E., and S. M. M. Carmichael, 1999, The Paleocene deepwater sandstone play West of Shetland: Geological Society of London, Petroleum Geology Conference series, v. 5, p. 645-659.

Li, M., H. Yao, M. G. Fowler, and L. D. Stasiuk, 1998, Geochemical constraints on models for secondary petroleum migration along the Upper Devonian Rimbey-Meadowbrook reef trend in central Alberta, Canada: Organic Geochemistry, v. 29, no. 1-3, p. 163-182.

Lillis, P. G., and D. Selby, 2013, Evaluation of the rhenium–osmium geochronometer in the Phosphoria petroleum system, Bighorn basin of Wyoming and Montana, USA: Geochimica et Cosmochimica Acta, v. 118, p. 312-330.

Ludwig, K., 2012, User's manual for Isoplot version 3.75-4.15: a geochronological toolkit for Microsoft: Excel Berkley Geochronological Center Special Publication, no. 5.

Magoon, L., and W. Dow, 1991, The petroleum system - From source to trap: AAPG Bulletin, v. 75, no.3, p. 627.

Mahdaoui, F., R. Michels, L. Reisberg, M. Pujol, and Y. Poirier, 2015, Behavior of Re and Os during contact between an aqueous solution and oil: Consequences for the application of the Re–Os geochronometer to petroleum: Geochimica et Cosmochimica Acta, v. 158, p. 1-21.

Mark, D. F., J. Parnell, S. P. Kelley, M. Lee, S. C. Sherlock, and A. Carr, 2005, Dating of multistage fluid flow in sandstones: Science, v. 309, no. 5743, p. 2048-2051.

Mark, D. F., J. Parnell, S. P. Kelley, M. R. Lee, and S. C. Sherlock, 2010, $^{40}Ar/^{39}Ar$ dating of oil generation and migration at complex continental margins: Geology, v. 38, no. 1, p. 75-78.

Marquez, X., 1994, Reservoir geology of Upper Devonian Leduc buildups, deep Alberta basin: Ph. D. Dissertation, McGill University, Montreal, Canada, 285 p.

McLean, R. A., and G. Klapper, 1998, Biostratigraphy of Frasnian (Upper Devonian) strata in western Canada, based on conodonts and rugose corals: Bulletin of Canadian Petroleum Geology, v. 46, no. 4, p. 515-563.

Miller, C. A., 2004, Re-Os dating of algal laminites reduction-enrichment of metals in the sedimentary environment and evidence for new geoporphyrins: Master of Science Dissertation, University of Saskatchewan, Saskatoon, Canada, 153 p.

Mountjoy, E. W., H. G. Machel, D. Green, J. Duggan, and A. E. Williams-Jones, 1999, Devonian matrix dolomites and deep burial carbonate cements: a comparison between the Rimbey-Meadowbrook reef trend and the deep basin of west-central Alberta: Bulletin of Canadian Petroleum Geology, v. 47, no. 4, p. 487-509.

Nowell, G., A. Luguet, D. Pearson, and M. Horstwood, 2008, Precise and accurate $^{186}Os/^{188}Os$ and $^{187}Os/^{188}Os$ measurements by multi-collector plasma ionisation mass spectrometry (MC-ICP-MS) part I: Solution analyses: Chemical Geology, v. 248, no. 3, p. 363-393.

Ogg, J., G. Ogg, and F. M. Gradstein, 2016, A Concise Geologic Time Scale 2016, Amsterdam, Elsevier, 242 p.

Peters, K. E., C. C. Walters, and J. M. Moldowan, 2005, The biomarker guide, volume 2 - Biomarkers and isotopes in petroleum exploration and earth history: Cambridge: Cambridge University Press, v. 475, 634 p.

Riediger, C. L., S. Ness, M. Fowler, and N. T. Akpulat, 2001, Timing of oil generation and migration, northeastern British Columbia and southern Alberta - Significance for understanding the development of the eastern Alberta tar sands deposits (abs.): AAPG Annual Convention Official Program, v. 10, p. A168.

Rogers, M. A., J. McAlary, and N. Bailey, 1974, Significance of reservoir bitumens to thermal-maturation studies, Western Canada basin: AAPG Bulletin, v. 58, no. 9, p. 1806-1824.

Rooney, A. D., D. M. Chew, and D. Selby, 2011, Re–Os geochronology of the Neoproterozoic–Cambrian Dalradian Supergroup of Scotland and Ireland: Implications for Neoproterozoic stratigraphy, glaciations and Re–Os systematics: Precambrian Research, v. 185, no. 3-4, p. 202-214.

Rooney, A. D., D. Selby, M. D. Lewan, P. G. Lillis, and J. P. Houzay, 2012, Evaluating Re–Os systematics in organic-rich sedimentary rocks in response to petroleum generation using hydrous pyrolysis experiments: Geochimica et Cosmochimica Acta, v. 77, p. 275-291.

Rostron, B. J., 1997, Fluid flow, hydrochemistry and petroleum entrapment in Devonian reef complexes, south-central Alberta, Canada. in S.G. Pemberton and D.P. James eds., Petroleum Geology of the Cretaceous Mannville Group: Canadian Society of Petroleum Geologists Memoir 18, Calgary, p. 169-190.

Ruble, T. E., M. Lewan, and R. Philp, 2001, New insights on the Green River petroleum system in the Uinta basin from hydrous pyrolysis experiments: AAPG bulletin, v. 85, no. 8, p. 1333-1371.

Selby, D., and R. A. Creaser, 2001, Re-Os geochronology and systematics in molybdenite from the Endako porphyry molybdenum deposit, British Columbia, Canada: Economic Geology, v. 96, no. 1, p. 197-204.

Selby, D., and R. A. Creaser, 2003, Re–Os geochronology of organic rich sediments: an evaluation of organic matter analysis methods: Chemical Geology, v. 200, no. 3-4, p. 225-240.

Selby, D., and R. A. Creaser, 2005a, Direct radiometric dating of hydrocarbon deposits using rhenium-osmium isotopes: Science, v. 308, no. 5726, p. 1293-1295.

Selby, D., and R. A. Creaser, 2005b, Direct radiometric dating of the Devonian-Mississippian time-scale boundary using the Re-Os black shale geochronometer: Geology, v. 33, no. 7, p. 545-548.

Selby, D., R. Creaser, K. Dewing, and M. Fowler, 2005, Evaluation of bitumen as a Re–Os geochronometer for hydrocarbon maturation and migration: A test case from the Polaris MVT deposit, Canada: Earth and Planetary Science Letters, v. 235, no. 1-2, p. 1-15.

Selby, D., 2007, Direct Rhenium-Osmium age of the Oxfordian-Kimmeridgian boundary, Staffin bay, Isle of Skye, UK, and the Late Jurassic time scale: Norwegian Journal of Geology, v. 87, no. 3, p. 291-299.

Selby, D., R. A. Creaser, and M. G. Fowler, 2007, Re–Os elemental and isotopic systematics in crude oils: Geochimica et Cosmochimica Acta, v. 71, no. 2, p. 378-386.

Simpson, G. P., 1999, Sulfate reduction and fluid chemistry of the Devonian Leduc and Nisku formations in south-central Alberta: Ph. D. Dissertation, University of Calgary, Canada, 228 p.

Smoliar, M. I., R. J. Walker, and J. W. Morgan, 1996, Re-Os ages of group IIA, IIIA, IVA, and IVB iron meteorites: Science, v. 271, no. 5252, p. 1099.

Speight, J., 2004, Petroleum Asphaltenes-Part 1: Asphaltenes, resins and the structure of petroleum: Oil & Gas Science and Technology, v. 59, no. 5, p. 467-477.

Stasiuk, L. D., 1997, The origin of pyrobitumens in upper Devonian Leduc formation gas reservoirs, Alberta, Canada: An optical and EDS study of oil to

gas transformation: Marine and Petroleum Geology, v. 14, no. 7-8, p. 915-929.

Stasiuk, L. D., and M. Fowler, 2002, Thermal maturity evaluation (vitrinite and vitrinite reflectance equivalent) of Middle Devonian, Upper Devonian and Devonian-Mississippian strata in the Western Canada Sedimentary basin: Geological Survey of Canada Open File Report 4341, 20 p.

Stoakes, F., and S. Creaney, 1984, Sedimentology of a carbonate source rock: the Duvernay Formation of Central Alberta, in L. Eliuk, eds., Carbonates in subsurface and outcrop: Canadian Society of Petroleum Geologists Core Conference, p. 132-147.

Stoakes, F., and S. Creaney, 1985, Controls on the accumulation and subsequent maturation and migration history of a carbonate source rock. Society of Economic Paleontologists and Mineralogists, in Proceedings SEPM Core Workshop Proceedings, Golden, Colorado, p. 343-375.

Switzer, S., W. Holland, D. Christie, G. Graf, A. Hedinger, R. McAuley, R. Wierzbicki, and J. Packard, 1994, Devonian Woodbend-Winterburn strata of the Western Canada sedimentary basin: Geological Atlas of the Western Canada sedimentary basin: Canadian Society of Petroleum Geologists and Alberta Research Council, p. 165-202.

Tozer, R. S., A. P. Choi, J. T. Pietras, and D. J. Tanasichuk, 2014, Athabasca oil sands: Megatrap restoration and charge timing: AAPG Bulletin, v. 98, no. 3, p. 429-447.

Völkening, J., T. Walczyk, and K.G. Heumann, 1991, Osmium isotope ratio determination by negative thermal ion mass spectrometry: International Journal of Mass Spectrometry and Ion Processes, v. 105, no. 2, p. 147–159.

Welte, D. H., B. Horsfield, and D. R. Baker, 2012, Petroleum and basin evolution: insights from petroleum geochemistry, geology and basin modeling: Berlin Heidelberg, Springer, 535 p.

Wenger, L. M., C. L. Davis, and G. H. Isaksen, 2001, Multiple controls on petroleum biodegradation and impact on oil quality: Proceedings SPE Annual Technical Conference and Exhibition, 14 p.

Whalen, M. T., G. P. Eberli, F. S. van Buchem, E. W. Mountjoy, and P. W. Homewood, 2000, Bypass margins, basin-restricted wedges, and platform-to-basin correlation, Upper Devonian, Canadian Rocky Mountains: implications for sequence stratigraphy of carbonate platform systems: Journal of Sedimentary Research, v. 70, no. 4, p. 913-936.

Wu, J., Z. Li, and X. C. Wang, 2016, Comment on “Behavior of Re and Os during contact between an aqueous solution and oil: Consequences for the application of the Re–Os geochronometer to petroleum” by Mahdaoui et al. (2015): Geochimica et Cosmochimica Acta, v. 186, p. 344-347.

Ziegler, W., and C. A. Sandberg, 1990, The Late Devonian standard conodont zonation: Courier Forschungsinstitut Senckenberg, v. 121, 115 p.

Table 3.1 Well locations and reservoir formations of the oil samples of this study.

Sample	Well	Latitude	Longitude	Depth (m)	Formation
L00864	14-35-48-27W4	53.19	-113.85	1920.0-1923.9	Leduc
L00873	10-9-48-27W4	53.13	-113.89	1781.9-1783.4	Nisku
L01558	01-3-37-20W4	52.15	-112.77	1604.8-1622.1	Nisku
L01810	12-11-49-12W5	53.21	-115.66	2997-3069	Nisku
L01827	11-14-42-2W5	52.62	-114.18	2373-2387	Leduc
L01831	8-35-48-12W5	53.18	-115.64	3059-3086	Nisku
L02037	16-16-41-2W5	52.54	-114.22	2431-2442	Nisku
L02083	12-13-41-23W4	52.53	-113.19	1742-1743	Nisku
L02155	10-31-39-23W4	52.4	-113.3	1781.3	Nisku
L02196	9-11-33-26W4	51.81	-113.59	2497.8	Leduc
L02197	9-14-33-26W4	51.83	-113.58	2202	Nisku
L02203	10-28-42-23W4	52.65	-113.25	1720	Nisku
L02220	11-35-36-20W4	52.14	-112.76	1606.3	Nisku
L02221	7-23-36-20W4	52.1	-112.75	1569.7-1617.9	Leduc/Nisku
L02225	15-22-38-20W4	52.29	-112.78	1563.6-1645.9	Leduc
L02226	12-10-38-20W4	52.25	-112.79	1569.7-1624.6	Leduc
L01822	2-27-37-20W4	52.2	-112.78	1599-1603	Leduc

Table 3.2 Re-Os data synopsis for the Duvernay Formation shale samples from multiple locations (wells) and their Os_i (378.5 Ma) and Os_g (66 Ma) values.

Sample	Depth (m)	Re (ppb)	±	Os (ppt)	±	^{192}Os (ppt)	±	$^{187}Re/^{188}Os$	±	$^{187}Os/^{188}Os$	±	rho	Os_i [a]	±	Os_g [b]	±
10-27-57-21W4		*53.96°N*		*113.03°W*												
DS18-12	1106	5.84	0.02	631.2	2.2	244.5	1.0	47.5	0.2	0.633	0.004	0.590	0.33	0.01	0.58	0.01
DS20-12	1124.5	14.37	0.04	1245.3	4.8	478.7	2.2	59.7	0.3	0.693	0.005	0.604	0.32	0.01	0.63	0.01
DS22-12	1128.45	13.23	0.04	1299.2	5.1	500.7	2.4	52.5	0.3	0.673	0.005	0.600	0.34	0.01	0.62	0.01
DS24-12	1139.7	12.36	0.04	1121.1	4.4	431.3	2.1	57.0	0.3	0.687	0.005	0.600	0.33	0.01	0.62	0.01
DS26-12	1144	16.86	0.05	947.8	3.8	355.5	1.5	94.4	0.5	0.899	0.005	0.598	0.30	0.01	0.80	0.01
DS28-12	1146.5	14.68	0.04	1392.9	5.2	537.7	2.4	54.3	0.3	0.659	0.004	0.598	0.32	0.01	0.60	0.01
DS30-12	1151	26.33	0.07	1965.2	6.9	751.1	2.9	69.8	0.3	0.742	0.004	0.584	0.30	0.01	0.67	0.01
DS32-12	1154	24.15	0.06	1537.6	5.6	579.5	2.2	82.9	0.4	0.859	0.005	0.582	0.34	0.01	0.77	0.01
DS34-12	1159.5	10.91	0.03	397.1	2.0	142.7	0.7	152.0	0.9	1.267	0.009	0.608	0.31	0.02	1.10	0.01
DS36-12	1161.25	25.43	0.07	1188.0	4.7	436.5	1.7	115.9	0.5	1.074	0.006	0.582	0.34	0.01	0.95	0.01
16-18-52-5W5		*53.5°N*		*114.72°W*												
DS1-12	2343	0.31	0.01	58.8	2.1	23.2	1.9	26.3	2.2	0.488	0.055	0.687	0.32	0.07	0.46	0.06
DS3-12	2343.5	1.25	0.01	242.5	2.5	95.6	1.9	26.0	0.5	0.491	0.014	0.683	0.33	0.02	0.46	0.02

To be continued.

Continue:

Sample	Depth (m)	Re (ppb)	±	Os (ppt)	±	^{192}Os (ppt)	±	^{187}Re/^{188}Os	±	^{187}Os/^{188}Os	±	rho	Os_i [a]	±	Os_g [b]	±
DS5-12	2344	2.03	0.01	178.1	1.3	68.5	0.8	58.9	0.7	0.693	0.012	0.671	0.32	0.02	0.63	0.01
DS7-12	2344.5	4.03	0.01	248.0	1.3	93.4	0.7	85.8	0.7	0.862	0.009	0.657	0.32	0.01	0.77	0.01
14-29-48-6W5		*53.18°N*		*114.84°W*												
DS9-12	2646.6	48.46	0.14	1370.7	8.2	474.1	2.9	203.3	1.4	1.611	0.014	0.646	0.32	0.02	1.39	0.02
DS11-12	2648.6	8.75	0.03	362.4	1.9	132.7	0.8	131.3	0.9	1.107	0.010	0.622	0.28	0.02	0.96	0.01
DS13-12	2650.6	10.82	0.03	482.0	2.3	176.0	0.9	122.3	0.7	1.129	0.008	0.609	0.36	0.01	0.99	0.01
DS15-12	2652.6	21.94	0.06	1827.3	6.6	700.6	2.8	62.3	0.3	0.716	0.004	0.576	0.32	0.01	0.65	0.01
DS17-12	2654.6	36.35	0.09	1726.5	8.7	636.2	3.4	113.7	0.7	1.050	0.009	0.589	0.33	0.01	0.93	0.01
2-6-47-4W5		*53.02°N*		*114.57°W*												
DS37-12	2629	0.53	0.01	29.0	1.0	10.8	0.9	98.2	8.0	0.94	0.11	0.701	0.32	0.16	0.83	0.12
DS38-12	2631	0.40	0.01	30.7	0.7	11.7	0.6	68.2	3.6	0.792	0.056	0.677	0.36	0.08	0.72	0.06
DS39-12	2633	1.36	0.01	62.2	0.9	22.8	0.6	118.5	3.2	1.110	0.042	0.694	0.36	0.06	0.98	0.05
DS40-12	2635	41.52	0.14	1218.3	4.2	423.1	1.0	195.2	0.8	1.575	0.005	0.403	0.34	0.01	1.36	0.01
DS41-12	2637	67.56	0.22	1721.5	7.0	587.5	1.7	228.8	1.0	1.736	0.007	0.476	0.29	0.01	1.48	0.01
DS42-12	2639	13.07	0.04	900.4	2.9	340.3	1.1	76.4	0.3	0.836	0.004	0.486	0.35	0.01	0.75	0.01

To be continued.

Continue:

Sample	Depth (m)	Re (ppb)	±	Os (ppt)	±	^{192}Os (ppt)	±	^{187}Re/^{188}Os	±	^{187}Os/^{188}Os	±	rho	Os_i [a]	±	Os_g [b]	±
DS43-12	2641	11.27	0.04	746.9	3.7	282.3	1.8	79.4	0.6	0.835	0.007	0.620	0.33	0.01	0.75	0.01
DS44-12	2643	5.99	0.02	430.7	1.8	163.0	0.8	73.1	0.4	0.823	0.006	0.576	0.36	0.01	0.74	0.01
DS45-12	2645	8.74	0.03	598.6	3.5	226.1	1.8	76.9	0.7	0.841	0.010	0.648	0.35	0.01	0.76	0.01
DS46-12	2647	28.75	0.09	1707.7	5.7	639.0	2.0	89.5	0.4	0.919	0.004	0.482	0.35	0.01	0.82	0.01
DS47-12	2649	41.79	0.14	1774.0	8.1	649.0	3.1	128.1	0.7	1.112	0.008	0.581	0.30	0.01	0.97	0.01
2-12-50-26W4		*53.30°N*		*113.67°W*		*Finlay et al. (2012)*										
DS44-03	1751.6	7.41	0.03	383	2	140	1	104.4	0.6	1.037	0.006	0.800	0.38	0.01	0.92	0.01
8-35-31-25W4		*51.70°N*		*113.43°W*		*Finlay et al. (2012)*										
DS69-03	2340.9	11.55	0.04	569	2	208	1	109.5	0.5	1.036	0.004	0.800	0.34	0.01	0.92	0.01
1-28-36-3W5		*52.20°N*		*114.36°W*		*Selby et al. (2007)*										
DS45-03-1-4	3013.1	8.10	0.03	219.6	1.2	75.3	0.4	214.1	1.2	1.689	0.012	0.542	0.34	0.02	1.45	0.01

[a] Os_i = initial ^{187}Os/^{188}Os ratio of shales during deposition which is calculated at 378.5 Ma (see text for discussion);

[b] Os_g = ^{187}Os/^{188}Os ratio of shales at oil generation calculated at 66 Ma (see text for discussion).

Table 3.3 Re-Os data synopsis for asphaltene fractions of the oil samples from the Duvernay petroleum system and their Os_i (66 Ma) values.

Sample	Asphaltene	Re (ppb)	±	Os (ppt)	±	^{192}Os (ppt)	±	^{187}Re/^{188}Os	±	^{187}Os/^{188}Os	±	rho	Os_i [a]	±
L00864	1.61%	0.12	0.07	9.4	0.5	3.6	0.5	66.8	37.1	0.78	0.11	0.211	0.70	0.15
L00864rpt	1.16%	0.13	0.05	8.2	0.4	3.0	0.3	84.9	31.1	0.98	0.12	0.270	0.89	0.15
L00864rpt2	1.81%	0.12	0.04	7.4	0.4	2.7	0.4	84.1	32.0	1.04	0.16	0.291	0.94	0.20
L00873	5.65%	0.42	0.03	8.8	0.3	3.3	0.2	256.1	26.1	1.01	0.09	0.621	0.72	0.12
L01558	3.60%	1.42	0.03	20.4	0.5	7.6	0.4	371.1	20.0	0.97	0.06	0.698	0.56	0.09
L02083	2.46%	1.26	0.04	11.2	0.4	3.9	0.3	641.6	51.8	1.52	0.13	0.814	0.82	0.19
L02155	1.45%	0.32	0.04	3.6	0.3	1.2	0.3	511.4	131.1	1.62	0.37	0.844	1.06	0.52
L02196	0.25%	0.04	0.00	0.6	0.1	0.2	0.1	351.4	81.0	1.10	0.28	0.918	0.72	0.36
L02203	1.39%	0.26	0.00	4.6	0.5	1.7	0.5	298.8	85.4	0.88	0.27	0.919	0.55	0.37
L02220	3.00%	1.41	0.03	19.1	0.5	7.0	0.4	400.4	22.9	1.10	0.07	0.712	0.66	0.10
L02221 [b]	14.10%	3.78	0.04	41.2	1.6	14.9	1.2	504.7	42.3	1.21	0.14	0.712	0.65	0.19
L02225 [b]	6.75%	0.51	0.04	6.4	0.4	2.3	0.3	442.6	74.5	1.28	0.22	0.760	0.80	0.30
L02226 [b]	5.84%	1.11	0.05	12.0	0.6	4.2	0.5	524.6	68.6	1.48	0.22	0.766	0.90	0.29
L01822 [c]	14.50%	2.03	0.07	25.3	1.6	8.8	0.6	457.1	72.3	1.49	0.24	0.500	0.99	0.32

To be continued.

Continue:

Sample	Asphaltene	Re (ppb)	±	Os (ppt)	±	^{192}Os (ppt)	±	^{187}Re/^{188}Os	±	^{187}Os/^{188}Os	±	rho	Os_i [a]	±
Data not applied on isochron														
L01810	0.35%	0.04	0.11	1.0	0.8			218.2	705.6	0.63	1.33	0.54		
L01831	0.52%	0.01	0.11	23.3	1.0			2.0	25.1	1.11	0.12	0.01		
L02196rpt	0.78%	0.02	0.05	0.6	0.4			210.4	562.6	0.52	0.92	0.51		
L02037	0.28%	0.05	0.17	-	-			-	-	-	-	-		
L02197	0.27	0.07	0.17	-	-			-	-	-	-	-		

[a] Os_i = initial ^{187}Os/^{188}Os ratios of oil at the timing of generation which are calculated at 66 Ma (see text for discussion);

[b] these samples are asphaltene fractions precipitated by *n*-pentane at the GSC;

[c] data from Selby et al. (2007).

Table 3.4 The compounds represented by the peak annotations in the geochemistry figures (Figures 3.8 - 3.10).

Peak	Compound	Peak	Compound
n-C_5	C_5 n-alkane	C_{26}TT	C_{26} tricyclic terpane
n-C_6	C_6 n-alkane	Ts	18α(H),22,29,30-trisnorhopane (Ts)
MCYC5	methylcyclopentane	Tm	17α(H),22,29,30-trisnorhopane (Tm)
n-C_7	C_7 n-alkane	C_{29}	17α(H),21β(H)-30-norhopane
MCYC6	methylcyclohexane	C_{29}Ts	18α(H),21β(H)-norneohopane
n-C_8	C_8 n-alkane	C_{30}H	17α(H),21β(H)-hopane
Pr	pristane	G	gammacerane
Ph	phytane	C_{34}	17α(H),21β(H)-tetrakishomohopanes
n-C_{15}	C_{15} n-alkane	C_{35}	17α(H),21β(H)-pentakishomohopanes
n-C_{20}	C_{20} n-alkane	C_{21}P	pregnane
n-C_{25}	C_{25} n-alkane	dC_{27}S20S	diacholestane 20S
C_{23}TT	C_{23} tricyclic terpane	dC_{29}S20S	diastigmastane 20S
C_{24}TeT	C_{24} tetracyclic terpane	C_{29}S20R	5α(H),14β(H),17β(H)-stigmastane 20R

Table 3.5 Re-Os data and calculated $^{187}Os/^{188}Os$ composition at 66 Ma for other oil prone strata of the WCSB.

Well	depth (m)	Re (ppb)	Os (ppt)	$^{187}Re/^{188}Os$	$^{187}Os/^{188}Os$	Os_g [a]
Lower Jurassic Gordondale Member *Finlay et al. (2012)*						
7-31-79-10W6	1557	574.9	6.34	550.4	2.116	1.51
14-24-80-7W6	1183.5	369.2	1.86	1674	5.900	4.06
14-24-80-7W6	1190.4	229.9	1.83	885.8	3.655	2.68
8-26-69-7W6	2271.4	195.3	6.13	178.6	1.372	1.18
10-17-84-22W5	2361	196.2	1.12	1352	4.748	3.26
6-29-85-11W5	1148.7	402.6	3.05	933.2	3.716	2.69

Selby et al. (2007) [b] *well 6-32-78-5W6 1218.0–1218.6 m*

Sample	$^{187}Re/^{188}Os$	$^{187}Os/^{188}Os$	Os_g [a]
TS22b.DD.GB	765.25	2.925	2.08
TS23c.DD.GB	432.40	1.914	1.44
TS24b.DD.GB	291.71	1.405	1.08
TS25b.DD.GB	424.18	1.926	1.46
TS26a.DD.GB	182.21	1.186	0.99

To be continued.

Continue:

Devonian-Mississippian Exshaw Formation

Selby and Creaser (2005) 51°05'29''N 115°09'29''W

within ~4 m lateral interval and 10 cm of vertical stratigraphy

Sample	Re (ppb)	Os (ppt)	$^{187}Re/^{188}Os$	$^{187}Os/^{188}Os$	Os_g [a]
DS53	15.6	367.8	253.5	1.948	1.67
DS54	17.5	375.9	283.8	2.141	1.83
DS55A	15.5	341.4	273.7	2.073	1.77
DS55B	16.4	363.5	277.3	2.100	1.80
DS55C	21.2	426.3	306.1	2.265	1.93
DS56	16.4	493.3	190.4	1.570	1.36
DS57	36.0	595.8	391.8	2.787	2.36
DS58A	15.2	458.7	189.3	1.563	1.35
DS58B	16.6	490.6	194.5	1.597	1.38

Selby et al. (2003); Creaser et al. (2002); Finlay et al. (2012)

Well	depth (m)	Re (ppb)	Os (ppb)	$^{187}Re/^{188}Os$	$^{187}Os/^{188}Os$	Os_g [a]
3-19-80-23W5	1752	70.0	0.69	487.1	3.517	2.98
3-19-80-23W5	1753	88.8	1.62	350.7	2.656	2.27
3-19-80-23W5	1754	22.8	0.50	279.8	2.195	1.89
3-19-80-23W5	1756.5	31.7	0.48	441.1	3.220	2.73
13-18-80-23W5	1748.8	47.9	0.64	518.3	3.546	2.98
13-18-80-23W5	1750.9	68.9	1.11	408.9	2.987	2.54
8-29-78-01W6	2099.1	128.6	1.70	538.4	3.806	3.21
8-29-78-01W6	2099.2	20.0	0.69	166.1	1.535	1.35
14-22-80-02W6	2058.3	31.8	0.67	287.5	2.095	1.78
6-19-78-25W5	2006.2	52.0	0.84	405.1	2.885	2.44
4-23-72-10W6	3570.4	31.3	0.29	916.8	5.968	4.96
4-23-72-10W6	3567.7	42.3	0.80	327.8	2.389	2.03

To be continued.

Continue:

Middle Devonian Keg River Formation, La Crete Basin

Miller (2004)

Sample	Re (ppb)	Os (ppb)	$^{187}Re/^{188}Os$	$^{187}Os/^{188}Os$	Os_g [a]
CM-KR-1	50.8	1.24	238	1.775	1.51
CM-KR-2	34.6	0.94	208	1.568	1.34
CM-KR-3	32.8	0.92	204	1.575	1.35
CM-KR-4	20.7	0.47	259	1.920	1.64
CM-KR-5	57.2	0.95	386	2.733	2.31
CM-KR-6	224.2	2.32	757	5.087	4.25
CM-KR-7	26.7	0.67	232	1.754	1.50
CM-KR-I-D	42.4	0.78	336	2.392	2.02
CM-KR-I-E	37.9	0.78	294	2.124	1.80

Ordovician Kukersites, Williston Basin

Miller (2004)

Sample	Re (ppb)	Os (ppb)	$^{187}Re/^{188}Os$	$^{187}Os/^{188}Os$	Os_g [a]
CM-13	2.60	0.085	146	1.608	1.45
CM-14	0.94	0.033	136	1.390	1.24
CM-15	1.01	0.031	155	1.742	1.57
CM-16 (rpt.)	0.60	0.069	44.7	0.776	0.73
CM-17 (rpt.)	0.27	0.074	18.5	0.476	0.46
CM-19 (rpt.)	0.40	0.063	31.4	0.514	0.48
CM-22 (rpt.)	0.40	0.067	30.2	0.580	0.55
CM-IV-A-iii.iv.v (rpt.)	0.22	0.019	54.7	0.899	0.84
CM-IV-A-v,vi,vii (rpt.)	0.24	0.023	50	0.894	0.84
CM-IV-A-xiii,xiv,xv	0.23	0.015	75.6	0.943	0.86
CM-IV-A-xvi	0.14	0.030	22.4	0.593	0.57
CM-24	6.58	0.070	752	6.190	5.36
CM-28	0.50	0.048	49.5	0.845	0.79

To be continued.

Continue:

Neoproterozoic Old Fort Point Formation, Jasper, Alberta

Kendall et al. (2004) *52.96°N* *118.48°W*

Sample	Re (ppb)	Os (ppt)	$^{187}Re/^{188}Os$	$^{187}Os/^{188}Os$	Os_g [a]	Os_i [c]
BK-01-014B	15.43	249.4	524.7	5.954	5.38	0.61
BK-01-015A	6.36	164.7	262.9	3.299	3.01	0.62
BK-01-015B	12.53	218.9	463.7	5.352	4.84	0.63
BK-01-015C	8.54	192.0	318.7	3.859	3.51	0.61
BK-01-015D	7.28	144.8	379.6	4.475	4.06	0.61

[a] Os_g = $^{187}Os/^{188}Os$ ratios of strata at the approximate timing of thermal maturation of most of the strata (adopting the Re-Os age of 66 Ma);

[b] No Re and Os abundance data available;

[c] Os_i = initial $^{187}Os/^{188}Os$ ratios of Old Fort Point Formation calculated at its Re-Os depositional age of 608 Ma.

Figure 3.1 Map of the study area showing the location of the oil and Duvernay Formation shale samples used in this study (modified from Fowler et al. 2001 with the permission of Canadian Society of Petroleum Geologists). The oils are from the Devonian Leduc and Nisku formations. The majority of the shale samples are located in the mature zone (16-18-52-5W5, 14-29-48-6W5, 2-12-50-26W4 and 2-6-47-4W5) with some from the immature zone (10-27-57-21W4) and the overmature zone (1-28-36-3W5 and 8-35-31-25W4). Solvent extracts of well 10-27-57-21W4 (low maturity) and 13-14-35-25W4 (high maturity) are used for organic geochemical analysis.

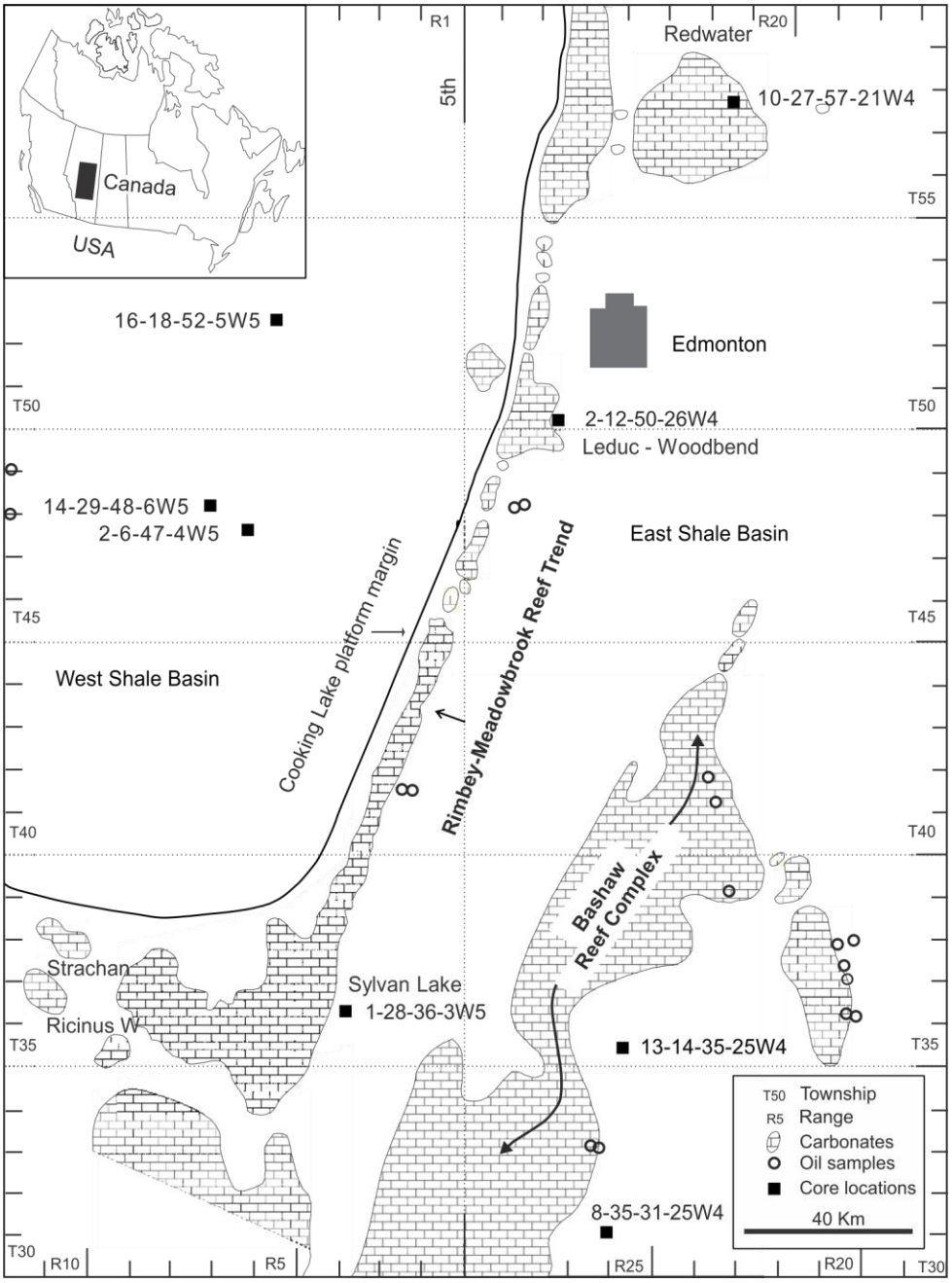
Canada
USA
R1
5th
R20
Redwater
10-27-57-21W4
T55
16-18-52-5W5
Edmonton
T50
T50
2-12-50-26W4
Leduc - Woodbend
14-29-48-6W5
2-6-47-4W5
East Shale Basin
T45
T45
West Shale Basin
Cooking Lake platform margin
Rimbey-Meadowbrook Reef Trend
T40
T40
Bashaw
Reef Complex
Strachan
Ricinus W
Sylvan Lake
1-28-36-3W5
T35
13-14-35-25W4
T35
T50 Township
R5 Range
Carbonates
Oil samples
Core locations
40 Km
8-35-31-25W4
T30
R10
R5
R25
R20
T30

Figure 3.2 Devonian stratigraphy of the study area, south-central Alberta (modified from Li et al. 1998 and Fowler et al. 2001). Late Devonian Woodbend Group Duvernay Formation interfingers with Leduc reefs. Also shown here are the organic-rich Devonian-Mississippian Exshaw Formation and Middle Devonian Keg River Formation.

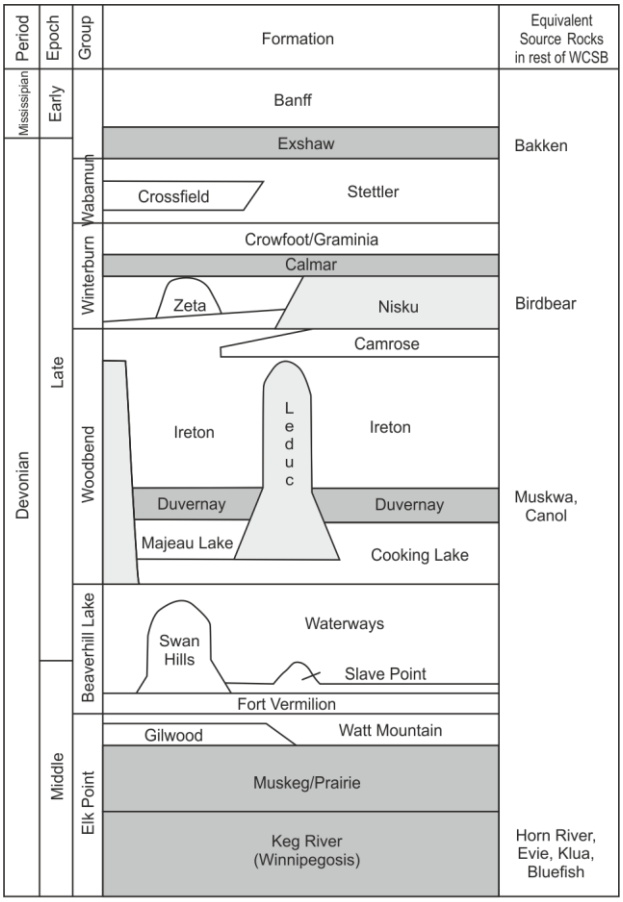
Period
Epoch
Group
Formation
Equivalent Source Rocks in rest of WCSB
Mississipian
Early
Devonian
Late
Middle
Banff
Exshaw
Bakken
Wabamun
Crossfield
Stettler
Winterburn
Crowfoot/Graminia
Calmar
Zeta
Nisku
Birdbear
Camrose
Woodbend
Ireton
Leduc
Ireton
Duvernay
Duvernay
Muskwa, Canol
Majeau Lake
Cooking Lake
Beaverhill Lake
Swan Hills
Waterways
Slave Point
Fort Vermilion
Elk Point
Gilwood
Watt Mountain
Muskeg/Prairie
Keg River (Winnipegosis)
Horn River, Evie, Klua, Bluefish

Figure 3.3 Migration of the Duvernay Formation generated oil (Modified from Switzer et al. 1994). Following oil generation the Duvernay oil migrated to adjacent Leduc reefs with the underlying Cooking Lake carbonates working as a "pipe line". In the Bashaw reef area, the differential compaction of the Ireton aquitard due to the underlying Leduc reefs leads to the thinning or absence of the aquitard. This facilitates the breach of Duvernay sourced oil from Leduc reefs to the overlying Nisku formation.

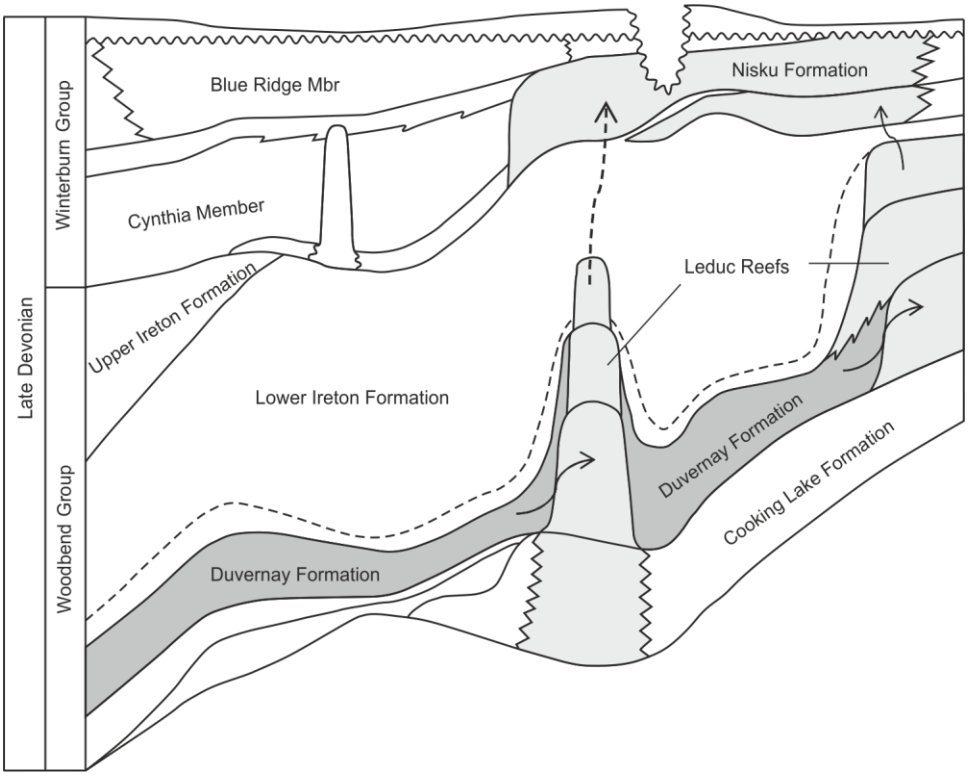
Late Devonian
Winterburn Group
Woodbend Group
Blue Ridge Mbr
Nisku Formation
Cynthia Member
Leduc Reefs
Upper Ireton Formation
Lower Ireton Formation
Duvernay Formation
Cooking Lake Formation
Duvernay Formation

Figure 3.4 Asphaltene content versus asphaltene Re (ppb) and unradiogenic Os (ppt, represented by ^{192}Os) abundance of the Duvernay oils.

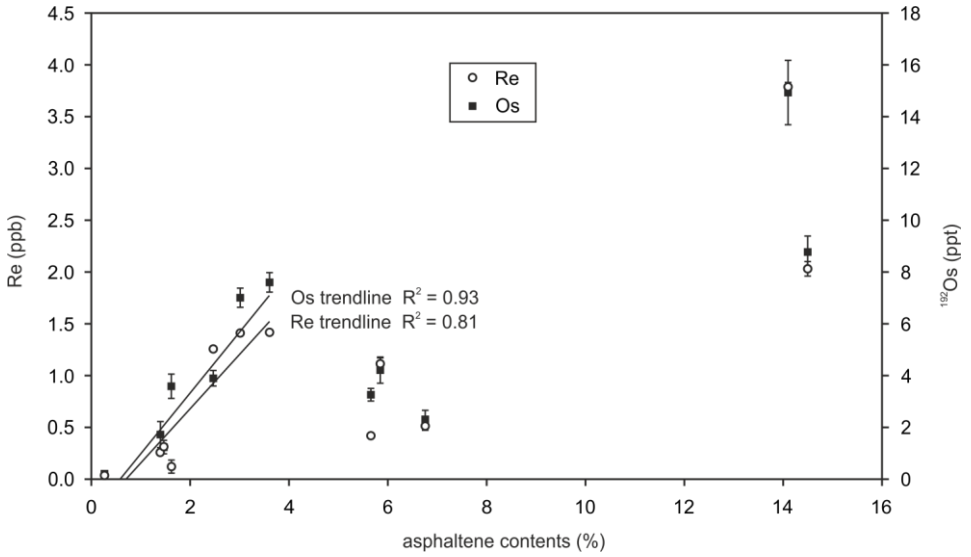
Re
Os
Os trendline R2 = 0.93
Re trendline R2 = 0.81
Re (ppb)
192Os (ppt)
asphaltene contents (%)
0.0
0.5
1.0
1.5
2.0
2.5
3.0
3.5
4.0
4.5
0
2
4
6
8
10
12
14
16
18

Figure 3.5 $^{187}Re/^{188}Os$ vs $^{187}Os/^{188}Os$ plot for the asphaltene fractions of the Duvernay oil.

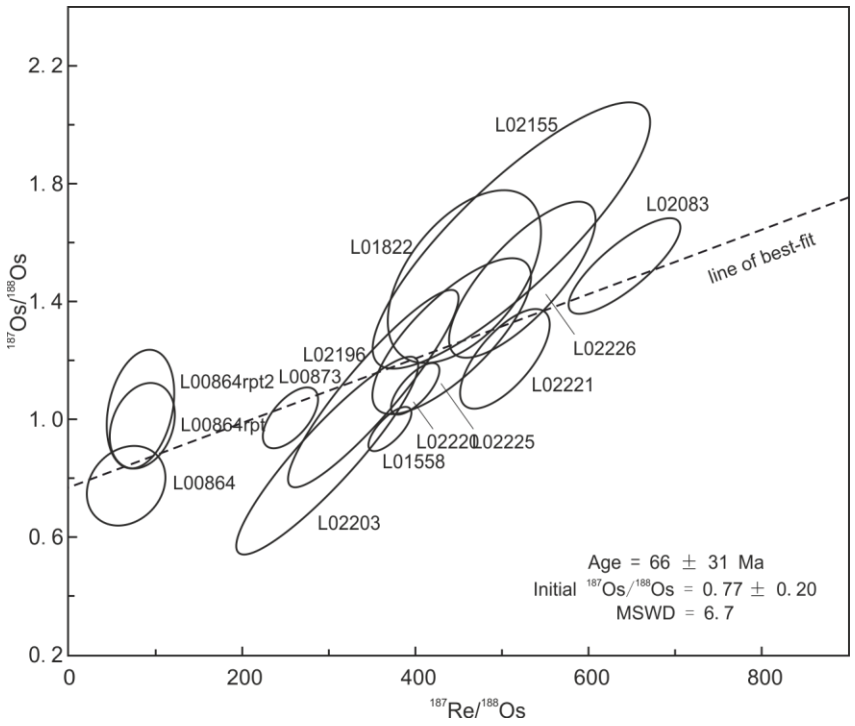
2.2
1.8
1.4
1.0
0.6
0.2
0
200
400
600
800
$^{187}Os/^{188}Os$
$^{187}Re/^{188}Os$
L02155
L02083
L01822
line of best-fit
L02226
L02196
L00873
L00864rpt2
L02221
L00864rpt
L02220
L02225
L01558
L00864
L02203
Age = 66 ± 31 Ma
Initial $^{187}Os/^{188}Os$ = 0.77 ± 0.20
MSWD = 6.7

Figure 3.6 The individually calculated Os_i values of asphaltene samples of the Duvernay oil.

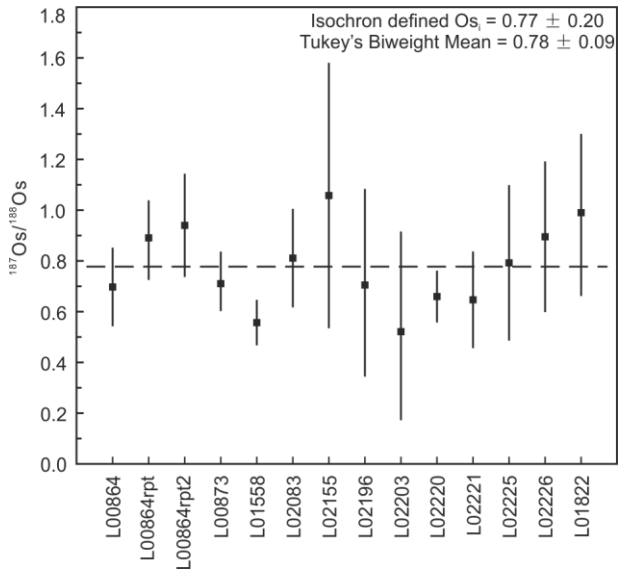
Isochron defined Os$_i$ = 0.77 ± 0.20
Tukey's Biweight Mean = 0.78 ± 0.09
$^{187}Os/^{188}Os$
1.8
1.6
1.4
1.2
1.0
0.8
0.6
0.4
0.2
0.0
L00864
L00864rpt
L00864rpt2
L00873
L01558
L02083
L02155
L02196
L02203
L02220
L02221
L02225
L02226
L01822

Figure 3.7 Duvernay Formation total organic carbon (TOC), Re and unradiogenic Os (^{192}Os as representative) abundances, and calculated $^{187}Os/^{188}Os$ compositions at the time of deposition (Os_i, 378.5 Ma) and oil generation (Os_g, 66 Ma). The depth of TOC does not correlate exactly with the Re and Os data (Fowler et al., 2003). Broadly the Re and Os abundances positively co-vary with the TOC content. The Os_i values show a limited (0.28 to 0.38) range, and yield a weighted average of ~0.33, reflecting a relatively nonradiogenic $^{187}Os/^{188}Os$ composition for contemporaneous seawater. The Os_g values of the Duvernay Formation calculated at 66 Ma are between 0.46 and 1.48, and yield a Tukey's Biweight average of 0.833 ± 0.009.

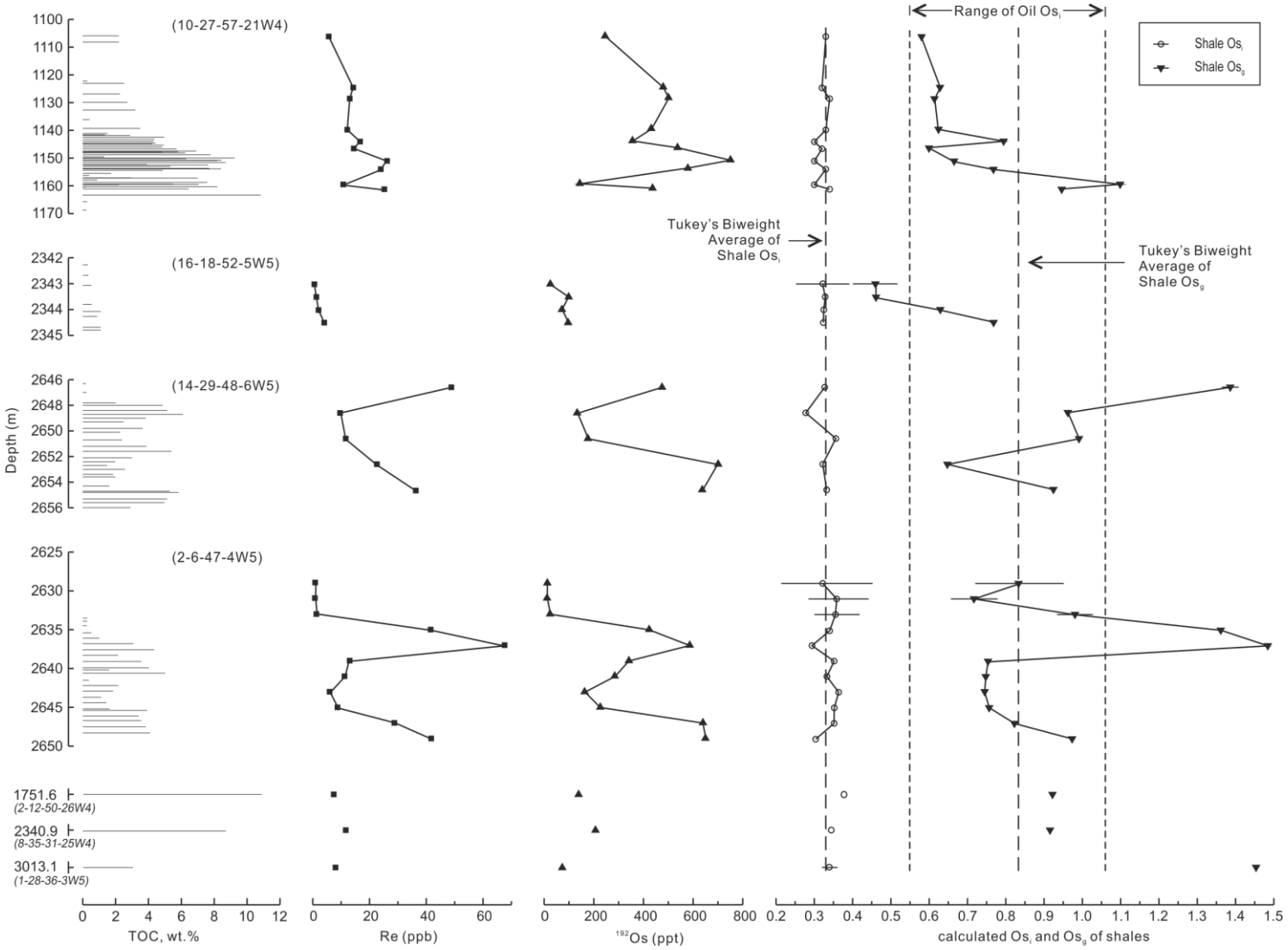
(10-27-57-21W4)
(16-18-52-5W5)
(14-29-48-6W5)
(2-6-47-4W5)
Depth (m)
1751.6
(2-12-50-26W4)
2340.9
(8-35-31-25W4)
3013.1
(1-28-36-3W5)
TOC, wt.%
Re (ppb)
192Os (ppt)
calculated Osi and Osg of shales
Range of Oil Osi
Shale Osi
Shale Osg
Tukey's Biweight Average of Shale Osi
Tukey's Biweight Average of Shale Osg

Figure 3.8a Representative gas chromatograms showing distributions of: 1) gasoline range hydrocarbons and 2) normal alkanes and isoprenoids in low (sample L02221), medium (sample L02155) and high (sample L02177) maturity Duvernay-sourced crude oils. The high maturity oils have very low asphaltene content and hence were not selected for Re-Os analysis. For peak annotations see Table 3.4.

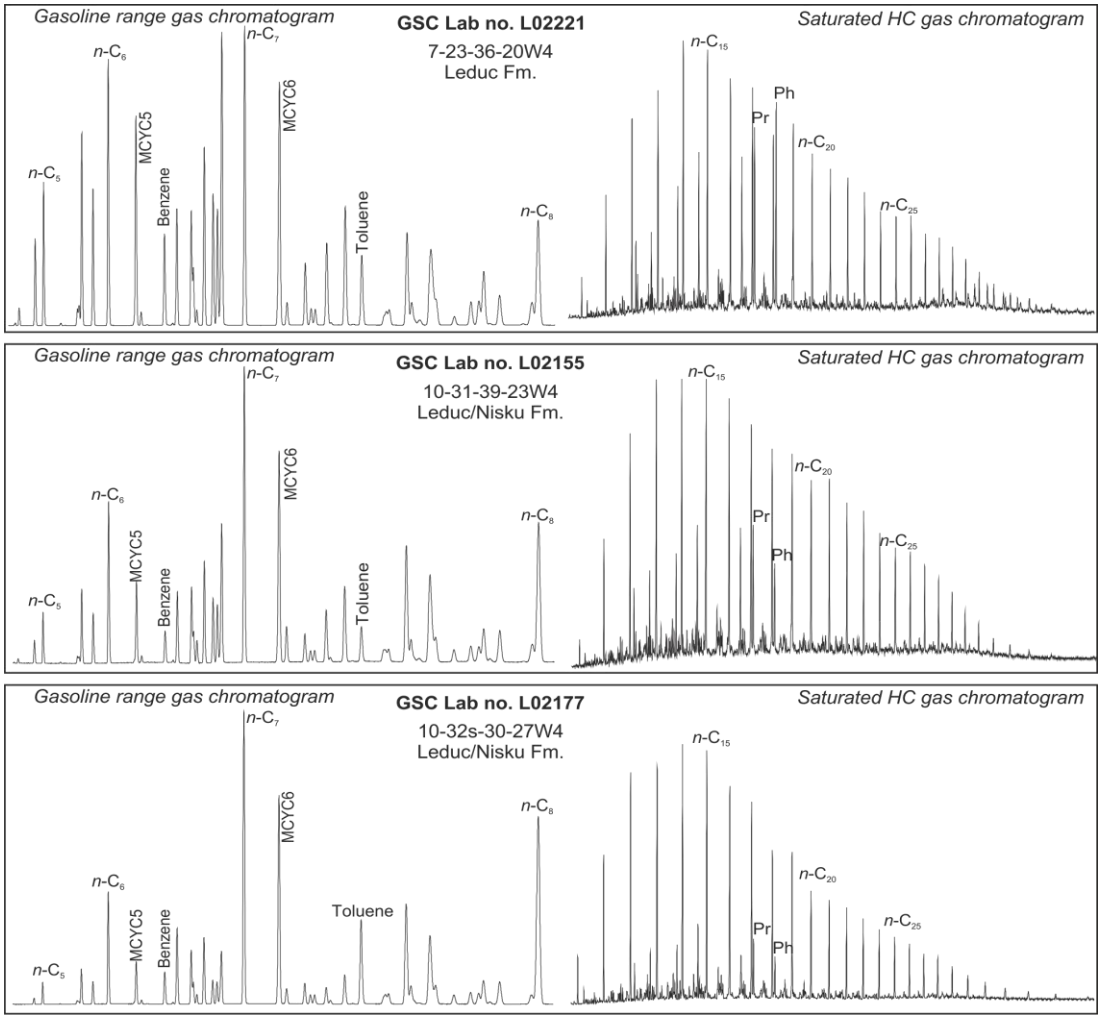
Gasoline range gas chromatogram
GSC Lab no. L02221
7-23-36-20W4
Leduc Fm.
Saturated HC gas chromatogram
n-C5
n-C6
MCYC5
Benzene
n-C7
MCYC6
Toluene
n-C8
n-C15
Pr
Ph
n-C20
n-C25
Gasoline range gas chromatogram
GSC Lab no. L02155
10-31-39-23W4
Leduc/Nisku Fm.
Saturated HC gas chromatogram
n-C5
n-C6
MCYC5
Benzene
n-C7
MCYC6
Toluene
n-C8
n-C15
Pr
Ph
n-C20
n-C25
Gasoline range gas chromatogram
GSC Lab no. L02177
10-32s-30-27W4
Leduc/Nisku Fm.
Saturated HC gas chromatogram
n-C5
n-C6
MCYC5
Benzene
n-C7
MCYC6
Toluene
n-C8
n-C15
Pr
Ph
n-C20
n-C25

Figure 3.8b Representative gas chromatograms showing distributions of: 3) terpanes and 4) steranes in low (sample L02221), medium (sample L02155) and high (sample L02177) maturity Duvernay-sourced crude oils.

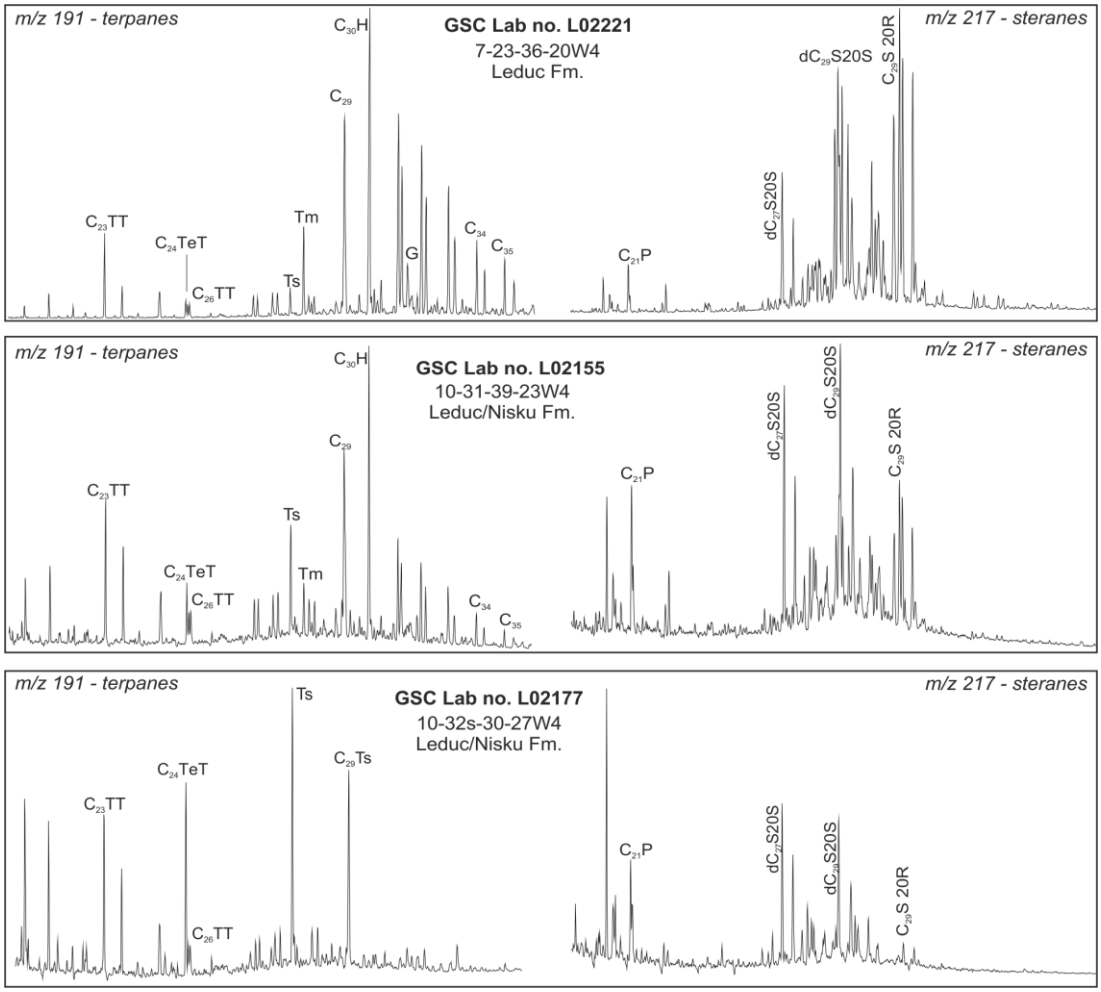
m/z 191 - terpanes
GSC Lab no. L02221
7-23-36-20W4
Leduc Fm.
m/z 217 - steranes
C23TT
C24TeT
C26TT
Ts
Tm
C29
C30H
G
C34
C35
C21P
dC27S20S
dC29S20S
C29S 20R
m/z 191 - terpanes
GSC Lab no. L02155
10-31-39-23W4
Leduc/Nisku Fm.
m/z 217 - steranes
C23TT
C24TeT
C26TT
Ts
Tm
C29
C30H
C34
C35
C21P
dC27S20S
dC29S20S
C29S 20R
m/z 191 - terpanes
GSC Lab no. L02177
10-32s-30-27W4
Leduc/Nisku Fm.
m/z 217 - steranes
C23TT
C24TeT
C26TT
Ts
C29Ts
C21P
dC27S20S
dC29S20S
C29S 20R

Figure 3.9 Saturate fraction gas chromatograms showing distributions of 1) normal alkanes and isoprenoids, 2) terpanes and 3) steranes in low and high maturity Duvernay Formation organic extracts. For peak annotations see Table 3.4.

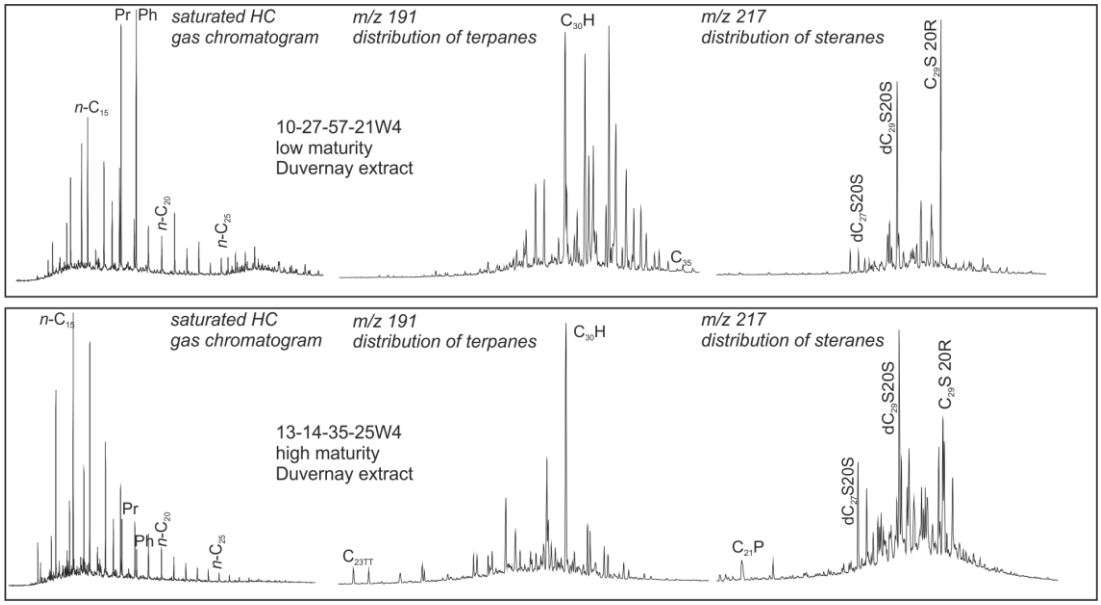
Pr
Ph
saturated HC
gas chromatogram
m/z 191
distribution of terpanes
C30H
m/z 217
distribution of steranes
C29S 20R
dC29S20S
dC27S20S
n-C15
n-C20
n-C25
10-27-57-21W4
low maturity
Duvernay extract
C25
n-C15
saturated HC
gas chromatogram
m/z 191
distribution of terpanes
C30H
m/z 217
distribution of steranes
C29S 20R
dC29S20S
dC27S20S
13-14-35-25W4
high maturity
Duvernay extract
Pr
Ph
n-C20
n-C25
C23TT
C21P

Figure 3.10 Oil-source correlation of a Nisku crude oil from Wood River field (within the Bashaw reef complex, 10-28-42-23W4, sample L02203) and Duvernay Formation organic extract from 13-14-35-25W4 showing strong similarities in the distributions of terpane and sterane biomarkers. For peak annotations see Table 3.4.

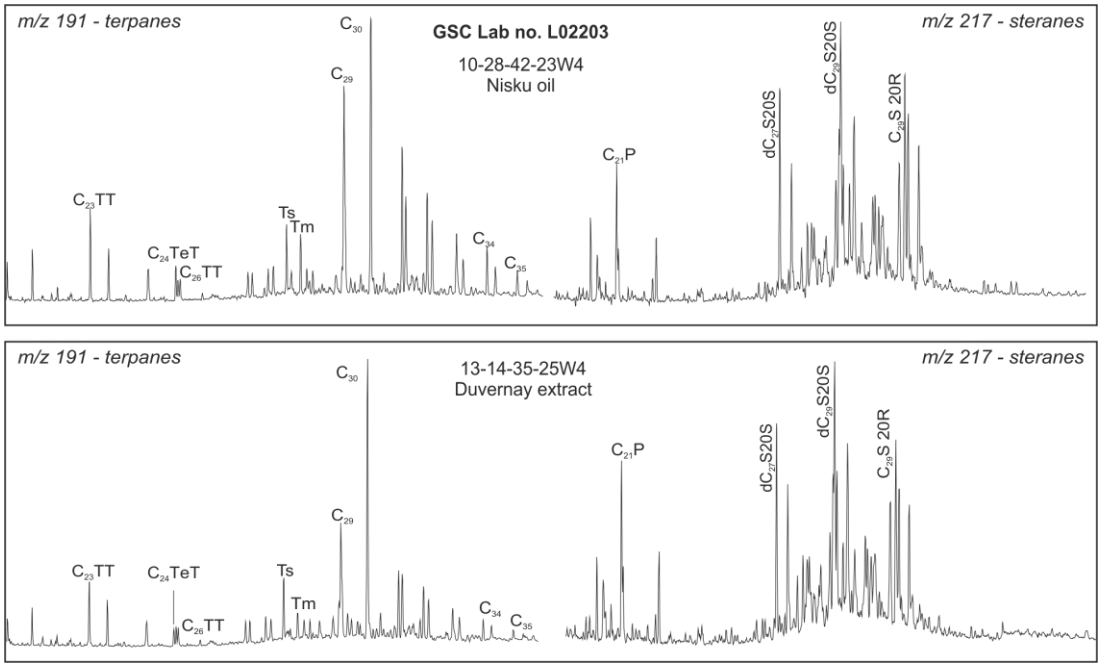
m/z 191 - terpanes
GSC Lab no. L02203
10-28-42-23W4
Nisku oil
m/z 217 - steranes
C30
C29
C23TT
C24TeT
C26TT
Ts
Tm
C34
C35
C21P
dC27S20S
dC28S20S
C29S 20R
m/z 191 - terpanes
13-14-35-25W4
Duvernay extract
m/z 217 - steranes
C30
C29
C23TT
C24TeT
C26TT
Ts
Tm
C34
C35
C21P
dC27S20S
dC28S20S
C29S 20R

Figure 3.11 $^{187}Re/^{188}Os$ vs $^{187}Os/^{188}Os$ plots for the Duvernay formation. A) core 10-27-57-21W4; B) core 16-18-52-5W5; C) core 14-29-48-6W5; D) core 2-6-47-4W5; and E) all data including samples from references (Selby et al., 2007; Finlay et al., 2012). See text for discussion.

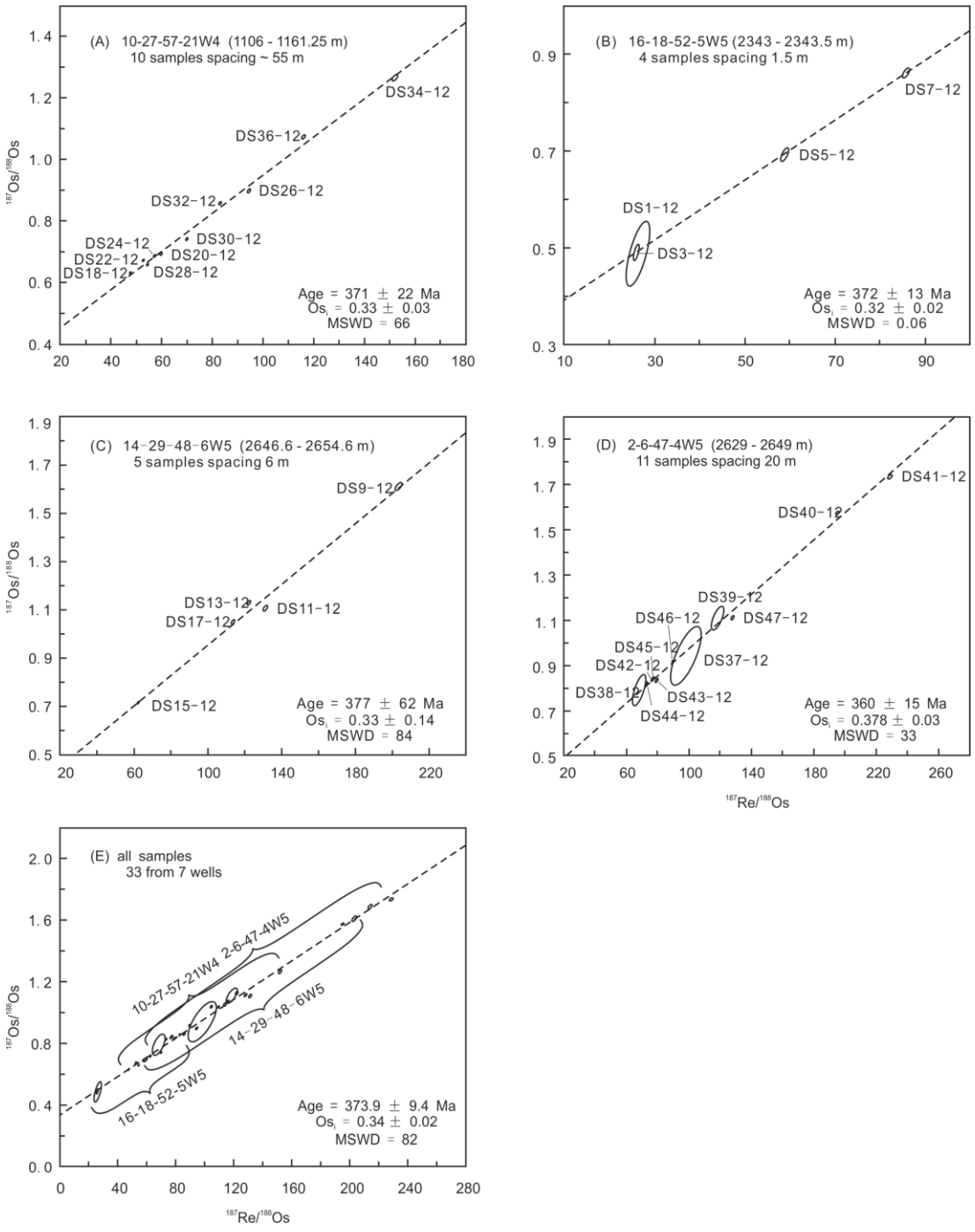
(A) 10-27-57-21W4 (1106 - 1161.25 m)
10 samples spacing ~ 55 m
DS34-12
DS36-12
DS32-12
DS26-12
DS24-12
DS30-12
DS22-12
DS20-12
DS18-12
DS28-12
Age = 371 ± 22 Ma
Os$_i$ = 0.33 ± 0.03
MSWD = 66
(B) 16-18-52-5W5 (2343 - 2343.5 m)
4 samples spacing 1.5 m
DS7-12
DS5-12
DS1-12
DS3-12
Age = 372 ± 13 Ma
Os$_i$ = 0.32 ± 0.02
MSWD = 0.06
(C) 14-29-48-6W5 (2646.6 - 2654.6 m)
5 samples spacing 6 m
DS9-12
DS13-12
DS17-12
DS11-12
DS15-12
Age = 377 ± 62 Ma
Os$_i$ = 0.33 ± 0.14
MSWD = 84
(D) 2-6-47-4W5 (2629 - 2649 m)
11 samples spacing 20 m
DS41-12
DS40-12
DS39-12
DS46-12
DS47-12
DS45-12
DS42-12
DS37-12
DS38-12
DS43-12
DS44-12
Age = 360 ± 15 Ma
Os$_i$ = 0.378 ± 0.03
MSWD = 33
^{187}Re/^{188}Os
(E) all samples
33 from 7 wells
10-27-57-21W4
2-6-47-4W5
14-29-48-6W5
16-18-52-5W5
Age = 373.9 ± 9.4 Ma
Os$_i$ = 0.34 ± 0.02
MSWD = 82
^{187}Os/^{188}Os
^{187}Re/^{188}Os

Figure 3.12 Comparison of the currently available $^{187}Os/^{188}Os$ compositions at 66 Ma for the WCSB Phanerozoic organic-rich intervals with the Duvernay shale Os_g and oil Os_i values.

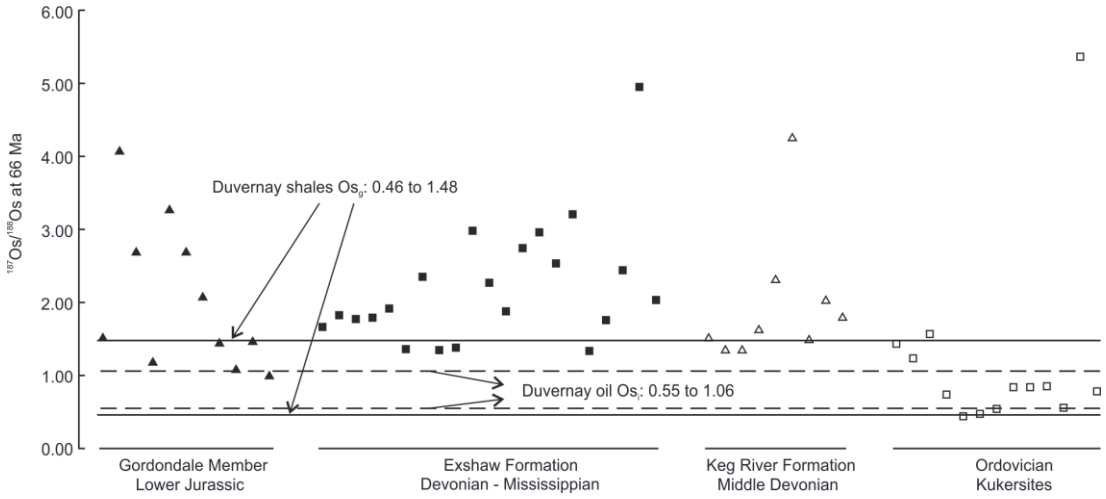
6.00
5.00
4.00
3.00
2.00
1.00
0.00
$^{187}Os/^{188}Os$ at 66 Ma
Duvernay shales Os_9: 0.46 to 1.48
Duvernay oil Os_7: 0.55 to 1.06
Gordondale Member
Lower Jurassic
Exshaw Formation
Devonian - Mississippian
Keg River Formation
Middle Devonian
Ordovician
Kukersites

Chapter 4 Further evaluation of the Re-Os systematics of crude oil: Implications for Re-Os geochronology of petroleum systems

A version of this chapter will be submitted to Geochimica et Cosmochimica Acta co-authored by David Selby, Paul G. Lillis, Honggang Zhou and Magali Pujol.

4.1 Introduction

The presence of rhenium (Re) and osmium (Os) in many bitumen and crude oil samples in measurable concentrations, typically > 1 ppb (parts per billion of weight, ng/g) Re and > 30 ppt (parts per trillion of weight, pg/g) Os, has been known for several decades (Poplavko et al., 1974; Barre et al., 1995; Selby et al., 2007). As a result, this has permitted the application of the Re-Os geochronometer to provide timing constraints for key petroleum events, e.g., crude oil generation, thermochemical sulphate reduction and thermal cracking, and also be a source tracer of the oil (Selby et al., 2005; Selby and Creaser, 2005; Finlay et al., 2011; Finlay et al., 2012; Lillis and Selby, 2013; Cumming et al., 2014; Ge et al., 2016; Chapter 3). Thus far, the validation of Re-Os crude oil and bitumen dates are commonly achieved through the comparison with the established chronologies of the studied petroleum system, e.g., basin modelling and/or apatite fission track and Ar-Ar dates (Eadington et al., 1991; Mark et al., 2005; Mark et al., 2010; Welte et al., 2012; Peyton and Carrapa, 2013). Therefore, it is critical to enhance the understanding of the geochemical behaviour of Re and Os in crude oil for the interpretation and further application of Re-Os geochronometer on petroleum systems.

It has been shown that, the asphaltene fraction isolated from crude oil by the addition of *n*-alkanes (e.g. *n*-pentane and *n*-heptane) is the main carrier of Re (> 90%) and Os (> 83%) in crude oil (Selby et al., 2007). The maltene fraction, which can be fractionated into saturates, aromatics and resin, contains the remaining Re and Os in crude oil. As a result, the $^{187}Re/^{188}Os$ and $^{187}Os/^{188}Os$ compositions of the whole oil are predominantly determined by the asphaltene fraction. The exact binding locations of both Re and Os in the asphaltene and maltene fractions still remain mostly unknown, although previous studies have proposed that Re and Os are present in the form of metalloporphyrins or to be bound by heteroatom ligands (Miller, 2004; Selby et al., 2007).

The typical molecular structure of asphaltene consists of a polycyclic aromatic hydrocarbon core with alkyl side chains (Figure 4.1; Figure 2, Mullins, 2010). The asphaltene molecular structure is demonstrated to aggregate at low concentrations (50-100 mg/l) in toluene (Gray et al., 2011; Mullins et al., 2012).The asphaltene aggregate structure is macro-porous, which enables the asphaltene to adsorb and occlude additional molecules (e.g., biomarkers) during their formation (Figure 4.2; Mujica et al., 2000; Liao et al., 2005; Derakhshesh et al., 2013; Snowdon et al., 2016). Asphaltene precipitation occurs in response to the changes in physical and chemical conditions within the petroleum system, e.g., pressure decrease and component changes, i.e. gas (CH_4 and CO_2) injection and oil mixing (Buenrostro-Gonzalez et al., 2004; Subramanian et al., 2016). However, the precipitation process is not well understood yet.

To date, the studies of Re-Os elemental and isotopic systematic have been conducted on the sequentially precipitated fractions from the asphaltene of two different oil samples. The sequential precipitation of asphaltene was conducted with a mixture of dichloromethane and *n*-heptane or *n*-pentane (Mahdaoui et al., 2013). The Re and Os abundances of the progressively precipitated asphaltene fractions decrease throughout the process, however, both the Re/Os and $^{187}Os/^{188}Os$ compositions of the fractions remain nearly constant. An additional study utilizing *n*-heptane-dichloromethane-methanol and acetone-toluene mixtures to progressively precipitate asphaltene fractions from two same asphaltene aliquots of a heavy oil sample, respectively (Dimarzio et al., 2016). This study showed that the highest Re and Os abundances are observed in the intermediate soluble fraction separated by *n*-heptane-dichloromethane-methanol and the most insoluble fraction separated by acetone-toluene. Different with the study of Mahdaoui et al. (2013), only the $^{187}Re/^{188}Os$ values of the fractions separated by acetone-toluene remain fairly constant throughout the progressive precipitation, the corresponding $^{187}Os/^{188}Os$ compositions of the fractions decrease during the process. For the fractions separated by *n*-heptane-dichloromethane-methanol, the $^{187}Re/^{188}Os$ increases and the $^{187}Os/^{188}Os$ composition increase first and then decrease throughout the progressive precipitation.

Recently, a new sampling methodology for Re-Os dating of crude oil was proposed to avoid the potential disadvantages for multiple crude oil samples from a large geographic area, e.g. different sources and different secondary/alteration histories

(Georgiev et al., 2016). The Re-Os analyses were conducted on multiple asphaltene and maltene fractions separated from the same crude oil sample with *n*-pentane, *n*-hexane, *n*-heptane and *n*-decane with the objective to obtain the necessary spread in the Re-Os isotopic compositions essential to develop an isochron. A Re-Os date (~200 Ma) was defined by the maltene fractions of an oil sample from the Streppenosa Formation and another Re-Os date (~ 29 Ma) was defined by the crude oil and asphaltene fractions of another two oils from the Noto and Siccia formations of Gela Oilfield, Italy. These Re-Os dates are interpreted to reflect the timing of oil generation (Georgiev et al., 2016).

Although the previous studies have greatly increased the knowledge of the Re-Os systematics within crude oil and asphaltene, the current understanding can potentially be limited considering the limited amount of samples employed and the substantial diversity and complexity of worldwide crude oils. Further, the ability of the single oil Re-Os dating method determining geological age also requires further validation before extensive application. In this study, the Re-Os isotopic systematics of six different crude oils were inspected by separating them into fractions with two different methodologies: 1) fractionating bulk asphaltene progressively with the increase of *n*-heptane percentage in its mixture with dichloromethane, and, 2) separating whole oil into asphaltene and maltene fractions by a series of *n*-alkane solutions (from *n*-C_5 to *n*-C_{10}) with dichloromethane-methanol. This study illustrates the observed decrease of Re and Os abundances and the different trends in the $^{187}Re/^{188}Os$ and $^{187}Os/^{188}Os$ compositions throughout the progressive precipitation for each sample. The variation of Re-Os isotopic compositions of the maltene fractions separated by a series of *n*-alkane solutions is more prominent than that of the asphaltene fractions. However, the Re-Os systematics of either the asphaltene or the maltene fractions cannot consistently yield geologically meaningful dates for all of the six oils in this study. This study also suggest the Re and Os to be bound in free molecules and asphaltene aggregates.

4.2 Samples and analytical protocols

4.2.1 The samples

Six crude oils from different geographic locations are used in this study, of which the Derby, Federal, Viking-Morel and Purisima oil samples were obtained from the U.S.

Geological Survey oil library in Denver, Colorado, the Persian oil was provided by Centre Scientifique et Technique Jean Féger (CSTJF) of the petroleum company, Total and the RM8505 was ordered from the U.S. National Institute of Standards and Technology (NIST).

The Derby oil (118.55°W, 42.69°N) is recovered from the Permian Phosphoria Formation of Derby field, Wind River basin, Wyoming, USA. The oil is sourced from the Permian Phosphoria Formation which is characterised by Type II-S kerogen. The oil is considered to have migrated significant distance (≥150 km). The onset of oil generation for is considered to be similar to that of the Big Horn basin Phosphoria petroleum system (~ 200 Ma, Lillis and Selby, 2013). The oil has an asphaltene abundance of 6%.

The Federal oil (106.78°W, 42.86°N) is recovered from the Pennsylvanian Tensleep Formation of South Casper Creek field, Wind River basin, Wyoming, USA. Same as the Derby oil, the source of Federal oil is the Permian Phosphoria Formation and probably also with the onset of oil generation in Late Triassic. The Federal oil is also considered to have migrated significant distance (≥150 km) and generated since Late Triassic (~ 200 Ma). The Federal oil possess an API gravity of 12°, sulphur content of 4.5% and asphaltene abundance of 12%.

The Viking-Morel oil (105.06°W, 44.58°N) is recovered from the Pennsylvanian-Permian Minnelusa Formation of Morel field, Powder River basin, Wyoming, USA. The oil is locally sourced from the Minnelusa Formation containing Type II medium sulphur kerogen (Clayton et al., 1992). The timing of oil generation is not known, but is considered to be during the Cretaceous. The oil has an API gravity of 25°, sulphur content of 3.3 % and asphaltene content of 9%.

The Purisima oil (120.42°W, 34.72°N) is recovered from the Miocene Monterey Formation of Lompoc field, Santa Maria basin, California, USA. The oil is considered to have generated during the last 5 million years from the Miocene Monterey Formation which is characterize by Type II-S kerogen (Isaacs and Rullkötter, 2001). The oil has an API gravity of 22.1° and asphaltene abundance of 16%.

The Persian oil is from a Cenomanian carbonate reservoir in Persian Gulf. The oil source rock is of Cretaceous and/or Late Jurassic marine origin with probably Type II-S kerogen (Nairn and Alsharhan, 1997). This oil has a total asphaltene abundance of 6%.

The RM8505 oil is a Venezuelan crude oil. No further geological details of the origin are available from NIST. The predominant source rocks of crude oil in Venezuela is from the Upper Cretaceous (Cenomanian-Turonian-Coniacian, 100 – 86 Ma) La Luna Formation (Type II kerogen) and its age equivalents, with only minor contributions from Palaeocene, Eocene and Miocene source rocks (James, 1990, 2000; Summa et al., 2003). The majority of oil generation of La Luna Formation is considered to have occurred since the Miocene (< 23 Ma), although oil generation is noted to have started as early as the Early Eocene (56 Ma; James, 2000; Summa et al., 2003). This oil has asphaltene content of ~ 13% (Chapter 2).

4.2.2 Sample preparation

For each oil sample, Re-Os determinations were taken on the whole oil, *n*-heptane separated bulk asphaltene and maltene, the progressively precipitated fractions of asphaltene via the mixture of *n*-heptane and dichloromethane, and the asphaltene and maltene fractions separated by a series of *n*-alkane-dichloromethane-methanol solutions.

Asphaltene and maltene were initially separated by a 40:1 *n*-heptane protocol from crude oils (Speight, 2004; Selby et al., 2007). In brief, ~ 40 ml of *n*-heptane was thoroughly mixed with per gram of crude oil. The mixture was put on a rocker overnight (for at least 8 hours) and then centrifuged for 20 minutes (4000 rpm). The supernatant of the *n*-heptane and soluble maltene fraction was decanted into a pre-weighed glass vial, with the *n*-heptane evaporated at 80 °C to recover the maltene fraction for Re-Os analyses. The precipitated asphaltene was also collected from the bottom of centrifuge tube into pre-weighed glass vial with ≤1 ml chloroform. The chloroform was evaporated to at 60 °C overnight to recover the asphaltene fraction. An aliquant of the bulk asphaltene (~ 0.250 mg) was set aside for Re-Os analysis, the remaining asphaltene fraction was used for progressive precipitation experiment (see below).

The progressive precipitation of asphaltene was achieved by using a binary mixture of dichloromethane (DCM, CH_2Cl_2) as the solvent and *n*-heptane as the precipitant (Figure 4.3; Nalwaya et al., 1999; Kaminski et al., 2000; Mahdaoui et al., 2013). It happens in response to the step-by-step increase of the percentage (5%, volume) of *n*-heptane in the binary mixture. The amount of asphaltene used for the progressive precipitation ranged between 2 – 4 g. The *n*-heptane-DCM mixture volumes are kept the same for every step (50 – 250 ml for different samples, Table 4.1). The bulk asphaltene fraction was firstly dissolved in DCM prior to the addition of *n*-heptane. The mixture was then left on a rocker overnight and centrifuged at 4000 rpm for 20 minutes to separate the precipitated and soluble fractions. After centrifuging, the supernatant was decanted and the precipitate was collected into pre-weighed glass vials with ≤1 ml chloroform and dried at 60 °C. The DCM and *n*-heptane were extracted from the decanted solution to recover the soluble fraction of asphaltene using a rotary evaporator (40 °C water-bath and 200 - 50 mBar pressure).The recovered soluble fraction of asphaltene is used for the following step with 5% (volume) more of *n*-heptane in the DCM: *n*-heptane (Figure 4.3). The last steps used 100% *n*-heptane. Starting from a *n*-heptane:DCM ratio of 50:50, the first precipitation of asphaltene occurred on the ratio of 65:35 or 70:30 for different samples (Table 4.1).

The six crude oils were also separated into their asphaltene and maltene fractions with a series of *n*-alkane solutions, i.e. *n*-pentane, *n*-hexane, *n*-heptane, *n*-octane, *n*-nonane and *n*-decane (i.e. *n*-C_5, *n*-C_6, *n*-C_7, *n*-C_8, *n*-C_9 and *n*-C_{10}) using the protocol based on Weiss et al. (2000) applied by Georgiev et al. (2016). In brief, 3 ml dichloromethane-methanol (93:7 v/v) was added to ~ 1 gram of oil to dissolve the oil. Then *n*-alkanes (40 ml/g oil) were added and the mixtures were then put on a rocker overnight for at least 8 hours. The asphaltene were separated by centrifuging the mixture at 4000 rpm for 20 minutes. The same 3 ml dichloromethane-methanol and 40 ml *n*-alkane procedure was repeated on the isolated asphaltene to remove any co-precipitates (Gürgey, 1998; Alboudwarej et al., 2001; Álvarez et al., 2015). Finally the asphaltene was separated by centrifuging the solution, with the asphaltene removed to a pre-weighed glass vial using chloroform, which was then evaporated at 60 °C. The remaining soluble fractions in *n*-alkane-dichloromethane-methanol solution of the two steps were added together and removed using a rotary evaporator

(30 - 70 °C water-bath and 400 - 30 mBar pressure) to fully recover the maltene fraction. The maltene was also collected with chloroform which was placed into a pre-weighed glass vial, with the chloroform evaporated at 60 °C.

4.2.3 Re-Os analyses of the samples

The Re-Os analyses were conducted on the whole oil, *n*-heptane separated asphaltene and maltene fractions, the progressively precipitated fractions of asphaltene, and the asphaltene and maltene separated by *n*-alkane-dichloromethane-methanol solutions of the six studied oils. The Re-Os analyses were conducted by Isotope Dilution – Negative Thermal Ionisation Mass Spectrometry (ID-NTIMS) at Durham University in the Laboratory for Source Rock and Sulphide Geochronology and Geochemistry (Selby et al., 2007). With the exception of asphaltene fractions that dried to a solid (i.e. could be powdered in an agate pestle and mortar), all samples were loaded into Carius tubes in ≤1 ml of chloroform, which was then evaporated at 60 ˚C overnight. The sample was digested by inverse *aqua regia* (3 ml 12 N HCl + 6 ml 15.5 N HNO_3) and equilibrated with a mixed tracer solution of ^{185}Re and ^{190}Os at 220 °C for 24 hours. The Os was extracted from the digested sample by solvent extraction using chloroform, and back extracted in 3 ml of 9 N HBr, and then further purified by CrO_3-H_2SO_4-HBr micro-distillation. The Re was purified by HCl-HNO_3 based anion exchange chromatography. Both the Re and Os purified fractions were loaded on Ni and Pt wire filaments, respectively, and measured for their isotopic composition by NTIMS, using static collection by Faraday cups and peak-hopping mode on a secondary electron multiplier, respectively.

The total procedural blanks during the study are 1.63 ± 0.67 picograms for Re and 65 ± 13 femtograms for Os, with an average $^{187}Os/^{188}Os$ of 0.23 ± 0.02 (2 SD, n = 8). The average $^{187}Os/^{188}Os$ value of the in-house Os standard, DROsS, is 0.1611 ± 0.0004 (1SD, n = 126). The average $^{185}Re/^{187}Re$ value of the Re standard, Restd, is 0.5989 ± 0.0019 (1SD, n = 116). The $^{185}Re/^{187}Re$ value of 0.5974 (Gramlich et al., 1973) is used for the Re sample mass fractionation correction. Data reduction includes the instrumental mass fractionation, isobaric oxygen interference and contribution of blanks and the tracer solution. The final uncertainties of the results include the fully propagated of uncertainties of sample-weighing, tracer calibration,

blank abundances and isotope compositions, and reproducibility of standard Re and Os isotope values.

4.3 Results

4.3.1 The progressive precipitation of asphaltene and the separation of crude oil by *n*-alkanes

The six crude oils used in this study possess between 5.7% to 16.1% bulk asphaltene as separated by *n*-heptane (Table 4.1). For the studied oils the order from least to most asphaltene enriched is, Persian (5.7%), Derby (5.8%), Viking-Morel (8.6%), Federal (11.9%), RM8505 (12.8%), and Purisima (16.1%). For the progressive precipitation of asphaltene via *n*-heptane-DCM solutions, four of the samples precipitated the first fractions of asphaltene from an *n*-heptane-DCM ratio of 65:35 (Federal, Viking Morel, Persian and Purisima). Asphaltenes of both the Derby and RM8505 oil first precipitated with an *n*-heptane-DCM ratio of 70:30. The fractions of the asphaltene account for between 2 to 22% of the original bulk asphaltene, with the exception of the first precipitation of RM8505, which accounts for 54% of the bulk asphaltene (Table 4.1; Figure 4.4). From 6.9 to 21.5% of the original asphaltene are still soluble in 100% *n*-heptane at the last step of the progressive precipitation (Figure 4.4). The total progressively precipitated asphaltene account for ~96 to 103% of originally employed bulk asphaltene for the six samples (Table 4.1). The physical appearance of the fractions of asphaltene changes gradually from hard shiny black particles to amorphous dull brown powder and high viscous fluids (the last 100% *n*-heptane soluble fraction) throughout the progressive precipitation, which is identical to previous studies, e.g., Nalwaya et al. (1999).

Four of the six oils (Derby, Federal, Viking Morel, Persian) separated using a *n*-alkane-DCM-methanol solution show a general decrease in asphaltene yields from *n*-C_5 to *n*-C_7, with similar yields from *n*-C_7 to *n*-C_{10} (Figure 4.5; Table 4.2). The exception are for the oil samples Purisima and RM8505, which show a decrease in asphaltene yields from *n*-C_5 to *n*-C_7, with a slight increase for *n*-C_8 and lower values for *n*-C_9 that are similar to yields of *n*-C_7, and finally show a greater yield for *n*-C_{10} (Table 4.2; Figure 4.5). The majority of the asphaltene yields from the *n*-alkane-DCM-methanol solutions are lower than that of using solely *n*-heptane (cf. Tables 4.1 and 4.2), e.g. *n*-pentane 10.6% and *n*-heptane 7.8% asphaltene yields of Federal

oil with DCM-methanol versus 11.9% asphaltene obtained solely by *n*-heptane. The difference in asphaltene yields is attributed to the use of DCM-methanol especially the DCM. The maltene yields are identical for each oil sample with slight variations: ~ 80% for Derby and Federal oil, ~ 75% for Viking-Morel oil, ~ 70% for Persian oil, from 35% to 50% for Purisima oil and ~ 88% for RM 8505 oil (Figure 4.5; Table 4.2). The less than 100% yield can be accounted for by the loss of any volatile phase and sometimes water in the oil. For example, 4.4% fraction was lost/evaporated by heating 0.3 g of RM8505 crude oil at 80 °C for 10 days (Chapter 2). The reduced loss of RM8505 in this study (4.2%) compared to the average loss of Chapter 2 (7.9%) could be attributed to the use of rotary evaporator rather than heating to recover the asphaltene and maltene from chloroform and *n*-alkane-DCM-methanol solutions. Further, water is present in the Purisima oil sample. Even though the sample was centrifuged to remove as much water as possible, small amount is still present in the oil. As such variable amounts of water present in the Purisima oil may have contributed to the inconsistency of the asphaltene and maltene yields and mass balance of the separate fractions.

4.3.2 Re and Os elemental abundances and distribution in the fractions of oil

4.3.2.1 Re-Os data of whole oil and asphaltene and maltene separated by n-heptane

The six crude oil samples contain relatively large ranges of Re and Os abundance and isotopic compositions (Table 4.3). For the whole oil, the six oils possess ~2 (RM8505), 3 (Persian), 8 (Federal), 12 (Purisima), 12 (Derby), 12 (Viking-Morel) ppb Re, and ~12 (Persian), 24 (RM8505), 42 (Purisima), 56 (Federal), 150 (Derby), 174 (Viking-Morel) ppt Os. For the bulk separated asphaltenes, they contain ~14 (RM8505), 50 (Persian), 59 (Federal), 61 (Purisima), 130 (Viking-Morel) and 164 (Derby) ppb Re and ~139 (RM8505), 161 (Persian), 210 (Purisima), 387 (Federal), 1737 (Viking-Morel) and 1827 (Derby) ppt Os. The bulk separated maltenes contain ~0.2 (RM8505), 0.3 (Persian), 0.6 (Purisima), 1.1 (Federal), 1.2 (Derby), 1.6 (Viking-Morel) ppb Re and ~5 (Persian), 6 (Purisima), 8 (RM8505), 13 (Federal), 18 (Derby), 32 (Viking-Morel) ppt Os.

4.3.2.2 Re-Os data of the progressively precipitated fractions of asphaltene

During the progressive precipitation of asphaltene using the *n*-heptane-DCM protocol, the earlier precipitated fractions contain higher Re and Os abundances (Table 4.3; Figures 4.6 - 4.7). The exceptions are the first precipitates of the Federal, Viking-Morel and Persian oil samples.

For the convenience of comparison, the Re and Os abundances of the progressively precipitated asphaltene fractions, whole oil and *n*-heptane maltene fraction are normalized to the Re and Os abundances of the bulk asphaltene (Figures 4.6 - 4.7).

In general, the abundances of the most Re and Os enriched first or second asphaltene precipitates (i.e. at *n*-heptane-DCM ratios of 65:35 and/or 70:30) are 1.4 to 2.7 times that of the bulk asphaltene isolated solely by *n*-heptane. The Re and Os abundances of the precipitates of the last steps of the progressive precipitation are 0.3 to 0.6 times that of the bulk asphaltene. The Re and Os abundances of the 100% *n*-heptane soluble fractions are lower than the last precipitates, but higher than the maltenes. Observed for all samples with the exception of the Derby sample, is a difference in the normalized Re and Os abundances throughout the progressive precipitation (Figures 4.6 - 4.7).

The total Re, unradiogenic Os (represented by ^{192}Os) and radiogenic ^{187}Os of all the fractions of asphaltene account for ~ 100%, 97%, 95%, and 105% of those of the original bulk asphaltene of Derby, Viking-Morel, Persian, and RM8505 samples, respectively (Table 4.3). The currently available four fractions of the Federal sample account for 44% of the original asphaltene mass while accounting for 72.6% of the Re, 65.2% of the ^{192}Os and 63.3% of the ^{187}Os. The currently available six fractions of Purisima oil account for 63% of the original asphaltene mass while accounting for 89.8% of the Re, 101.9% of the ^{192}Os and 100.1% of the ^{187}Os of the original asphaltene.

4.3.2.3 Re-Os data of the asphaltene and maltene fractions separated by n-alkane-DCM-methanol

The Re and Os abundances of the asphaltenes separated by the *n*-alkane-DCM-methanol protocol are normalized to the values of the *n*-heptane separated asphaltene fractions (Figures 4.6 - 4.7). The Re and Os abundances of the maltene fraction separated by the *n*-alkane-DCM-methanol protocol are normalized by the values of *n*-heptane separated maltene fractions (Figures 4.6 - 4.7).

Compared to the asphaltene and maltene fractions separated solely by *n*-heptane, the asphaltenes and maltenes separated by the *n*-alkanes plus DCM and methanol protocol are generally more enriched in Re and Os, with the exception of asphaltenes isolated using *n*-C_5 and *n*-C_6 of the Derby oil (Tables 4.4 - 4.5; Figures 4.6 - 4.7). The enhanced abundances should be attributed to the reduced yield of asphaltene. The Re and Os abundances of *n*-alkanes asphaltenes can be as high as 1.7 (RM8505) and 1.6 (Purisima) times that of the *n*-heptane isolated asphaltenes, respectively. The Re and Os abundances of the *n*-alkane-DCM-methanol isolated maltenes can be as high as 6 (RM8505) and 3 (Viking-Morel) times that of the *n*-heptane isolated maltene fractions, respectively.

In a close relationship to the asphaltene yields, the Re and Os abundances of the asphaltene and maltene generally increase with the increase in chain length of the *n*-alkane used as a precipitant, especially from *n*-C_5 to *n*-C_7 (Figures 4.6 - 4.7). From *n*-C_7 to *n*-C_{10} the Re and Os abundances either increase (e.g. Viking-Morel and RM8505 maltenes), become relatively similar (e.g. Derby, Federal and Persian maltenes) or decrease (Derby and Federal asphaltenes).

As observed for the progressively precipitated asphaltene fractions using *n*-heptane-DCM solutions, the normalized Re and Os abundances are different for both the asphaltene and maltene fractions isolated using the *n*-alkane-DCM-methanol protocol for all samples. This is especially the case for the maltene fractions of the Purisima, Persian and RM8505 oils (Tables 4.3 - 4.5; Figures 4.6 - 4.7).

The total Re and Os contents of the pairs of asphaltene and maltene isolated using the same *n*-alkane-DCM-methanol solution are comparable to the Re-Os contents of the original whole oil (Table 4.6). No significant difference in Re or Os is observed for the Derby, Federal, Viking-Morel and Persian oil samples despite the ~ 13, 12, 19 and 27% loss of sample by evaporation. However, the total Re and Os contents of pairs of asphaltene and maltene of the Purisima oil are variable and show up to 43% Re and 33% Os less than the measured whole oil, considering the variable loss of up to 53% of sample during separation. The total Re and Os contents of the asphaltene and maltene pairs of RM8505 are ~2.2 to 2.8 ppb Re and ~28 to 30 ppt Os. These values are higher than the whole oil (~1.7 to 2.2 ppb Re and ~21 to 27 ppt Os, n = 18;

Liu et al., in press; Chapter 2), but similar to the two analyses reported by Georgiev et al. (2016) (~2.3 ppb Re; ~31 and 29 ppt Os).

4.3.3 Re-Os isotopic systematics

4.3.3.1 Re-Os isotopic compositions of whole oil and asphaltene and maltene separated by n-heptane

The six oil samples exhibit a large spread in Re-Os isotopic compositions (Tables 4.3 - 4.5; Figures 4.8 - 4.9). The $^{187}Re/^{188}Os$ values of the six oils are ~454 (RM8505), 469 (Viking-Morel), 529 (Derby), 1063 (Federal), 1542 (Persian) and 1549 (Purisima) and the $^{187}Os/^{188}Os$ compositions are ~0.95 (Purisima), 1.54 (RM8505), 2.63 (Persian), 2.84 (Derby), 2.98 (Viking-Morel) and 4.19 (Federal). The asphaltene $^{187}Re/^{188}Os$ values and $^{187}Os/^{188}Os$, compositions, although similar, are generally higher and more radiogenic than that of the whole oil (Figures 4.8 - 4.9). In contrast, the maltene fractions possess lower $^{187}Re/^{188}Os$ values and less radiogenic $^{187}Os/^{188}Os$ compositions to that of the whole oil and asphaltene (Figures 4.8 - 4.9). The $^{187}Re/^{188}Os$ values of the bulk separated six asphaltene samples are ~495 (Viking-Morel), 566 (RM8505), 595 (Derby), 1134 (Federal), 1157 (Purisima) and 2057 (Persian) and the $^{187}Os/^{188}Os$ compositions are ~0.97 (Purisima), 1.64 (RM8505), 2.99 (Derby), 3.01 (Viking-Morel), 3.03 (Persian) and 4.23 (Federal). The $^{187}Re/^{188}Os$ values of the bulk separated six maltene samples are ~155 (RM8505), 326 (Viking-Morel), 429 (Derby), 453 (Persian), 480 (Purisima) and 577 (Federal) and the $^{187}Os/^{188}Os$ compositions are ~0.70 (Purisima), 1.22 (RM8505), 1.09 (Persian), 2.83 (Viking-Morel), 2.96 (Derby) and 3.50 (Federal).

4.3.3.2 Re-Os isotopic compositions of the progressively precipitated fractions of asphaltene

The Re-Os isotopic compositions of the progressively precipitated asphaltene fractions from *n*-heptane-DCM solutions exhibit very different characteristics. For example, broadly, the Re-Os isotopic compositions for the progressively precipitated asphaltene fraction for the Derby and Federal oils are similar, whereas the Re-Os compositions for Viking-Morel, RM8505 and Purisima oils show a linear-like distribution on a $^{187}Re/^{188}Os$-$^{187}Os/^{188}Os$ plot, and finally the Persian oil shows a negative distribution in $^{187}Re/^{188}Os$-$^{187}Os/^{188}Os$ space (Figures 4.8 - 4.9). Below we

present in detail the Re-Os isotopic data for the progressively precipitated asphaltene fractions for each oil sample.

For the Derby oil, the $^{187}Re/^{188}Os$ values of most of the asphaltene fractions (70:30 to 95:5) are ~600; whereas for the 100:0 and 100:0 soluble fractions the $^{187}Re/^{188}Os$ values are lower (~556 and 500, respectively). With the exception of 100:0 and 100:0 soluble fractions, the whole oil and maltene fraction possess lower and less radiogenic $^{187}Re/^{188}Os$ and $^{187}Os/^{188}Os$ values, respectively.

For the Federal oil, the $^{187}Re/^{188}Os$ values are similar (~ 1150), with the exception to the 70:30 fraction that possesses a slightly higher $^{187}Re/^{188}Os$ value (~1260). All asphaltene fractions possess higher $^{187}Re/^{188}Os$ values to that of the bulk asphaltene (~1135). Only slight variations are observed in the $^{187}Os/^{188}Os$ compositions (~3.95 to 4.19). These are also similar to the values of bulk asphaltene (4.23) and whole oil (4.19), but much more radiogenic in comparison to the maltene fraction (~3.5), which also possesses a much lower $^{187}Re/^{188}Os$ value (~577).

The $^{187}Re/^{188}Os$ values of the asphaltene fractions of Viking-Morel oil sample decrease from ~515 shown by the first three fractions to ~230 of the last 100:0 soluble fraction in comparison to the 326, 470 and 495 of the maltene, whole oil and bulk asphaltene, respectively. The $^{187}Os/^{188}Os$ compositions for the asphaltene fractions are very similar (~3.00).

For the Purisima oil, the $^{187}Re/^{188}Os$ values increase from ~1140 of the first precipitate to the 1560 of the 95:5 fraction of Purisima asphaltene in comparison to the 480, 1550 and 1560 of the maltene, whole oil and bulk asphaltene, respectively. The $^{187}Os/^{188}Os$ compositions for the asphaltene fractions are very similar (~0.95).

The $^{187}Re/^{188}Os$ and $^{187}Os/^{188}Os$ compositions of the Persian asphaltene fractions are highly variable, typically showing with increased progressive precipitation a trend to lower (~2149 to 1337) and more radiogenic (~2.79 to 3.34) values, respectively (Figure 4.9).The exceptions are for the 65:35 and 100 soluble fractions which yield Re-Os isotopic compositions similar to the whole oil and maltene fraction, respectively (Figure 4.9).

The $^{187}Re/^{188}Os$ and $^{187}Os/^{188}Os$ compositions of the RM8505 asphaltene fractions exhibit with progressively precipitation a trend to lower (~609 to 151) and less

radiogenic (~1.71 to 1.07) values, respectively (Figure 4.9). The whole oil, within uncertainty, possesses similar Re-Os isotopic compositions to the 80:20 and 85:15 precipitated fractions. Likewise, the 100 soluble fraction has an alike Re-Os isotopic composition to that of the maltene fraction.

4.3.3.3 Re-Os isotopic compositions of the asphaltene and maltene fractions separated by n-alkane-DCM-methanol

The $^{187}Os/^{188}Os$ values of the asphaltenes separated by the *n*-alkane-DCM-methanol protocol are very similar to each other and that of bulk separated asphaltene by *n*-heptane. The $^{187}Re/^{188}Os$ values of the asphaltene fractions are variable, but are generally similar to each other for the six oil samples (Figures 4.8 - 4.9).

The $^{187}Os/^{188}Os$ compositions of the maltene fractions separated by the *n*-alkane-DCM-methanol protocol for each oil sample are, including uncertainties, very similar. These values are lower than that of the whole oil. A trend to slightly more radiogenic $^{187}Os/^{188}Os$ values for the maltene fractions recovered from *n*-C_5 to *n*-C_{10} solutions is observed for all oils, with exception to the RM8505 and Viking-Morel oil sample. The $^{187}Re/^{188}Os$ values of the maltene fractions are higher than that of the bulk maltene from a *n*-heptane separation, but lower than the values for the whole oil. A general trend increasing $^{187}Re/^{188}Os$ values is observed for the maltene fractions precipitated from *n*-C_5 to *n*-C_8 and even to *n*-C_{10}.

4.4 Discussion

4.4.1 The residence of Re and Os in crude oil and asphaltene

4.4.1.1 Asphaltene is the main carrier of Re and Os of crude oil

The Re-Os analyses of the asphaltene and maltene fractions separated by both solely *n*-heptane and *n*-alkane-DCM-methanol solutions in this study demonstrate again that the asphaltene is the main carrier of Re and Os in crude oil (Selby et al., 2007; Rooney et al., 2012; Lillis and Selby, 2013; Cumming et al., 2014; Georgiev et al., 2016). When separated by solely *n*-heptane, the asphaltene fraction accounts for ≥ 78% Re (of Derby oil sample), and ≥ 71% Os (of Derby oil sample), which are lower than the values of Selby et al. (2007), i.e. >90 and 83% of the Re and Os, respectively. When separated by *n*-alkane-DCM-methanol solutions, the asphaltene fraction accounts for ≥ 64% Re (of Derby oil sample with *n*-hexane), and ≥ 57% Os (of

Federal oil sample with *n*-decane), which are comparable to the values of Georgiev et al. (2016), i.e. 55-79% Re and Os.

Also, consistent with a previous study (Mahdaoui et al., 2013), we observe that the first and/or second precipitated fractions of asphaltene by progressive precipitation possess a higher abundance of Re and Os, with a decrease in Re-Os abundance observed throughout the progressive precipitation (Figures 4.6 - 4.7). This finding may suggests a similar complexation in addition to distribution of Re and Os in crude oil.

4.4.1.2 The binding sites of Re and Os

Multiple heteroatomic complexes and stable porphyrins are proposed to be the host of Re and Os in crude oil (Selby and Creaser, 2003; Miller, 2004; Selby et al., 2007). Predominantly (90%) porphyrins are occluded into the asphaltene, with the remaining 10% occurring as free molecules in crude oil (Yarranton et al., 2013 and references therein). It is possible that these proposed Re and Os bearing species can be adsorbed and occluded into the asphaltene aggregates like many other compounds (Mujica et al., 2000; Liao et al., 2005; Liao et al., 2006b, a; Liao et al., 2009; Acevedo et al., 2012; Derakhshesh et al., 2013; Zhao et al., 2013; Liu et al., 2015; Castillo and Vargas, 2016; Snowdon et al., 2016; Evdokimov et al., 2017). Based on the understanding of asphaltene nanoaggregates, we propose that Re and Os may exist either as free stable porphyrins and/or multiple heteroatomic complexes, or bound by the asphaltene molecules directly, or by Re and Os bearing compounds occluded/absorbed by the asphaltene aggregates. The *n*-heptane bulk separated asphaltene captures the majority, but not all, of the largest aromatic components of a crude oil that aggregate (Mullins, 2011) and most structural units and functional groups can be identified in both the maltene and asphaltene fractions (Redelius, 2009). As such, although such structural and functional groups are limited in the maltene fraction, the Re and Os may exist in the same forms as in asphaltene, i.e. free compounds and occluded/absorbed molecules in large aromatic molecules.

4.4.1.3 Re and Os in the progressively precipitated asphaltene fractions

Clues of how Re and Os reside in asphaltene may be understood from the variation in abundance throughout the progressive precipitation and the controlling factors of the progressive precipitation. Multiple forces or factors are considered to control the

precipitation, of asphaltene, e.g., polarity, aromaticity, asphaltene molecular mass and aggregate size, and the roles of metal and porphyrin components (Groenzin et al., 2003; Porte et al., 2003; Spiecker et al., 2003; Gawrys et al., 2006; Stoyanov et al., 2008; Yin et al., 2008; Daaou et al., 2009; Redelius, 2009; Durand et al., 2010; Rogel et al., 2010; Petrova et al., 2013; Tavakkoli et al., 2014; Zhang et al., 2014; Liu et al., 2015; Ortega et al., 2015; Painter et al., 2015; Rogel et al., 2015). Asphaltene with a larger aggregate size or aromatic core is proposed to comprise the earlier precipitated asphaltene fractions. Further, a molecular size study reveals that the progressively precipitated fractions of asphaltene contain the same molecular species, but the ratio of each species in a given fraction varies (Groenzin et al., 2003). The N, S and O contents of an asphaltene are not enriched in any of the progressively precipitated asphaltene fractions. This suggests that polarity may not be the controlling factor of asphaltene precipitation, although some studies have shown the NSO contents do change throughout the progressive precipitation (Kaminski et al., 2000; Gawrys et al., 2006; Kharrat, 2009; Adebiyi and Thoss, 2014). Further, metals are considered to facilitate the aggregation and trigger the fluctuation of asphaltene, with the earlier precipitated asphaltene fraction being more metal enriched (Gawrys et al., 2006; Duyck et al., 2007), which is consistent for the abundance trends shown for Re and Os. The latter may suggest a strong affinity of Re and Os with asphaltene comprised of a larger aggregate size or aromatic core.

However, an exception to the overall decrease in Re and Os abundance with progressive precipitation is shown by three oils that precipitated asphaltene with a *n*-heptane-DCM ratio of 65:35. For the Federal, Viking-Morel and Persian oils the 65:35 asphaltene fraction possesses less Re and Os compared to the asphaltene that precipitated with a *n*-heptane-DCM ratio of 70:30 (Figures 4.6 - 4.7). The 65:35 asphaltene fraction of the Persian oil sample contains a colourless crystalline wax. Wax is also observed to co-precipitate with asphaltene during the bulk *n*-heptane separation of asphaltene (Thanh et al., 1999; Leontaritis, 2007; Sun et al., 2017). Typically, the wax consists mainly of linear alkanes and small amounts of branched alkanes and aromatic compounds (García, 2000; Speight, 2014), which are not likely to be a host for Re and Os, and this may be the reason of the low Re and Os abundances of the 65:35 fraction of the Persian asphaltene. It may also be the reason

of the lower Re and Os abundances of the first precipitated fractions of the Federal and Viking-Morel asphaltene.

Additionally, for the Viking-Morel, Persian and RM8505 oil samples, the decrease in Re abundance throughout the progressive precipitation is greater than that shown for Os (Figures 4.6 - 4.7). This suggests that the complexation of Os in crude oil is potentially more variable than for Re. This suggests the existence of different Re and Os bearing complexes in crude oil, and different adsorption/occlusion abilities by asphaltene aggregates and/or co-precipitation properties.

4.4.2 Insights to Re-Os behaviour in oil based on the Re-Os isotopic systematics of crude oil fractions

For all of the six crude oil samples in this study, differences in the $^{187}Re/^{188}Os$ and $^{187}Os/^{188}Os$ compositions exist between the whole oil, bulk separated asphaltene and maltene fractions solely by *n*-heptane, progressively precipitated asphaltene fractions by *n*-heptane-DCM solutions, and the asphaltene and maltene fractions separated by *n*-alkane-DCM-methanol solutions (Figures 4.8 - 4.9).

The $^{187}Re/^{188}Os$ values decrease throughout the progressive precipitation for the Viking-Morel, Persian and RM8505 oil samples which is related to the greater decrease in Re abundance compared to Os (Table 4.3; Figures 4.6 - 4.7). In contrast, the $^{187}Re/^{188}Os$ values increase throughout the progressive precipitation for the Purisima oil sample. And lastly, the $^{187}Re/^{188}Os$ values of the Derby and Federal oil samples show either no relationship with the progressive precipitation or have similar $^{187}Re/^{188}Os$ values, respectively. Although differences exist, the $^{187}Os/^{188}Os$ composition of the progressively precipitated asphaltene fractions are quite similar (e.g. Derby, Federal, Viking-Morel, and Purisima), with the exception of the Persian and RM8505 oil samples (Figures 4.8 - 4.9). These differences may relate to the migration of radiogenic ^{187}Os. For example, the Re abundance and $^{187}Re/^{188}Os$ values decrease throughout the progressive precipitation of the Viking-Morel oil sample, whereas the $^{187}Os/^{188}Os$ composition are the same within uncertainty, with the exception of the 100:0 fraction (Table 4.3; Figure 4.8). For this sample, the ^{187}Os is proportional to the ^{188}Os abundance and shows basically no relationship with the Re abundance. We suggest that the radiogenic ^{187}Os could decouple from the parent ^{187}Re and behaves similarly to the other Os isotopes. However, for the Persian oil

sample, although shows a decrease in $^{187}Re/^{188}Os$ values with progressive precipitation, the $^{187}Os/^{188}Os$ compositions become more radiogenic. As such, the ^{187}Os is not proportional to either the ^{187}Re or the ^{188}Os abundances. We consider that the radiogenic ^{187}Os has decoupled from the parent ^{187}Re and has migrated or become bound to particular fractions which are not as enriched in other Os isotopes. This may also be the case for the Purisima oil sample. Further, for the RM8505 oil sample, coupled with the decrease in $^{187}Re/^{188}Os$ values with progressive precipitation is also a trend to less radiogenic $^{187}Os/^{188}Os$ compositions (Figure 4.9). As such, the radiogenic ^{187}Os is proportional to the parent ^{187}Re rather than all other isotopes of Os. We suggest that the radiogenic ^{187}Os is likely still in the same/similar complexation location as the parent ^{187}Re following beta decay. This scenario is most likely to happen when the Re is predominantly housed in the asphaltene aggregates rather the free stable porphyrins and multiple heteroatomic complexes, the radiogenic ^{187}Os may still be trapped in the asphaltene aggregates, but not likely in the free molecules. The Re in the Persian and Viking-Morel oil samples should predominantly be in the free stable porphyrins and/or multiple heteroatomic complexes.

4.4.3 Re-Os geochronology from the fractions of crude oil

4.4.3.1 The Re-Os geochronology information obtained

In the study of Georgiev et al. (2016), the Re-Os data of fractions of a single oil were interpreted to determine a Re-Os age which define the timing of oil generation. Here, we discuss the application of the Re-Os isotope systematics of the asphaltene and maltene fractions separated by *n*-alkane-dichloromethane-methanol solutions for geochronology to the six crude oil samples in this study. In addition, we discuss the Re-Os geochronology with the *n*-heptane separated fractions (whole oil, bulk asphaltene, bulk maltene), the progressively precipitated fractions of asphaltene by *n*-heptane-DCM, and the fractions separated by *n*-alkane-DCM-methanol. The regression analysis using *Isoplot* v. 4.15 of the Re-Os isotopic data for these fractions for all oil samples are listed in Table 4.7.

Regardless of any combination of the crude oil fractions, no meaningful geological dates can be obtained systematically for every oil sample (Table 4.7). The most precise date values are obtained by the progressively precipitated fractions of

asphaltene of sample RM8505 (98.4 ± 9.5 Ma) and by the maltene fractions separated by *n*-alkane-DCM-methanol solutions for the Purisima sample (27.4 ± 8.7 Ma). In both cases the dates obtained are close to the deposition age of their source rocks (James, 1990, 2000; Isaacs and Rullkötter, 2001; Summa et al., 2003), respectively, rather than the timing of oil generation. The Re-Os data of a few fractions of the progressively precipitated asphaltene fractions of Derby and Purisima samples define Re-Os dates of 167 ± 51 Ma and 5.6 ± 2.5 Ma, which are close to their known (Lillis and Selby, 2013) or estimated oil generation age, respectively. However, such combinations cannot yield geologically meaningful Re-Os ages for the other samples of this study (Table 4.7).

4.4.3.2 Implication on Re-Os geochronology from the progressive precipitation of asphaltene

The observation of the similar $^{187}Re/^{188}Os$ and $^{187}Os/^{188}Os$ for the majority of the asphaltene fraction (Mahdaoui et al., 2013; this study) concludes that the sequential loss of asphaltene in natural petroleum systems will not greatly change the Re-Os isotopic systematics of crude oil, and thus will not impede the application of Re-Os geochronology on petroleum samples. However, both changes of $^{187}Re/^{188}Os$ and $^{187}Os/^{188}Os$ compositions are observed in the six samples of this study during the progressive precipitation with similar mixture of DCM and *n*-heptane versus DCM and *n*-pentane. For the instances which a difference exists in $^{187}Re/^{188}Os$ and/or $^{187}Os/^{188}Os$ composition among the solubility class of asphaltene, the precipitated fractions containing different Re-Os isotopic systematics to the remaining crude oil will certainly lead to the change of $^{187}Re/^{188}Os$ and/or $^{187}Os/^{188}Os$ compositions of the whole oil. The effect of precipitation will depend on the degree of the loss of asphaltene, the relative abundances of Re and Os in the precipitates to the remaining fraction and how different the isotopic systematics are between the two.

The similarity of the $^{187}Os/^{188}Os$ composition and difference of the $^{187}Re/^{188}Os$ value of the progressively precipitated asphaltene fractions for some crude oils may provide the chance of dating the natural events associated with the precipitation of asphaltene, e.g., injection of gas (methane and carbon dioxide) originated from mantle degassing, metamorphic reactions or magmatic processes.

The heterogeneous Re-Os isotopic systematics inside a single oil sample and asphaltene is observed through the progressive precipitation of asphaltene and the *n*-alkane separation of crude oil for many samples. In presenting this heterogeneity, separating the crude oil or asphaltene with a binary mixture such as DCM and *n*-heptane seems to be a more powerful methodology than separating crude oil with different *n*-alkane (*n*-C_5, *n*-C_6, *n*-C_7, *n*-C_8, *n*-C_9 and *n*-C_{10}).

4.4.3.3 Implication on Re-Os geochronology from the asphaltene and maltene fractions separated by n-alkane-DCM-methanol solutions

The asphaltene yields are shown to decrease with the increase of *n*-alkane C number in some studies (Buenrostro-Gonzalez et al., 2004; Georgiev et al., 2016). However, in this study (Figure 4.5) and some other studies (Figure 1, Mitchell and Speight, 1973; Figure 6, Corbett and Petrossi, 1978; Haji-Akbari et al., 2015), the asphaltene yields decrease from *n*-C_5 to *n*-C_7, and then level off from approximately *n*-C_7 onwards to *n*-C_{10}. The maltene yields vary according to the change of asphaltene yields and also the influence of water contents (e.g. the Purisima sample).

However, the different asphaltene yields have limited influence on the asphaltene Re-Os elemental and isotopic systematics. The Re and Os abundance increase with the decrease of asphaltene yields, with the $^{187}Os/^{188}Os$ (± 2%) remaining almost unchanged and the $^{187}Re/^{188}Os$ (± 5%) show a small change. As stated above, the $^{187}Re/^{188}Os$ and $^{187}Os/^{188}Os$ of the *n*-alkane asphaltene fractions for all of the six samples cannot define a meaningful Re-Os age.

The change on the Re-Os elemental and isotopic systematics of the maltene fractions by different *n*-alkane is more prominent than for the asphaltene fractions. The maltene fractions Re and Os abundances increase with the increase of C number of the *n*-alkane used as the precipitant. The maltene fractions exhibit greater variation in their $^{187}Re/^{188}Os$ (± 35%) and $^{187}Os/^{188}Os$ (± 17%) compositions than the asphaltene fractions (Figures 4.8 - 4.9). However, only the Purisima maltene fractions determine a Model 1 best-fit line giving a Re-Os date of 27.4 ± 8.7, which is close to the age of the source rock (Figure 4.9). None of the remaining maltene fractions determine any meaningful Re-Os dates. The asphaltene and maltene fractions of Persian and RM8505 oils determine best-fit lines give Re-Os dates of 26 ± 10 Ma and 86 ± 18 Ma, respectively, being close to the age of source rock (Figure

4.9). However, the asphaltene and maltene fractions are basically two distinct clusters.

The same is true for the three samples of Georgiev et al. (2016). The Re-Os isotopic systematics of the asphaltene series of each of the three samples are very similar and cannot determine any geologically meaningful Re-Os dates. Only the maltene fractions of one out of the three oil samples were able to define a Re-Os date that was interpreted as the best estimate of the timing of oil generation age by the authors.

Obtaining Re-Os geochronology information from one single oil sample is a desirable approach considering the uncertainties and complex situation of multiple samples Re-Os dating, even though the problems of multiple samples methodology can also be true for the single oil methodology, i.e. mixing source and the effect of alteration on the Re-Os isotopic systematics within a crude oil. Utilizing this heterogeneity to obtain geochronology information and further the understanding of the residence of Re and Os in crude oil are nevertheless desirable goals.

4.5 Conclusion

In this study, Re-Os measurements were taken on six crude oil samples and their fractions. The crude oils were firstly separated by *n*-heptane into asphaltene and maltene fractions and then the asphaltene fractions were further progressively precipitated using mixtures of dichloromethane and *n*-heptane. The crude oils were also separated into asphaltene and maltene fractions by *n*-pentane, *n*-hexane, *n*-heptane, *n*-octane, *n*-nonane and *n*-decane by using a mix of dichloromethane and methanol.

Consistent with previous studies, asphaltene fractions are the main carrier of Re and Os in crude oil, no matter if separated solely by *n*-heptane or by *n*-alkane-dichloromethane-methanol solutions. The Re and Os abundance of the fractions of asphaltene decreases throughout the progressive precipitation, with the except to the first precipitate containing wax for the Persian, Federal and Viking-Morel oil samples. Throughout the progressive precipitation, both the $^{187}Re/^{188}Os$ and the $^{187}Os/^{188}Os$ values can remain constant, decrease or increase for the six samples – no consistent pattern is observed. Based on the proposed binding sites of Re and Os in crude oil and the structure of asphaltene, this study propose that the Re and Os in crude oil are to be bound in multiple free compounds, e.g. stable porphyrins and

molecules with heteroatomic ligands, and such molecules occluded/absorbed in the asphaltene aggregate structure. Further, the radiogenic ^{187}Os may decouple from the parent ^{187}Re during the progressive precipitation if the majority of the decay from ^{187}Re to ^{187}Os happens from Re bound to free asphaltene compounds rather than inside the asphaltene aggregates.

However, no combinations of the fractions of a single crude oil can consistently yield a geologically meaningful Re-Os age for each one of the six oil samples of this study. Therefore, the extensive application of using a single oil to obtain meaningful geological dates related to the petroleum system may not be fully viable.

4.6 References

Acevedo, S., K. Guzmán, H. Labrador, H. Carrier, B. Bouyssiere, and R. Lobinski, 2012, Trapping of metallic porphyrins by asphaltene aggregates: a size exclusion microchromatography with high-resolution inductively coupled plasma mass spectrometric detection study: Energy & Fuels, v. 26, no. 8, p. 4968-4977.

Adebiyi, F. M., and V. Thoss, 2014, Organic and elemental elucidation of asphaltene fraction of Nigerian crude oils: Fuel, v. 118, p. 426-431.

Alboudwarej, H., W. Svrcek, H. Yarranton, and K. Akbarzadeh, 2001, Asphaltene Characterization: Sensitivity of Asphaltene Properties to Extration Techniques, Canadian International Petroleum Conference: Calgary, Alberta, Petroleum Society of Canada, p. 11.

Álvarez, E., F. Trejo, G. Marroquín, and J. Ancheyta, 2015, The Effect of Solvent Washing on Asphaltenes and Their Characterization: Petroleum Science and Technology, v. 33, no. 3, p. 265-271.

Barre, A., A. Prinzhofer, and C. Allegre, 1995, Osmium isotopes in the organic matter of crude oil and asphaltenes: Terra Abs, v. 7, p. 199.

Buenrostro-Gonzalez, E., C. Lira-Galeana, A. Gil-Villegas, and J. Wu, 2004, Asphaltene precipitation in crude oils: Theory and experiments: AIChE Journal, v. 50, no. 10, p. 2552-2570.

Castillo, J., and V. Vargas, 2016, Metal porphyrin occlusion: Adsorption during asphaltene aggregation: Petroleum Science and Technology, v. 34, no. 10, p. 873-879.

Clayton, J. L., A. Warden, T. A. Daws, P. G. Lillis, G. E. Michael, and M. Dawson, 1992, Organic geochemistry of black shales, marlstones, and oils of Middle Pennsylvanian rocks from the northern Denver and southeastern Powder River basins, Wyoming, Nebraska, and Colorado, 1917K.

Corbett, L. W., and U. Petrossi, 1978, Differences in distillation and solvent separated asphalt residua: Industrial & Engineering Chemistry Product Research and Development, v. 17, no. 4, p. 342-346.

Cumming, V. M., D. Selby, P. G. Lillis, and M. D. Lewan, 2014, Re–Os geochronology and Os isotope fingerprinting of petroleum sourced from a Type I lacustrine kerogen: Insights from the natural Green River petroleum system in the Uinta Basin and hydrous pyrolysis experiments: Geochimica et Cosmochimica Acta, v. 138, p. 32-56.

Daaou, M., D. Bendedouch, Y. Bouhadda, L. Vernex-Loset, A. Modaressi, and M. Rogalski, 2009, Explaining the Flocculation of Hassi Messaoud Asphaltenes in Terms of Structural Characteristics of Monomers and Aggregates: Energy & Fuels, v. 23, no. 11, p. 5556-5563.

Derakhshesh, M., A. Bergmann, and M. R. Gray, 2013, Occlusion of Polyaromatic Compounds in Asphaltene Precipitates Suggests Porous Nanoaggregates: Energy & Fuels, v. 27, no. 4, p. 1748-1751.

Dimarzio, J. M., S. V. Georgiev, H. J. Stein, and J. L. Hannah, 2016, Residence of Rhenium and Osmium (Re-Os) within asphaltene and maltene sub-fractions of a heavy crude oil (abs.), GSA Annual Meeting: Denver, Colorado, USA.

Durand, E., M. Clemancey, J. M. Lancelin, J. Verstraete, D. Espinat, and A. A. Quoineaud, 2010, Effect of Chemical Composition on Asphaltenes Aggregation: Energy & Fuels, v. 24, no. 2, p. 1051-1062.

Duyck, C., N. Miekeley, C. L. Porto da Silveira, R. Q. Aucélio, R. C. Campos, P. Grinberg, and G. P. Brandão, 2007, The determination of trace elements in crude oil and its heavy fractions by atomic spectrometry: Spectrochimica Acta Part B: Atomic Spectroscopy, v. 62, no. 9, p. 939-951.

Eadington, P., P. Hamilton, and G. Bai, 1991, Fluid history analysis - A new concept for prospect evaluation: Australian Petroleum Exploration Association Journal, v. 31, no. 1, p. 282-294.

Evdokimov, I. N., A. A. Fesan, and A. P. Losev, 2017, Occlusion of Foreign Molecules in Primary Asphaltene Aggregates from Near-UV–Visible Absorption Studies: Energy & Fuels, v. 31, no. 2, p. 1370-1375.

Finlay, A. J., D. Selby, and M. J. Osborne, 2011, Re-Os geochronology and fingerprinting of United Kingdom Atlantic Margin oil: Temporal implications for regional petroleum systems: Geology, v. 39, no. 5, p. 475-478.

Finlay, A. J., D. Selby, and M. J. Osborne, 2012, Petroleum source rock identification of United Kingdom Atlantic Margin oil fields and the Western Canadian Oil Sands using Platinum, Palladium, Osmium and Rhenium: Implications for global petroleum systems: Earth and Planetary Science Letters, v. 313-314, p. 95-104.

García, M. d. C., 2000, Crude Oil Wax Crystallization. The Effect of Heavy n-Paraffins and Flocculated Asphaltenes: Energy & Fuels, v. 14, no. 5, p. 1043-1048.

Gawrys, K. L., G. A. Blankenship, and P. K. Kilpatrick, 2006, On the Distribution of Chemical Properties and Aggregation of Solubility Fractions in Asphaltenes: Energy & Fuels, v. 20, no. 2, p. 705-714.

Ge, X., C. Shen, D. Selby, D. Deng, and L. Mei, 2016, Apatite fission-track and Re-Os geochronology of the Xuefeng uplift, China: Temporal implications for dry gas associated hydrocarbon systems: Geology, v. 44, no. 6, p. 491-494.

Georgiev, S. V., H. J. Stein, J. L. Hannah, R. Galimberti, M. Nali, G. Yang, and A. Zimmerman, 2016, Re-Os dating of maltenes and asphaltenes within single samples of crude oil: Geochimica et Cosmochimica Acta, v. 179, p. 53-75.

Gramlich, J. W., T. J. Murphy, E. L. Garner, and W. R. Shields, 1973, Absolute isotopic abundance ratio and atomic weight of a reference sample of rhenium: J. Res. Natl. Bur. Stand. A, v. 77, p. 691-698.

Gray, M. R., R. R. Tykwinski, J. M. Stryker, and Tan, X., 2011, Supramolecular Assembly Model for Aggregation of Petroleum Asphaltenes: Energy & Fuels, v. 25, no. 7, p. 3125-3134.

Groenzin, H., O. C. Mullins, S. Eser, J. Mathews, M. G. Yang, and D. Jones, 2003, Molecular Size of Asphaltene Solubility Fractions: Energy & Fuels, v. 17, no. 2, p. 498-503.

Gürgey, K., 1998, Geochemical effects of asphaltene separation procedures: changes in sterane, terpane, and methylalkane distributions in maltenes and asphaltene co-precipitates: Organic Geochemistry, v. 29, no. 5, p. 1139-1147.

Haji-Akbari, N., P. Teeraphapkul, A. T. Balgoa, and H. S. Fogler, 2015, Effect of n-Alkane Precipitants on Aggregation Kinetics of Asphaltenes: Energy & Fuels, v. 29, no. 4, p. 2190-2196.

Isaacs, C. M., and J. Rullkötter, 2001, The Monterey Formation: From Rocks to Molecules, New York, Columbia University Press, 553 p.

James, K., 1990, The Venezuelan hydrocarbon habitat: Geological Society, London, Special Publications, v. 50, no. 1, p. 9-35.

James, K., 2000, The Venezuelan hydrocarbon habitat, part 1: tectonics, structure, palaeogeography and source rocks: Journal of Petroleum Geology, v. 23, no. 1, p. 5-53.

Kaminski, T. J., H. S. Fogler, N. Wolf, P. Wattana, and A. Mairal, 2000, Classification of Asphaltenes via Fractionation and the Effect of Heteroatom Content on Dissolution Kinetics: Energy & Fuels, v. 14, no. 1, p. 25-30.

Kharrat, A. M., 2009, Characterization of Canadian Heavy Oils Using Sequential Extraction Approach: Energy & Fuels, v. 23, no. 2, p. 828-834.

Leontaritis, K. J., 2007, The Asphaltene and Wax Deposition Envelopes: Fuel Science and Technology International, v. 14, no. 1-2, p. 13-39.

Liao, Z., A. Geng, A. Graciaa, P. Creux, A. Chrostowska, and Y. Zhang, 2006a, Different Adsorption/Occlusion Properties of Asphaltenes Associated with Their Secondary Evolution Processes in Oil Reservoirs: Energy & Fuels, v. 20, no. 3, p. 1131-1136.

Liao, Z., A. Geng, A. Graciaa, P. Creux, A. Chrostowska, and Y. Zhang, 2006b, Saturated hydrocarbons occluded inside asphaltene structures and their geochemical significance, as exemplified by two Venezuelan oils: Organic Geochemistry, v. 37, no. 3, p. 291-303.

Liao, Z., J. Zhao, P. Creux, and C. Yang, 2009, Discussion on the Structural Features of Asphaltene Molecules: Energy & Fuels, v. 23, no. 12, p. 6272-6274.

Liao, Z. W., H. G. Zhou, A. Graciaa, A. Chrostowska, P. Creux, and A. Geng, 2005, Adsorption/occlusion characteristics of asphaltenes: Some implication for asphaltene structural features: Energy & Fuels, v. 19, no. 1, p. 180-186.

Lillis, P. G., and D. Selby, 2013, Evaluation of the rhenium–osmium geochronometer in the Phosphoria petroleum system, Bighorn Basin of Wyoming and Montana, USA: Geochimica et Cosmochimica Acta, v. 118, p. 312-330.

Liu, H., C. Lin, Z. Wang, A. Guo, and K. Chen, 2015, Ni, V, and Porphyrinic V Distribution and Its Role in Aggregation of Asphaltenes: Journal of Dispersion Science and Technology, v. 36, no. 8, p. 1140-1146.

Mahdaoui, F., L. Reisberg, R. Michels, Y. Hautevelle, Y. Poirier, and J.P. Girard, 2013, Effect of the progressive precipitation of petroleum asphaltenes on the Re–Os radioisotope system: Chemical Geology, v. 358, p. 90-100.

Mark, D. F., J. Parnell, S. P. Kelley, M. Lee, S. C. Sherlock, and A. Carr, 2005, Dating of multistage fluid flow in sandstones: Science, v. 309, no. 5743, p. 2048-2051.

Mark, D. F., J. Parnell, S. P. Kelley, M. R. Lee, and S. C. Sherlock, 2010, $^{40}Ar/^{39}Ar$ dating of oil generation and migration at complex continental margins: Geology, v. 38, no. 1, p. 75-78.

Miller, C. A., 2004, Re-Os dating of algal laminites reduction-enrichment of metals in the sedimentary environment and evidence for new geoporphyrins: Master of Science Dissertation, University of Saskatchewan, Saskatoon, Canada, 153 p.

Mitchell, D. L., and J. G. Speight, 1973, The solubility of asphaltenes in hydrocarbon solvents: Fuel, v. 52, no. 2, p. 149-152.

Mujica, V., P. Nieto, L. Puerta, and S. Acevedo, 2000, Caging of Molecules by Asphaltenes. A Model for Free Radical Preservation in Crude Oils: Energy & Fuels, v. 14, no. 3, p. 632-639.

Mullins, O. C., 2010, The Modified Yen Model: Energy & Fuels, v. 24, no. 4, p. 2179-2207.

Mullins, O. C., H. Sabbah, J. Eyssautier, A. E. Pomerantz, L. Barré, A. B. Andrews, Y. Ruiz-Morales, F. Mostowfi, R. McFarlane, L. Goual, R. Lepkowicz, T. Cooper, J. Orbulescu, R. M. Leblanc, J. Edwards, and R. N. Zare, 2012, Advances in Asphaltene Science and the Yen–Mullins Model: Energy & Fuels, v. 26, no. 7, p. 3986-4003.

Nairn, A., and A. Alsharhan, 1997, Sedimentary basins and petroleum geology of the Middle East, Amsterdam, Elsevier, 943 p.

Nalwaya, V., V. Tantayakom, P. Piumsomboon, and S. Fogler, 1999, Studies on Asphaltenes through Analysis of Polar Fractions: Industrial & Engineering Chemistry Research, v. 38, no. 3, p. 964-972.

Ortega, L. C., E. Rogel, J. Vien, C. Ovalles, H. Guzman, F. Lopez-Linares, and P. Pereira-Almao, 2015, Effect of Precipitating Conditions on Asphaltene Properties and Aggregation: Energy & Fuels, v. 29, no. 6, p. 3664-3674.

Painter, P., B. Veytsman, and J. Youtcheff, 2015, Asphaltene Aggregation and Solubility: Energy & Fuels, v. 29, no. 4, p. 2120-2133.

Petrova, L., N. Abbakumova, D. Borisov, M. Yakubov, I. Zaidullin, and G. Romanov, 2013, Interrelation of Flocculation, Precipitation, and Structure of Asphaltene Fractions: Chemistry and Technology of Fuels and Oils, v. 49, no. 1, p. 25-31.

Peyton, S. L., and B. Carrapa, 2013, An Introduction to Low-temperature Thermochronologic Techniques, Methodology, and Applications, in C. Knight, and J. Cuzella, eds., Application of structural methods to Rocky Mountain hydrocarbon exploration and development, Volume 65, p. 15-36.

Poplavko, Y., V. Ivanov, T. Karasik, A. Miller, V. Orekhov, S. Taliyev, Y. Tarkhov, and V. Fadeyeva, 1974, On the concentration of rhenium in petroleum, petroleum bitumens and oil shales: Geochemistry International, v. 11, no. 5, p. 969-972.

Porte, G., H. G. Zhou, and V. Lazzeri, 2003, Reversible description of asphaltene colloidal association and precipitation: Langmuir, v. 19, no. 1, p. 40-47.

Redelius, P., 2009, Asphaltenes in bitumen, what they are and what they are not: Road Materials and Pavement Design, v. 10, no. sup1, p. 25-43.

Rogel, E., C. Ovalles, and M. Moir, 2010, Asphaltene Stability in Crude Oils and Petroleum Materials by Solubility Profile Analysis: Energy & Fuels, v. 24, no. 8, p. 4369-4374.

Rogel, E., M. Roye, J. Vien, and T. Miao, 2015, Characterization of Asphaltene Fractions: Distribution, Chemical Characteristics, and Solubility Behavior: Energy & Fuels, v. 29, no. 4, p. 2143-2152.

Rooney, A. D., D. Selby, M. D. Lewan, P. G. Lillis, and J. P. Houzay, 2012, Evaluating Re–Os systematics in organic-rich sedimentary rocks in response to petroleum generation using hydrous pyrolysis experiments: Geochimica et Cosmochimica Acta, v. 77, p. 275-291.

Selby, D., R. Creaser, K. Dewing, and M. Fowler, 2005, Evaluation of bitumen as a Re–Os geochronometer for hydrocarbon maturation and migration: A test case from the Polaris MVT deposit, Canada: Earth and Planetary Science Letters, v. 235, no. 1-2, p. 1-15.

Selby, D., and R. A. Creaser, 2005, Direct radiometric dating of hydrocarbon deposits using rhenium-osmium isotopes: Science, v. 308, no. 5726, p. 1293-1295.

Selby, D., R. A. Creaser, and M. G. Fowler, 2007, Re–Os elemental and isotopic systematics in crude oils: Geochimica et Cosmochimica Acta, v. 71, no. 2, p. 378-386.

Snowdon, L. R., J. K. Volkman, Z. Zhang, G. Tao, and P. Liu, 2016, The organic geochemistry of asphaltenes and occluded biomarkers: Organic Geochemistry, v. 91, p. 3-15.

Speight, J. G., 2004, Petroleum Asphaltenes-Part 1: Asphaltenes, resins and the structure of petroleum: Oil & gas science and technology, v. 59, no. 5, p. 467-477.

Speight, J. G., 2014, The chemistry and technology of petroleum, CRC press.

Spiecker, P. M., K. L. Gawrys, and P. K. Kilpatrick, 2003, Aggregation and solubility behavior of asphaltenes and their subfractions: Journal of Colloid and Interface Science, v. 267, no. 1, p. 178-193.

Stoyanov, S. R., S. Gusarov, and A. Kovalenko, 2008, Multiscale modelling of asphaltene disaggregation: Molecular Simulation, v. 34, no. 10-15, p. 953-960.

Subramanian, S., S. Simon, and J. Sjöblom, 2016, Asphaltene Precipitation Models: A Review: Journal of Dispersion Science and Technology, v. 37, no. 7, p. 1027-1049.

Summa, L., E. Goodman, M. Richardson, I. Norton, and A. Green, 2003, Hydrocarbon systems of Northeastern Venezuela: plate through molecular scale-analysis of the genesis and evolution of the Eastern Venezuela Basin: Marine and Petroleum Geology, v. 20, no. 3, p. 323-349.

Sun, W., W. Wang, Y. Gu, X. Xu, and J. Gong, 2017, Study on the wax/asphaltene aggregation with diffusion limited aggregation model: Fuel, v. 191, p. 106-113.

Tavakkoli, M., S. R. Panuganti, V. Taghikhani, M. R. Pishvaie, and W. G. Chapman, 2014, Understanding the polydisperse behavior of asphaltenes during precipitation: Fuel, v. 117, Part A, p. 206-217.

Thanh, N. X., M. Hsieh, and R. P. Philp, 1999, Waxes and asphaltenes in crude oils: Organic Geochemistry, v. 30, no. 2-3, p. 119-132.

Weiss, H., A. Wilhelms, N. Mills, J. Scotchmer, P. Hall, K. Lind, and T. Brekke, 2000, NIGOGA-The Norwegian Industry Guide to Organic Geochemical Analyses: Norsk Hydro, Statoil, Geolab Nor, SINTEF Petroleum Research and the Norwegian Petroleum Directorate, 102 p.

Welte, D. H., B. Horsfield, and D. R. Baker, 2012, Petroleum and basin evolution: insights from petroleum geochemistry, geology and basin modeling, Springer Science & Business Media.

Yarranton, H. W., D. P. Ortiz, D. M. Barrera, E. N. Baydak, L. Barré, D. Frot, J. Eyssautier, H. Zeng, Z. Xu, G. Dechaine, M. Becerra, J. M. Shaw, A. M. McKenna, M. M. Mapolelo, C. Bohne, Z. Yang, and J. Oake, 2013, On the Size Distribution of Self-Associated Asphaltenes: Energy & Fuels, v. 27, no. 9, p. 5083-5106.

Yin, C. X., X. Tan, K. Müllen, J. M. Stryker, and M. R. Gray, 2008, Associative π−π Interactions of Condensed Aromatic Compounds with Vanadyl or Nickel Porphyrin Complexes Are Not Observed in the Organic Phase: Energy & Fuels, v. 22, no. 4, p. 2465-2469.

Zhang, L. L., G. H. Yang, J. Q. Wang, Y. Li, L. Li, and C. H. Yang, 2014, Study on the polarity, solubility, and stacking characteristics of asphaltenes: Fuel, v. 128, p. 366-372.

Zhao, X., Y. Liu, C. Xu, Y. Yan, Y. Zhang, Q. Zhang, S. Zhao, K. Chung, M. R. Gray, and Q. Shi, 2013, Separation and Characterization of Vanadyl Porphyrins in Venezuela Orinoco Heavy Crude Oil: Energy & Fuels, v. 27, no. 6, p. 2874-2882.

Table 4.1 Details of the bulk asphaltene, solvent/precipitant volume and the progressively precipitated fractions of asphaltene.

Sample	asphaltene content (%)	asphaltene adopted (g)	DCM + *n*-C_7 (ml)	fractions (*n*-C_7: DCM) (g)									sum (g)	sum (%)
				65:35	70:30	75:25	80:20	85:15	90:10	95:5	100:0	soluble		
Derby	5.8	3.9620	250	0.0000	0.7397	0.8014	0.4824	0.3753	0.4572	0.2032	0.5561	0.3564	3.9716	100.2
Federal	11.9	2.4159	200	0.0727	0.4624	0.2071	0.3239	0.1849	0.3064	0.2211	0.2612	0.4390	2.4787	102.6
Viking-Morel	8.6	2.6435	200	0.1786	0.4300	0.3100	0.3660	0.2122	0.2491	0.1366	0.2321	0.5673	2.6819	101.5
Purisima	16.1	2.2225	200	0.0352	0.3642	0.2834	0.1544	0.3579	0.2070	0.2433	0.2562	0.3666	2.2683	102.1
Persian	5.7	4.0956	250	0.2234	0.5023	0.8012	0.6563	0.5945	0.1956	0.4817	0.3631	0.2815	4.0995	100.1
RM8505	12.8	2.5800	50	0.0000	1.3992	0.1956	0.2077	0.0847	0.1209	0.0561	0.0479	0.3740	2.4860	96.4

Table 4.2 The separation of crude oils by *n*-alkanes (*n*-C_5, *n*-C_6, *n*-C_7, *n*-C_8, *n*-C_9 and *n*-C_{10}) and dichloromethane and methanol of Derby, Federal, Viking-Morel, Persian, Purisima and RM8505 oil samples.

Alkanes	oil (g)	Asphalene (g)	Asphaltene (%)	Maltene (g)	Maltene (%)	Lost (%)
Derby oil						
n-C_5	0.99496	0.06312	6.3	0.75895	76.3	17.4
n-C_6	0.99726	0.04972	5.0	0.70854	71.0	24.0
n-C_7	1.01089	0.05117	5.1	0.82369	81.5	13.5
n-C_8	1.12069	0.05545	4.9	0.91910	82.0	13.0
n-C_9	1.11289	0.05437	4.9	0.91384	82.1	13.0
n-C_{10}	1.01597	0.04958	4.9	0.85195	83.9	11.3
Federal oil						
n-C_5	0.98687	0.10435	10.6	0.62743	63.6	25.8
n-C_6	1.00850	0.08491	8.4	0.79873	79.2	12.4
n-C_7	0.96435	0.07498	7.8	0.77333	80.2	12.0
n-C_8	0.96546	0.07049	7.3	0.77422	80.2	12.5
n-C_9	0.96236	0.07123	7.4	0.77299	80.3	12.3
n-C_{10}	1.03674	0.07468	7.2	0.82562	79.6	13.2
Viking-Morel oil						
n-C_5	0.99882	0.08070	8.1	0.72507	72.6	19.3
n-C_6	1.00929	0.06901	6.8	0.75534	74.8	18.3
n-C_7	1.00585	0.06473	6.4	0.7536	74.9	18.6
n-C_8	1.01179	0.06374	6.3	0.75964	75.1	18.6
n-C_9	1.05958	0.06287	5.9	0.79222	74.8	19.3
n-C_{10}	1.00253	0.05951	5.9	0.75509	75.3	18.7
Purisima oil						
n-C_5	1.00860	0.12887	12.8	0.47412	47.0	40.2
n-C_6	1.01059	0.11445	11.3	0.52489	51.9	36.7
n-C_7	1.00100	0.07989	8.0	0.38971	38.9	53.1
n-C_8	1.00107	0.08107	8.1	0.42302	42.3	49.6
n-C_9	1.03770	0.08064	7.8	0.45279	43.6	48.6
n-C_{10}	1.00403	0.10430	10.4	0.34919	34.8	54.8

To be continued.

Continue:

Alkanes	oil (g)	Asphalene (g)	Asphaltene (%)	Maltene (g)	Maltene (%)	Lost (%)
Persian oil						
n-C_5	0.99286	0.05135	5.2	0.68212	68.7	26.1
n-C_6	0.99885	0.04280	4.3	0.68706	68.8	26.9
n-C_7	1.00035	0.03586	3.6	0.69802	69.8	26.6
n-C_8	1.00058	0.03527	3.5	0.68989	68.9	27.5
n-C_9	1.00015	0.03465	3.5	0.68988	69.0	27.6
n-C_{10}	0.99429	0.03453	3.5	0.69784	70.2	26.3
RM8505 oil						
n-C_5	1.00373	0.09846	9.8	0.87147	86.8	3.4
n-C_6	1.19398	0.10209	8.6	1.04103	87.2	4.3
n-C_7	0.90893	0.06147	6.8	0.80135	88.2	5.1
n-C_8	0.983	0.08358	8.5	0.86275	87.8	3.7
n-C_9	0.97629	0.06405	6.6	0.85379	87.5	6.0
n-C_{10}	1.06586	0.08740	8.2	0.94822	89.0	2.8

Table 4.3 Re-Os data synopsis for the progressively precipitated asphaltene fractions and the whole oil, *n*-heptane asphaltene and maltene for the six oils. The mass balance calculation of Re, unradiogenic Os (^{192}Os) and radiogenic ^{187}Os for the progressive precipitation is also presented. See text for discussion.

Sample	Re (ppb)	±	Os (ppt)	±	^{192}Os (ppt)	±	^{187}Re/ ^{188}Os	±	^{187}Os/ ^{188}Os	±	rho	fraction (%)	Re (ppb) [a]	^{192}Os (ppt) [a]	^{187}Os (ppt) [b]
Derby oil															
70:30	244.2	0.7	2756	16	832.7	3.5	583	3	2.94	0.02	0.61	18.7	45.6	155.4	144.2
75:25	218.9	0.6	2407	14	724.0	3.2	601	3	2.99	0.02	0.61	20.2	44.3	146.4	138.1
80:20	195.7	0.5	2143	13	643.9	2.9	605	3	3.00	0.02	0.62	12.2	23.8	78.4	74.2
85:15	177.4	0.5	1926	12	579.0	2.7	610	3	2.99	0.02	0.63	9.5	16.8	54.8	51.8
90:10	144.9	0.4	1609.7	9.5	483.8	2.1	596	3	2.99	0.02	0.62	11.5	16.7	55.8	52.8
95:5	125.3	0.3	1389.6	8.5	419.0	1.9	595	3	2.96	0.02	0.62	5.1	6.4	21.5	20.1
100:0	65.3	0.2	773.9	4.6	233.3	1.0	556	3	2.96	0.02	0.63	14.0	9.2	32.7	30.6
100:0 soluble	8.2	0.1	107.9	1.3	32.6	0.6	500	9	2.94	0.06	0.76	9.0	0.7	2.9	2.7
whole oil	12.1	0.1	149.7	2.3	45.6	0.9	529	11	2.84	0.08	0.67	Sum [c]:			
asphaltene	164.1	0.5	1827	11	549.0	2.5	595	3	2.99	0.02	0.62	100.2	163.5	548.1	514.5
maltene	1.2	0.0	18.2	0.6	5.5	0.4	429	33	2.96	0.24	0.75	Recovery [d]:	99.6%	99.8%	99.1%

To be continued.

Continue:

Sample	Re (ppb)	±	Os (ppt)	±	^{192}Os (ppt)	±	^{187}Re/ ^{188}Os	±	^{187}Os/ ^{188}Os	±	rho	fraction (%)	Re (ppb) [a]	^{192}Os (ppt) [a]	^{187}Os (ppt) [b]
Federal oil															
65:35	68.1	0.2	436.4	3.3	118.1	0.8	1148	8	4.15	0.03	0.76	3.0	2.1	3.6	4.7
70:30	113.5	0.3	665.7	4.1	179.7	0.7	1256	6	4.19	0.02	0.62	19.1	21.7	34.4	45.5
75:25	90.0	0.3	567.6	5.0	156.3	1.3	1145	10	3.95	0.04	0.72	8.6	7.7	13.4	16.7
80:20	86.5	0.2	548.8	3.5	149.8	0.6	1148	6	4.06	0.02	0.64	13.4	11.6	20.1	25.7
whole oil	8.0	0.0	55.5	1.0	15.0	0.4	1063	29	4.19	0.14	0.78	Sum [c]:			
asphaltene	59.4	0.2	387.0	3.1	104.1	0.7	1134	8	4.23	0.04	0.73	44.1	43.1	67.9	88.0
maltene	1.1	0.0	13.3	0.7	3.8	0.4	577	67	3.50	0.48	0.76	Recovery [d]:	72.6%	65.2%	63.3%

To be continued.

Continue:

Sample	Re (ppb)	±	Os (ppt)	±	^{192}Os (ppt)	±	^{187}Re/ ^{188}Os	±	^{187}Os/ ^{188}Os	±	rho	fraction (%)	Re (ppb) [a]	^{192}Os (ppt) [a]	^{187}Os (ppt) [b]
Viking-Morel oil															
65:35	178.5	0.4	2289	12	686.6	2.5	517	2	3.01	0.02	0.59	6.8	12.1	46.4	44.2
70:30	201.1	0.5	2576	14	773.0	2.7	518	2	3.01	0.02	0.58	16.3	32.7	125.7	119.5
75:25	185.0	0.5	2390	13	717.9	2.6	513	2	3.00	0.02	0.59	11.7	21.7	84.2	79.8
80:20	167.4	0.4	2209	12	663.7	2.5	502	2	2.99	0.02	0.59	13.8	23.2	91.9	86.9
85:15	146.8	0.4	2000	11	601.3	2.4	486	2	2.99	0.02	0.60	8.0	11.8	48.3	45.6
90:10	122.0	0.3	1744	10	524.7	2.3	463	2	2.98	0.02	0.61	9.4	11.5	49.4	46.6
95:5	100.0	0.3	1476.0	9.9	443.4	2.4	448	3	3.00	0.02	0.64	5.2	5.2	22.9	21.7
100:0	63.7	0.2	996.7	8.8	301.3	2.6	421	4	2.93	0.04	0.68	8.8	5.6	26.5	24.5
100:0 soluble	5.4	0.0	153.9	1.5	46.2	0.5	230	3	3.00	0.04	0.61	21.5	1.1	9.9	9.4
whole oil	12.3	0.0	173.6	2.3	52.2	0.9	469	8	2.98	0.07	0.70	Sum [c]:			
asphaltene	129.6	0.3	1736.8	9.5	521.0	1.9	495	2	3.01	0.02	0.59	101.5	124.8	505.2	478.1
maltene	1.6	0.0	31.5	0.8	9.6	0.5	326	18	2.83	0.18	0.69	Recovery [d]:	96.3%	97.0%	96.4%

To be continued.

Continue:

Sample	Re (ppb)	±	Os (ppt)	±	^{192}Os (ppt)	±	^{187}Re/^{188}Os	±	^{187}Os/^{188}Os	±	rho	fraction (%)	Re (ppb) [a]	^{192}Os (ppt) [a]	^{187}Os (ppt) [b]
Purisima oil															
65:35	119.5	0.4	559.2	3.4	208.7	1.8	1139	10	0.94	0.01	0.74	1.6	1.9	3.3	1.0
70:30	125.2	0.3	518.3	2.1	193.0	0.8	1291	6	0.96	0.01	0.63	16.4	20.5	31.6	9.6
75:25	104.9	0.3	398.1	1.8	148.1	0.8	1409	9	0.97	0.01	0.69	12.8	13.4	18.9	5.8
80:20	92.5	0.2	359.8	1.4	134.7	0.6	1366	7	0.92	0.01	0.64	6.9	6.4	9.4	2.7
85:15	56.2	0.1	197.6	1.0	73.6	0.5	1521	11	0.96	0.01	0.73	16.1	9.1	11.8	3.6
90:10	38.2	0.1	130.8	0.8	48.8	0.4	1560	15	0.95	0.01	0.82	9.3	3.6	4.5	1.4
whole oil	12.1	0.0	41.6	0.5	15.5	0.4	1549	38	0.95	0.03	0.80	Sum [c]:			
asphaltene	61.1	0.2	210.0	1.1	78.1	0.5	1557	11	0.97	0.01	0.75	63.1	54.8	79.6	24.1
maltene	0.6	0.0	6.3	0.3	2.4	0.3	480	62	0.70	0.09	0.77	Recovery [d]:	89.8%	101.9%	100.1%

To be continued.

Continue:

Sample	Re (ppb)	±	Os (ppt)	±	^{192}Os (ppt)	±	^{187}Re/ ^{188}Os	±	^{187}Os/ ^{188}Os	±	rho	fraction (%)	Re (ppb) [a]	^{192}Os (ppt) [a]	^{187}Os (ppt) [b]
Persian oil															
65:35	15.9	0.1	56.5	1.3	17.6	0.9	1799	88	2.65	0.13	0.96	5.5	0.9	1.0	0.8
70:30	79.3	0.2	239.5	1.6	73.4	0.4	2149	13	2.79	0.02	0.71	12.3	9.7	9.0	7.9
75:25	66.7	0.2	202.5	1.3	61.4	0.3	2162	13	2.90	0.02	0.72	19.6	13.0	12.0	11.0
80:20	62.3	0.2	195.4	1.4	59.2	0.4	2096	15	2.91	0.03	0.75	16.0	10.0	9.5	8.7
85:15	48.0	0.1	158.0	1.3	47.3	0.4	2017	17	3.03	0.03	0.77	14.5	7.0	6.9	6.6
90:10	42.2	0.1	147.6	1.3	43.9	0.4	1912	20	3.09	0.04	0.77	4.8	2.0	2.1	2.1
95:5	31.3	0.1	124.9	1.2	36.6	0.4	1700	20	3.27	0.05	0.77	11.8	3.7	4.3	4.4
100:0	12.6	0.1	64.3	0.8	18.7	0.4	1337	26	3.34	0.07	0.85	8.9	1.1	1.7	1.8
100:0 soluble	2.1	0.0	21.4	0.5	6.5	0.3	630	30	2.83	0.13	0.87	6.9	0.1	0.4	0.4
whole oil	2.8	0.0	11.7	0.4	3.6	0.3	1542	130	2.63	0.24	0.88	Sum [c]:			
asphaltene	49.8	0.1	160.9	1.2	48.2	0.4	2057	16	3.03	0.03	0.79	100.1	47.5	46.8	43.7
maltene	0.3	0.0	4.6	0.4	1.5	0.3	453	104	2.09	0.45	0.79	Recovery [d]:	95.4%	97.2%	94.7%

To be continued.

Continue:

Sample	Re (ppb)	±	Os (ppt)	±	^{192}Os (ppt)	±	^{187}Re/^{188}Os	±	^{187}Os/^{188}Os	±	rho	fraction (%)	Re (ppb) [a]	^{192}Os (ppt) [a]	^{187}Os (ppt) [b]
RM8505															
70:30	20.7	0.1	197.9	1.8	67.7	0.8	609	8	1.71	0.03	0.69	54.2	11.2	36.7	19.9
75:25	14.7	0.1	160.4	1.8	55.9	0.9	524	9	1.54	0.04	0.70	7.6	1.1	4.2	2.1
80:20	12.0	0.1	142.8	1.8	50.2	1.0	474	10	1.47	0.04	0.70	8.0	1.0	4.0	1.9
85:15	9.9	0.1	126.6	2.7	44.8	1.9	439	19	1.40	0.08	0.71	3.3	0.3	1.5	0.7
90:10	7.2	0.1	104.2	3.9	37.1	3.0	388	32	1.35	0.15	0.71	4.7	0.3	1.7	0.7
95:5	5.7	0.1	98.9	3.7	36.1	3.0	315	27	1.15	0.13	0.70	2.2	0.1	0.8	0.3
100:0	4.1	0.1	81.5	3.2	29.5	2.6	275	25	1.21	0.14	0.69	1.9	0.1	0.5	0.2
100:0 soluble	0.4	0.0	15.2	0.6	5.6	0.5	151	19	1.07	0.13	0.55	14.5	0.1	0.8	0.3
whole oil	1.9	0.0	23.6	0.9	8.2	0.7	454	41	1.54	0.18	0.72	Sum [c]:			
asphaltene	13.6	0.1	138.8	1.8	47.8	0.5	566	12	1.64	0.05	0.71	96.4	14.2	50.4	26.0
maltene	0.2	0.0	8.2	0.4	3.0	0.4	155	36	1.22	0.19	0.48	Recovery [d]:	104.7%	105.2%	104.7%

[a] : the values are derived by the Re and ^{192}Os abundances of each fraction times by their mass percentage during the progressive precipitation;

[b] : the ^{187}Os values equals ^{192}Os times ^{188}Os/^{192}Os times ^{187}Os/^{188}Os of each fraction. ^{188}Os/^{192}Os is a fixed value;

[c] : these are the sums of the mass percentage of each fraction of asphaltenes during progressive precipitation, the sums of the Re abundance of each fraction, the sum of the ^{192}Os abundance of each fraction, and the sum of ^{187}Os abundance of each fraction;

[d] : the recovery refers to the sum of Re, ^{192}Os and ^{187}Os of each fraction from the progressive precipitation divided by the values of the bulk asphaltene.

Table 4.4 Re-Os data synopsis for the asphaltene fractions separated by *n*-alkane-dichloromethane-methanol from the six oil samples.

Alkanes	Re (ppb)	±	Os (ppt)	±	^{192}Os (ppt)	±	^{187}Re/^{188}Os	±	^{187}Os/^{188}Os	±	rho
Derby oil											
n-C_5	152.4	0.4	1709	10	514.3	2.3	590	3	2.98	0.02	0.62
n-C_6	154.7	0.4	1745	10	525.5	2.5	585	3	2.97	0.02	0.64
n-C_7	169.2	0.5	1820	11	548.0	2.6	614	3	2.97	0.02	0.63
n-C_8	167.7	0.4	1861	11	560.0	2.6	596	3	2.98	0.02	0.63
n-C_9	168.6	0.4	1822	11	548.5	2.6	612	3	2.97	0.02	0.63
n-C_{10}	165.8	0.4	1786	11	537.9	2.6	613	3	2.97	0.02	0.64
Federal oil											
n-C_5	66.4	0.2	395	3	106.9	0.7	1236.4	9	4.17	0.04	0.72
n-C_6	73.9	0.2	441	3	119.2	0.9	1234.3	9	4.16	0.04	0.72
n-C_7	73.2	0.2	450	4	121.9	1.0	1194.3	10	4.15	0.04	0.73
n-C_8	77.8	0.2	456	4	123.5	1.0	1253.0	11	4.13	0.04	0.74
n-C_9	75.3	0.2	444	4	120.2	1.0	1247.3	11	4.15	0.04	0.74
n-C_{10}	72.7	0.2	442	4	119.9	1.0	1206.7	10	4.14	0.04	0.73
Viking-Morel oil											
n-C_5	143.7	0.4	1826	11	548.3	2.4	521	3	3.00	0.02	0.62
n-C_6	153.6	0.4	1917	12	575.5	2.6	531	3	3.00	0.02	0.62
n-C_7	157.7	0.4	1896	12	569.4	2.6	551	3	3.00	0.02	0.63
n-C_8	152.5	0.4	1892	12	568.2	2.6	534	3	3.00	0.02	0.62
n-C_9	158.8	0.4	1875	11	563.1	2.6	561	3	3.00	0.02	0.62
n-C_{10}	152.8	0.4	1858	11	558.3	2.6	544	3	3.00	0.02	0.63

To be continued.

Continue:

Alkanes	Re (ppb)	±	Os (ppt)	±	^{192}Os (ppt)	±	^{187}Re/^{188}Os	±	^{187}Os/^{188}Os	±	rho
Purisima oil											
n-C_5	70.1	0.2	253.7	1.2	94.3	0.6	1478	9	0.97	0.01	0.70
n-C_6	75.6	0.2	291.0	1.4	108.2	0.6	1390	9	0.97	0.01	0.70
n-C_7	79.4	0.2	308.2	1.6	114.7	0.8	1376	10	0.97	0.01	0.74
n-C_8	84.2	0.2	321.2	1.7	119.6	0.8	1400	10	0.96	0.01	0.72
n-C_9	96.0	0.2	333.7	1.7	124.2	0.8	1538	11	0.97	0.01	0.72
n-C_{10}	76.1	0.2	296.6	2.6	110.5	1.6	1370	20	0.96	0.02	0.78
Persian oil											
n-C_5	51.0	0.2	164.5	2.0	49.7	0.9	2041	38	2.93	0.06	0.88
n-C_6	57.7	0.2	182.1	2.3	55.3	1.1	2073	40	2.88	0.06	0.89
n-C_7	60.0	0.2	198.7	2.6	60.6	1.3	1970	41	2.83	0.06	0.90
n-C_8	60.6	0.4	194.8	3.9	59.9	2.5	2013	83	2.76	0.12	0.93
n-C_9	64.3	0.3	201.3	2.6	61.4	1.3	2084	44	2.84	0.06	0.90
n-C_{10}	63.3	0.3	200.1	2.6	61.3	1.3	2055	44	2.79	0.06	0.90
RM8505											
n-C_5	19.3	0.1	189.8	1.9	65.9	1.0	583	9	1.57	0.03	0.71
n-C_6	20.3	0.1	197.6	2.0	68.5	1.0	591	9	1.59	0.03	0.71
n-C_7	23.3	0.1	217.3	2.3	75.2	1.2	616	11	1.61	0.03	0.73
n-C_8	18.8	0.1	174.9	1.9	60.2	1.0	621	11	1.65	0.04	0.71
n-C_9	22.9	0.1	213.8	2.3	74.0	1.2	616	10	1.60	0.03	0.73
n-C_{10}	19.1	0.1	178.0	1.9	61.6	1.0	617	10	1.61	0.03	0.72

Table 4.5 Re-Os data synopsis for the maltene fractions separated by *n*-alkane-dichloromethane-methanol from the six oil samples.

Alkanes	Re (ppb)	±	Os (ppt)	±	^{192}Os (ppt)	±	^{187}Re/^{188}Os	±	^{187}Os/^{188}Os	±	rho
Derby oil											
n-C_5	1.81	0.01	27.9	1.2	8.8	0.8	410	36	2.54	0.30	0.74
n-C_6	2.61	0.01	36.6	1.5	11.4	1.0	457	39	2.64	0.31	0.73
n-C_7	3.41	0.02	46.1	2.0	14.3	1.2	476	41	2.68	0.32	0.73
n-C_8	3.78	0.02	48.9	2.1	15.2	1.3	496	42	2.67	0.31	0.72
n-C_9	3.62	0.02	47.9	2.0	14.8	1.2	487	41	2.70	0.31	0.72
n-C_{10}	3.71	0.02	47.8	2.0	14.7	1.2	501	42	2.74	0.32	0.72
Federal oil											
n-C_5	1.33	0.01	15.6	0.8	4.6	0.5	576	61	3.20	0.43	0.79
n-C_6	2.10	0.02	20.6	1.0	5.8	0.6	715	71	3.62	0.46	0.77
n-C_7	2.54	0.02	22.5	1.1	6.3	0.6	801	76	3.73	0.46	0.76
n-C_8	3.03	0.02	28.2	1.3	8.1	0.7	742	67	3.46	0.42	0.74
n-C_9	3.01	0.02	26.5	1.2	7.5	0.7	794	72	3.60	0.44	0.74
n-C_{10}	3.20	0.02	28.2	1.3	8.0	0.7	797	72	3.64	0.44	0.74
Viking-Morel oil											
n-C_5	2.03	0.02	37.3	1.6	11.4	1.0	355	31	2.83	0.33	0.73
n-C_6	3.24	0.02	60.7	2.6	18.5	1.5	347	29	2.82	0.33	0.71
n-C_7	4.38	0.02	70.8	3.0	21.4	1.8	407	33	2.92	0.34	0.71
n-C_8	4.62	0.02	73.3	3.1	22.4	1.8	410	34	2.82	0.32	0.71
n-C_9	5.34	0.02	84.3	3.5	25.6	2.1	415	34	2.88	0.33	0.71
n-C_{10}	5.80	0.02	95.2	4.0	28.9	2.4	399	33	2.87	0.33	0.71

To be continued.

Continue:

Alkanes	Re (ppb)	±	Os (ppt)	±	^{192}Os (ppt)	±	^{187}Re/^{188}Os	±	^{187}Os/^{188}Os	±	rho
Purisima oil											
n-C_5	0.70	0.01	7.7	0.4	3.0	0.4	456	58	0.47	0.08	0.77
n-C_6	1.13	0.01	7.1	0.4	2.8	0.4	811	109	0.63	0.10	0.81
n-C_7	1.39	0.01	8.2	0.4	3.2	0.4	879	108	0.65	0.10	0.80
n-C_8	1.48	0.01	8.5	0.4	3.3	0.4	900	108	0.68	0.10	0.79
n-C_9	1.83	0.01	10.0	0.5	3.9	0.4	942	106	0.69	0.10	0.79
n-C_{10}	1.31	0.02	7.5	0.4	2.9	0.4	903	124	0.66	0.11	0.82
Persian oil											
n-C_5	0.57	0.04	5.0	0.4	1.6	0.3	694	143	2.10	0.44	0.86
n-C_6	0.86	0.04	5.8	0.4	1.9	0.3	913	157	2.22	0.41	0.86
n-C_7	1.20	0.04	6.9	0.4	2.2	0.3	1096	168	2.49	0.42	0.86
n-C_8	1.22	0.04	6.8	0.4	2.1	0.3	1142	176	2.52	0.43	0.86
n-C_9	1.25	0.04	7.6	0.4	2.4	0.3	1042	152	2.50	0.41	0.85
n-C_{10}	1.45	0.04	7.3	0.4	2.3	0.3	1259	188	2.57	0.43	0.86
RM8505											
n-C_5	0.75	0.04	12.4	0.5	4.6	0.5	324	37	1.04	0.13	0.69
n-C_6	0.58	0.04	13.2	0.6	4.8	0.5	238	29	1.17	0.15	0.64
n-C_7	0.81	0.05	16.1	0.7	5.8	0.6	274	33	1.19	0.16	0.66
n-C_8	0.92	0.06	17.0	0.8	6.1	0.6	299	36	1.21	0.16	0.68
n-C_9	1.11	0.05	17.5	0.8	6.3	0.6	349	39	1.20	0.16	0.70
n-C_{10}	1.39	0.05	17.7	0.8	6.4	0.6	434	46	1.23	0.16	0.72

Table 4.6 The sum of Re and Os of asphaltenes and maltenes separated by *n*-alkanes, and the percentage they account for of the crude oil .

Separation	asphaltene + maltene		asphaltene portion		maltene portion		lost Re and Os		lost oil
by *n*-alkanes	Re (ppb)	Os (ppt)	Re (%)	Os (%)	Re (%)	Os (%)	Re (%)	Os (%)	(%)
Derby oil	12.1	149.7							
n-C_5	11.0	129.7	79.7	72.4	11.3	14.2	9.0	13.3	17.4
n-C_6	9.6	113.0	63.5	58.1	15.3	17.4	21.2	24.5	24.0
n-C_7	11.3	129.7	70.6	61.6	22.9	25.1	6.5	13.3	13.5
n-C_8	11.4	132.2	68.4	61.5	25.6	26.8	6.1	11.7	13.0
n-C_9	11.2	128.4	67.9	59.5	24.5	26.3	7.6	14.2	13.0
n-C_{10}	11.2	127.3	66.7	58.3	25.6	26.8	7.7	15.0	11.3
n-C_7 only			78.4	70.7					
Federal oil	8.0	55.5							
n-C_5	7.9	51.7	87.8	75.3	10.6	17.9	1.7	6.9	25.8
n-C_6	7.9	53.4	77.8	66.8	20.8	29.4	1.4	3.8	12.4
n-C_7	7.7	53.0	71.1	63.1	25.5	32.5	3.4	4.5	12.0
n-C_8	8.1	55.9	71.0	59.9	30.4	40.8	-1.4	-0.7	12.5
n-C_9	8.0	54.2	69.7	59.1	30.2	38.4	0.1	2.4	12.3
n-C_{10}	7.8	54.3	65.5	57.4	31.8	40.4	2.7	2.2	13.2
n-C_7 only			88.3	83.0					

Continue:

Alkanes	asphaltene + maltene		asphaltene portion		maltene portion		lost Re and Os		lost oil
	Re (ppb)	Os (ppt)	Re (%)	Os (%)	Re (%)	Os (%)	Re (%)	Os (%)	(%)
Viking-Morel oil	12.3	173.6							
n-C_5	13.1	174.6	94.3	85.0	12.0	15.6	-6.3	-0.6	19.3
n-C_6	12.9	176.5	85.3	75.5	19.7	26.2	-5.0	-1.7	18.3
n-C_7	13.4	175.0	82.5	70.3	26.7	30.5	-9.1	-0.8	18.6
n-C_8	13.1	174.2	78.1	68.7	28.2	31.7	-6.2	-0.4	18.6
n-C_9	13.4	174.3	76.5	64.1	32.4	36.3	-9.0	-0.4	19.3
n-C_{10}	13.4	182.0	73.7	63.6	35.5	41.3	-9.2	-4.9	18.7
n-C_7 only			90.6	86.1					
Purisima oil	12.1	41.6							
n-C_5	9.3	36.0	74.2	78.0	2.7	8.7	23.1	13.3	40.2
n-C_6	9.1	36.7	71.0	79.3	4.9	8.9	24.2	11.8	36.7
n-C_7	6.9	27.8	52.5	59.2	4.5	7.7	43.0	33.1	53.1
n-C_8	7.4	29.6	56.5	62.6	5.2	8.6	38.3	28.8	49.6
n-C_9	8.3	30.3	61.8	62.4	6.6	10.5	31.5	27.1	48.6
n-C_{10}	8.6	34.7	65.5	74.1	5.6	9.3	28.9	16.6	54.8
n-C_7 only			81.7	81.5					

Continue:

Alkanes	asphaltene + maltene		asphaltene portion		maltene portion		lost Re and Os		lost oil
	Re (ppb)	Os (ppt)	Re (%)	Os (%)	Re (%)	Os (%)	Re (%)	Os (%)	(%)
Persian oil	2.8	11.7							
n-C_5	3.0	11.9	93.4	72.6	13.9	29.3	-7.3	-2.0	26.1
n-C_6	3.1	11.8	87.4	66.6	20.9	33.9	-8.3	-0.5	26.9
n-C_7	3.0	11.9	76.2	60.8	29.6	41.1	-5.8	-1.9	26.6
n-C_8	3.0	11.5	75.6	58.6	29.7	39.7	-5.3	1.6	27.5
n-C_9	3.1	12.2	78.8	59.5	30.4	44.5	-9.2	-4.0	27.6
n-C_{10}	3.2	12.1	77.8	59.3	36.0	43.9	-13.9	-3.2	26.3
n-C_7 only			100.5	78.3					
RM8505 oil	1.9	23.6							
n-C_5	2.5	29.4	101.0	78.8	34.6	45.8	-35.5	-24.6	3.4
n-C_6	2.2	28.4	92.7	71.6	26.7	48.9	-19.4	-20.4	4.3
n-C_7	2.3	28.9	83.8	62.2	37.8	60.3	-21.6	-22.5	5.1
n-C_8	2.4	29.8	85.1	63.0	43.1	63.0	-28.2	-26.0	3.7
n-C_9	2.5	29.3	80.1	59.4	51.7	64.7	-31.8	-24.1	6.0
n-C_{10}	2.8	30.3	83.5	61.9	65.9	66.6	-49.4	-28.5	2.8
n-C_7 only			92.8	75.3					

Table 4.7 Geochronology of the fractions of the six crude oil samples in this study.

Sample	source rock	oil generation	asphaltene and maltene (*n*-heptane), crude oil	asphaltene fractions by progressive precipitation	selection of asphaltene fractions	Maltenes separated by *n*-alkanes
Derby	Permian Phosphoria Formation	Late Trassic	Isoplot Model III, 20 ± 810 Ma (Os_i = 2.8 ± 7.3, MSWD = 6.0)	Isoplot Model III, 32 ± 40 Ma (Os_i = 2.7 ± 0.4, MSWD = 4.8)	70:30, 75:25, 80:20, 95:5; Model I, 167 ± 51 Ma (Os_i = 1.3 ± 0.5, MSWD = 0.7)	Isoplot Model I, 114 ± 200 Ma (Os_i = 1.8 ± 1.6, MSWD = 0.04)
Federal	Permian Phosphoria Formation	Late Trassic	Isoplot Model I, 70 ± 41 Ma (Os_i = 2.9 ± 0.8, MSWD = 0.7)	Isoplot Model III, 74 ± 270 Ma (Os_i = 2.6 ± 5.3, MSWD = 43)	/	Isoplot Model I, 114 ± 110 Ma (Os_i = 2.1 ± 1.3, MSWD = 0.25)
Viking-Morel	Pennsylvanian-Permian Minnelusa Formation	unkown	Isoplot Model I, 64 ± 55 Ma (Os_i = 2.5 ± 0.5, MSWD = 0.01)	Isoplot Model III, 4 ± 14 Ma (Os_i = 3.0 ± 0.1, MSWD = 2.7)	/	Isoplot Model I, 40 ± 280 Ma (Os_i = 2.6 ± 1.8, MSWD = 0.06)
Purisima	Miocene Monterey Formation	in the last 5 million years	Isoplot Model I, 15 ± 4 Ma (Os_i = 0.6 ± 0.1, MSWD = 4)	Isoplot Model III, 2 ± 11 Ma (Os_i = 0.9 ± 0.2, MSWD = 55)	65:35, 70:30, 75:25; Model I, 5.6 ± 2.5 Ma (Os_i = 0.8 ± 0.1, MSWD = 0.5)	Isoplot Model I, 27.4 ± 8.7 Ma (Os_i = 0.26 ± 0.12, MSWD = 0.07)

To be continued.

Continue:

Sample	source rock	oil generation	asphaltene and maltene (*n*-heptane), crude oil	asphaltene fractions by progressive precipitation	selection of asphaltene fractions	Maltenes separated by *n*-alkanes
Persian	Cretaceous and/or Late Jurassic	unknown	Isoplot Model I, 39 ± 12 Ma (Os_i = 1.7 ± 0.4, MSWD = 0.9)	Isoplot Model III, -4 ± 24 Ma (Os_i = 3.1 ± 0.7, MSWD = 39)	/	Isoplot Model I, 53 ± 43 Ma (Os_i = 1.50 ± 0.75, MSWD = 0.18)
RM8505	Upper Cretaceous	Since Miocene	Isoplot Model I, 62 ± 25 Ma (Os_i = 1.1 ± 0.2, MSWD = 0.04)	Isoplot Model I, 98.4 ± 9.5 Ma (Os_i = 0.7 ± 0.1, MSWD = 2)	/	Isoplot Model I, -1 ± 63 Ma (Os_i = 1.17 ± 0.34, MSWD = 1.3)

Figure 4.1 The modified Yen model of asphaltene molecule, aggregate and cluster structure (Mullins, 2010).

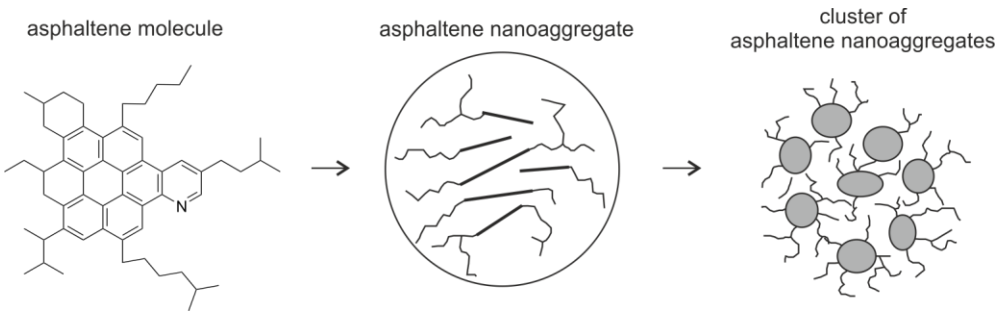
asphaltene molecule
asphaltene nanoaggregate
cluster of
asphaltene nanoaggregates
N

Figure 4.2 Free metal complexes and the absorption and occlusion by asphaltene aggregates (Modified from Snowdon et al. 2016).

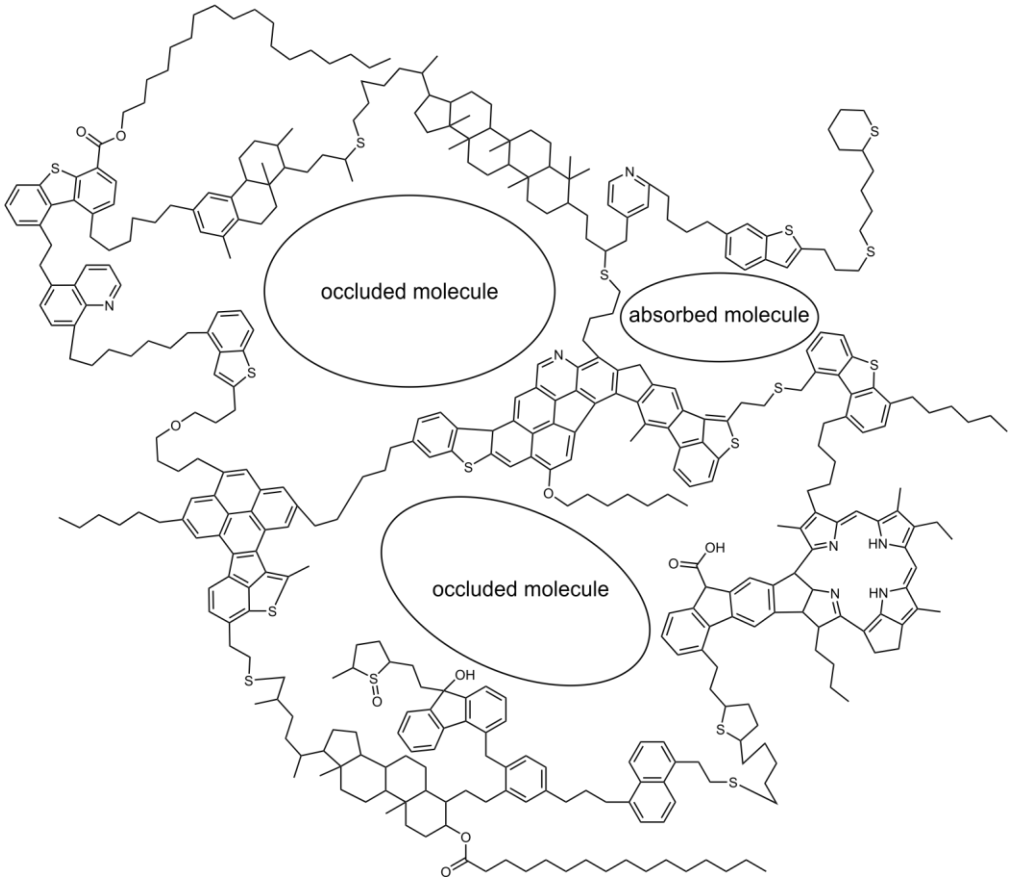
occluded molecule
absorbed molecule
occluded molecule

Figure 4.3 The procedure of asphaltene progressive precipitation.

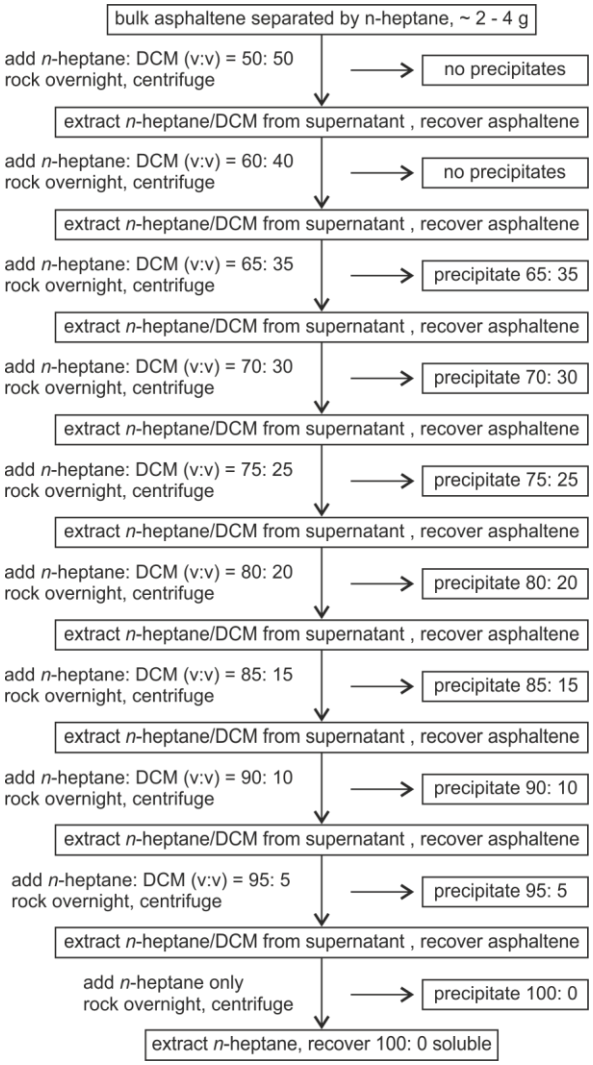
bulk asphaltene separated by n-heptane, ~ 2 - 4 g
add n-heptane: DCM (v:v) = 50: 50
rock overnight, centrifuge
no precipitates
extract n-heptane/DCM from supernatant , recover asphaltene
add n-heptane: DCM (v:v) = 60: 40
rock overnight, centrifuge
no precipitates
extract n-heptane/DCM from supernatant , recover asphaltene
add n-heptane: DCM (v:v) = 65: 35
rock overnight, centrifuge
precipitate 65: 35
extract n-heptane/DCM from supernatant , recover asphaltene
add n-heptane: DCM (v:v) = 70: 30
rock overnight, centrifuge
precipitate 70: 30
extract n-heptane/DCM from supernatant , recover asphaltene
add n-heptane: DCM (v:v) = 75: 25
rock overnight, centrifuge
precipitate 75: 25
extract n-heptane/DCM from supernatant , recover asphaltene
add n-heptane: DCM (v:v) = 80: 20
rock overnight, centrifuge
precipitate 80: 20
extract n-heptane/DCM from supernatant , recover asphaltene
add n-heptane: DCM (v:v) = 85: 15
rock overnight, centrifuge
precipitate 85: 15
extract n-heptane/DCM from supernatant , recover asphaltene
add n-heptane: DCM (v:v) = 90: 10
rock overnight, centrifuge
precipitate 90: 10
extract n-heptane/DCM from supernatant , recover asphaltene
add n-heptane: DCM (v:v) = 95: 5
rock overnight, centrifuge
precipitate 95: 5
extract n-heptane/DCM from supernatant , recover asphaltene
add n-heptane only
rock overnight, centrifuge
precipitate 100: 0
extract n-heptane, recover 100: 0 soluble

Figure 4.4 Mass percentages of the progressively precipitated fractions of the asphaltenes.

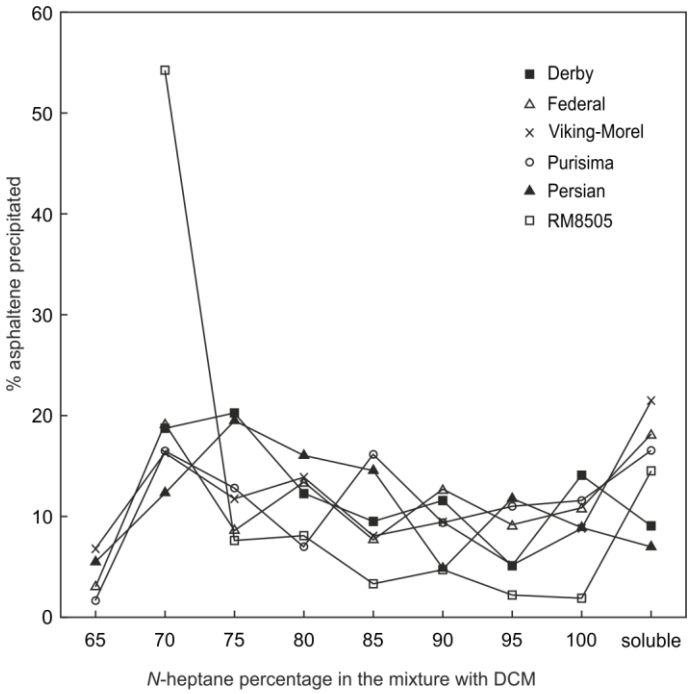
60
50
40
30
20
10
0
% asphaltene precipitated
Derby
Federal
Viking-Morel
Purisima
Persian
RM8505
65
70
75
80
85
90
95
100
soluble
N-heptane percentage in the mixture with DCM

Figure 4.5 Asphaltene (a) and maltene (b) percentages separated by *n*-alkane-DCM-methanol and their total (c).

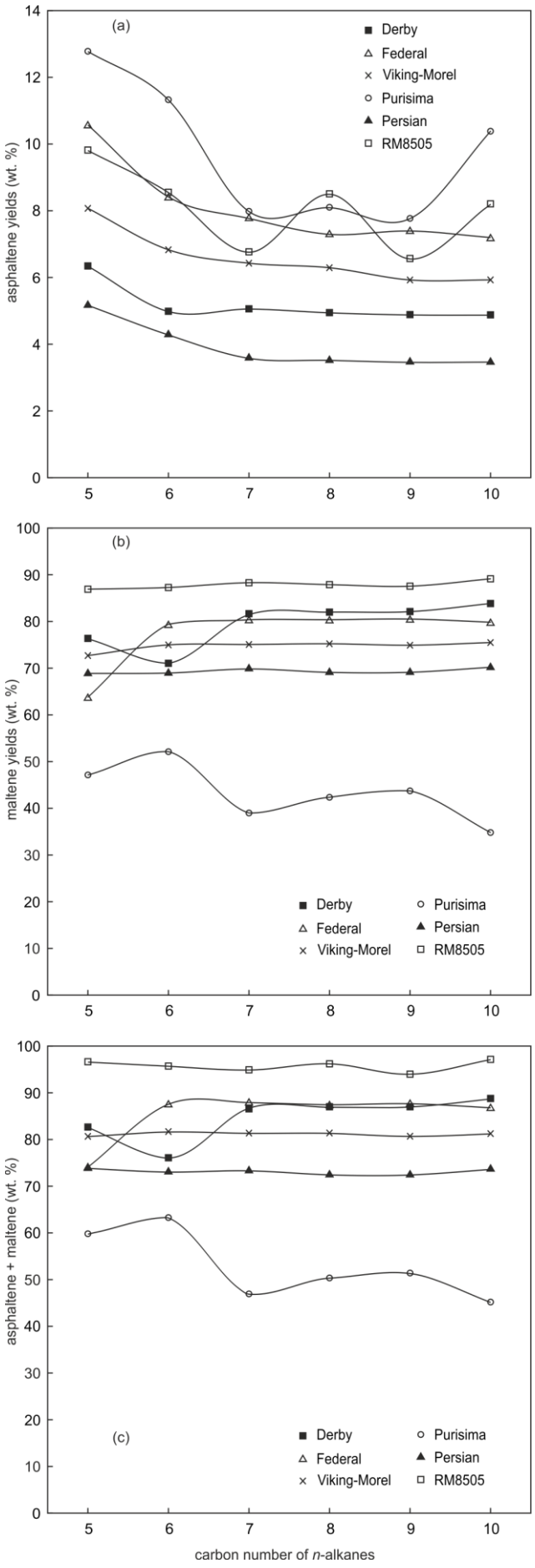
(a)
Derby
Federal
Viking-Morel
Purisima
Persian
RM8505
asphaltene yields (wt. %)
(b)
maltene yields (wt. %)
(c)
asphaltene + maltene (wt. %)
carbon number of n-alkanes

Figure 4.6 Normalized Re and Os abundances of the fractions of Derby oil, Federal oil and Viking-Morel oil. The Re and Os abundances of whole oil, *n*-heptane separated maltene, progressively precipitated asphaltene fractions, asphaltenes separated by *n*-alkane-DCM-methanol are normalized by those of the *n*-heptane separated asphaltenes. The Re and Os abundances of maltenes precipitated by *n*-alkane-DCM-methanol are normalized by those of the *n*-heptane separated maltenes.

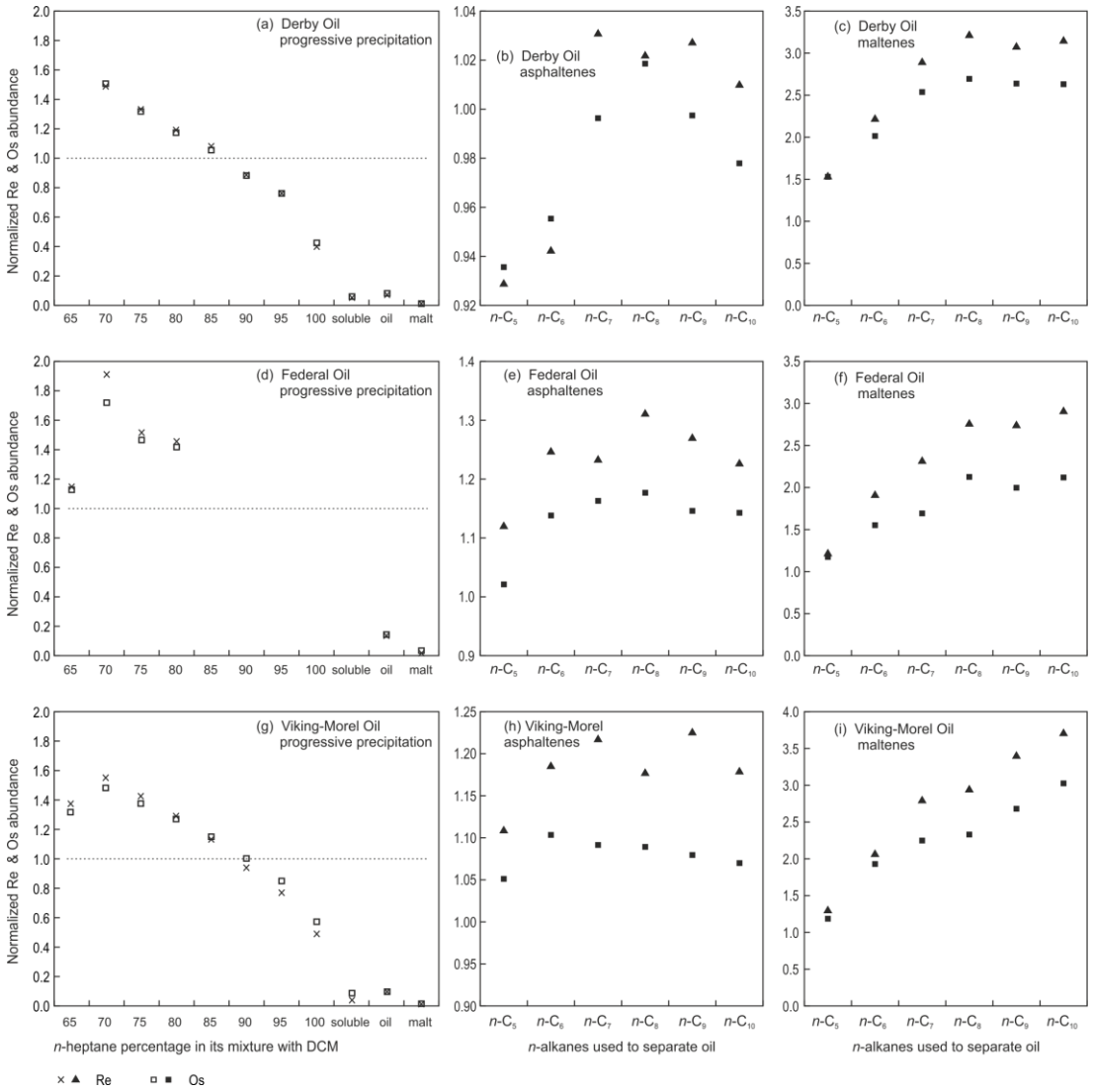
(a) Derby Oil progressive precipitation
(b) Derby Oil asphaltenes
(c) Derby Oil maltenes
(d) Federal Oil progressive precipitation
(e) Federal Oil asphaltenes
(f) Federal Oil maltenes
(g) Viking-Morel Oil progressive precipitation
(h) Viking-Morel asphaltenes
(i) Viking-Morel Oil maltenes
Normalized Re & Os abundance
65 70 75 80 85 90 95 100 soluble oil malt
n-heptane percentage in its mixture with DCM
n-C5 n-C6 n-C7 n-C8 n-C9 n-C10
n-alkanes used to separate oil
Re
Os

Figure 4.7 Normalized Re and Os abundances of Persian oil, Purisima oil and RM8505 oil. The Re and Os abundances of whole oil, *n*-heptane separated maltene, progressively precipitated asphaltene fractions, asphaltenes separated by *n*-alkane-DCM-methanol are normalized by those of the *n*-heptane separated asphaltenes. The Re and Os abundances of maltenes precipitated by *n*-alkane-DCM-methanol are normalized by those of the *n*-heptane separated maltenes.

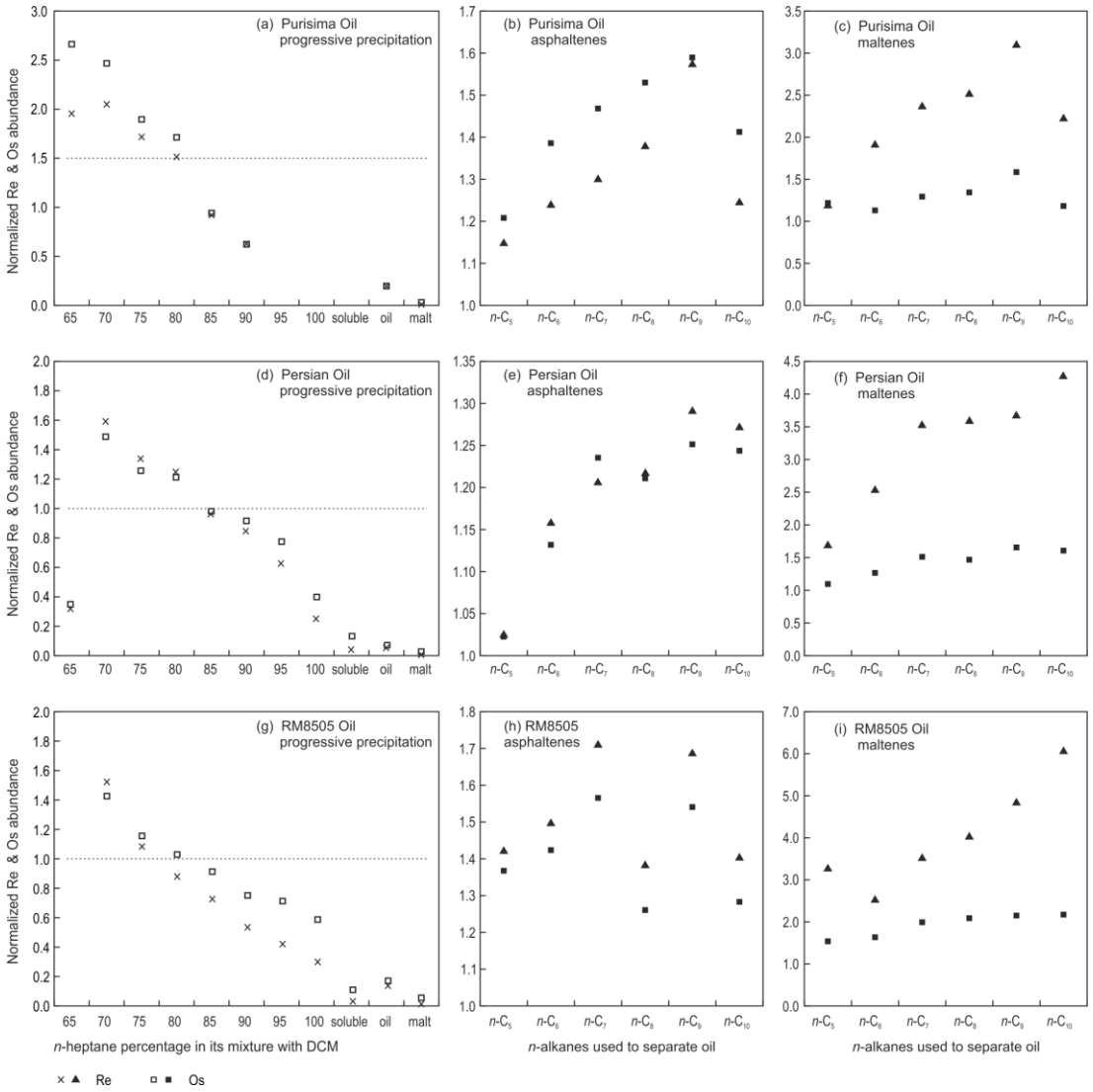
(a) Purisima Oil
progressive precipitation
(b) Purisima Oil
asphaltenes
(c) Purisima Oil
maltenes
(d) Persian Oil
progressive precipitation
(e) Persian Oil
asphaltenes
(f) Persian Oil
maltenes
(g) RM8505 Oil
progressive precipitation
(h) RM8505
asphaltenes
(i) RM8505 Oil
maltenes
Normalized Re & Os abundance
65 70 75 80 85 90 95 100 soluble oil malt
n-C5 n-C6 n-C7 n-C8 n-C9 n-C10
n-heptane percentage in its mixture with DCM
n-alkanes used to separate oil
Re
Os

Figure 4.8 The Re-Os isotopic ratios of Derby oil, Federal oil and Viking-Morel oil. The $^{187}Re/^{188}Os$ and $^{187}Os/^{188}Os$ values of the progressively precipitated asphaltene fractions are presented with those of the corresponding whole oils and *n*-heptane separated asphaltene and maltene fractions. The $^{187}Re/^{188}Os$ and $^{187}Os/^{188}Os$ values of the *n*-alkane-DCM-methanol separated asphaltene and maltene fractions are presented with those of the corresponding whole oils and *n*-heptane asphaltene and maltene fractions, too. (5, 6, 7, 8, 9, 10: carbon number of alkane; A: asphaltene; M: maltene)

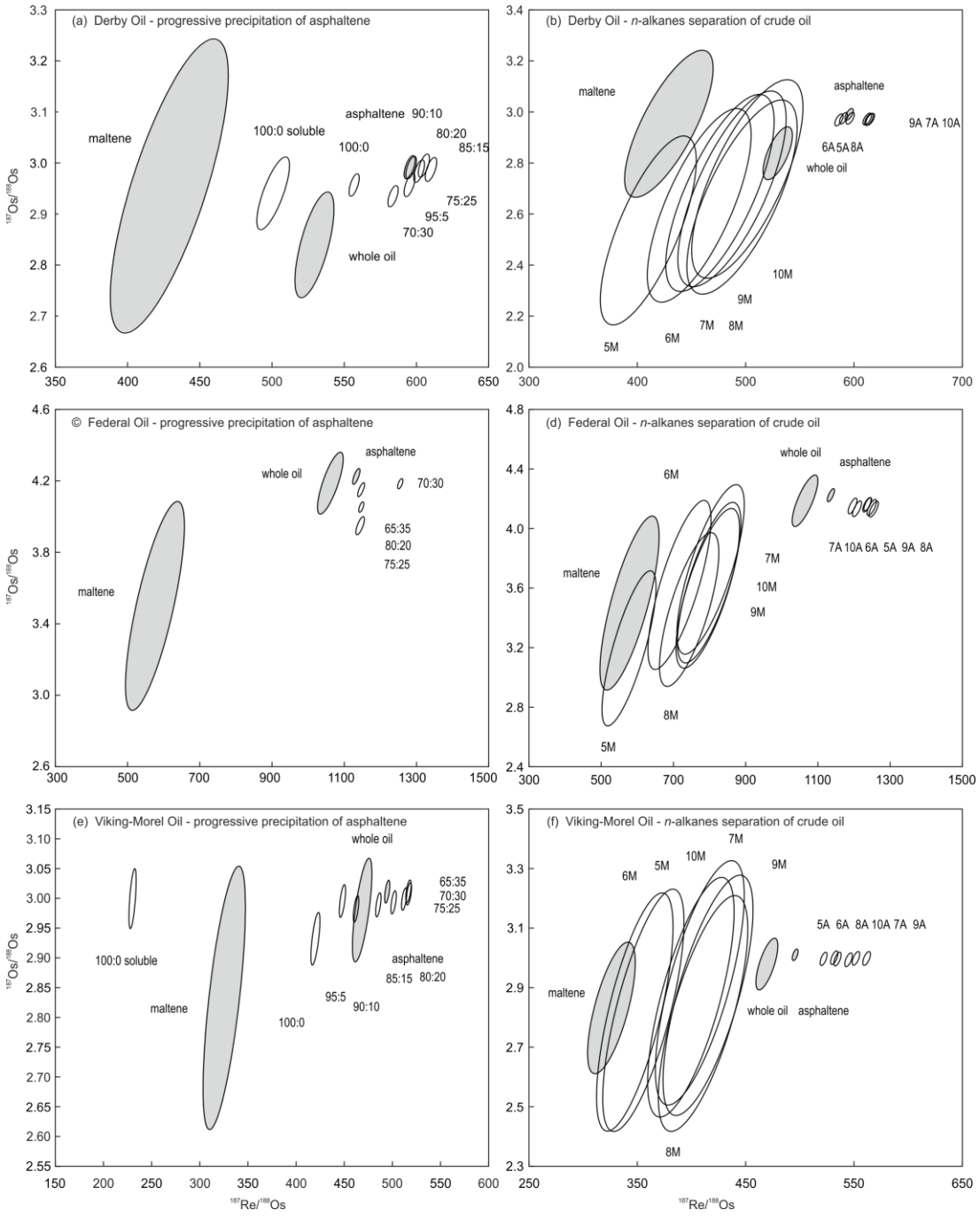
(a) Derby Oil - progressive precipitation of asphaltene
maltene
100:0 soluble
asphaltene 90:10
80:20
85:15
100:0
75:25
95:5
70:30
whole oil
(b) Derby Oil - n-alkanes separation of crude oil
maltene
asphaltene
9A 7A 10A
6A 5A 8A
whole oil
10M
9M
7M 8M
6M
5M
© Federal Oil - progressive precipitation of asphaltene
whole oil
asphaltene
70:30
65:35
80:20
75:25
maltene
(d) Federal Oil - n-alkanes separation of crude oil
whole oil
asphaltene
6M
7A 10A 6A 5A 9A 8A
7M
maltene
10M
9M
8M
5M
(e) Viking-Morel Oil - progressive precipitation of asphaltene
whole oil
65:35
70:30
75:25
asphaltene
85:15 80:20
100:0 soluble
maltene
95:5
90:10
100:0
(f) Viking-Morel Oil - n-alkanes separation of crude oil
7M
6M
5M
10M
9M
5A 6A 8A 10A 7A 9A
maltene
whole oil asphaltene
8M
187Os/188Os
187Re/188Os

Figure 4.9 The Re-Os isotopic ratios of Persian oil, Purisima oil and RM8505 oil. The $^{187}Re/^{188}Os$ and $^{187}Os/^{188}Os$ values of the progressively precipitated asphaltene fractions are presented with those of the corresponding whole oils and *n*-heptane separated asphaltene and maltene fractions. The $^{187}Re/^{188}Os$ and $^{187}Os/^{188}Os$ values of the *n*-alkane-DCM-methanol separated asphaltene and maltene fractions are presented with those of the corresponding whole oils and *n*-heptane asphaltene and maltene fractions, too. (5, 6, 7, 8, 9, 10: carbon number of alkane; A: asphaltene; M: maltene)

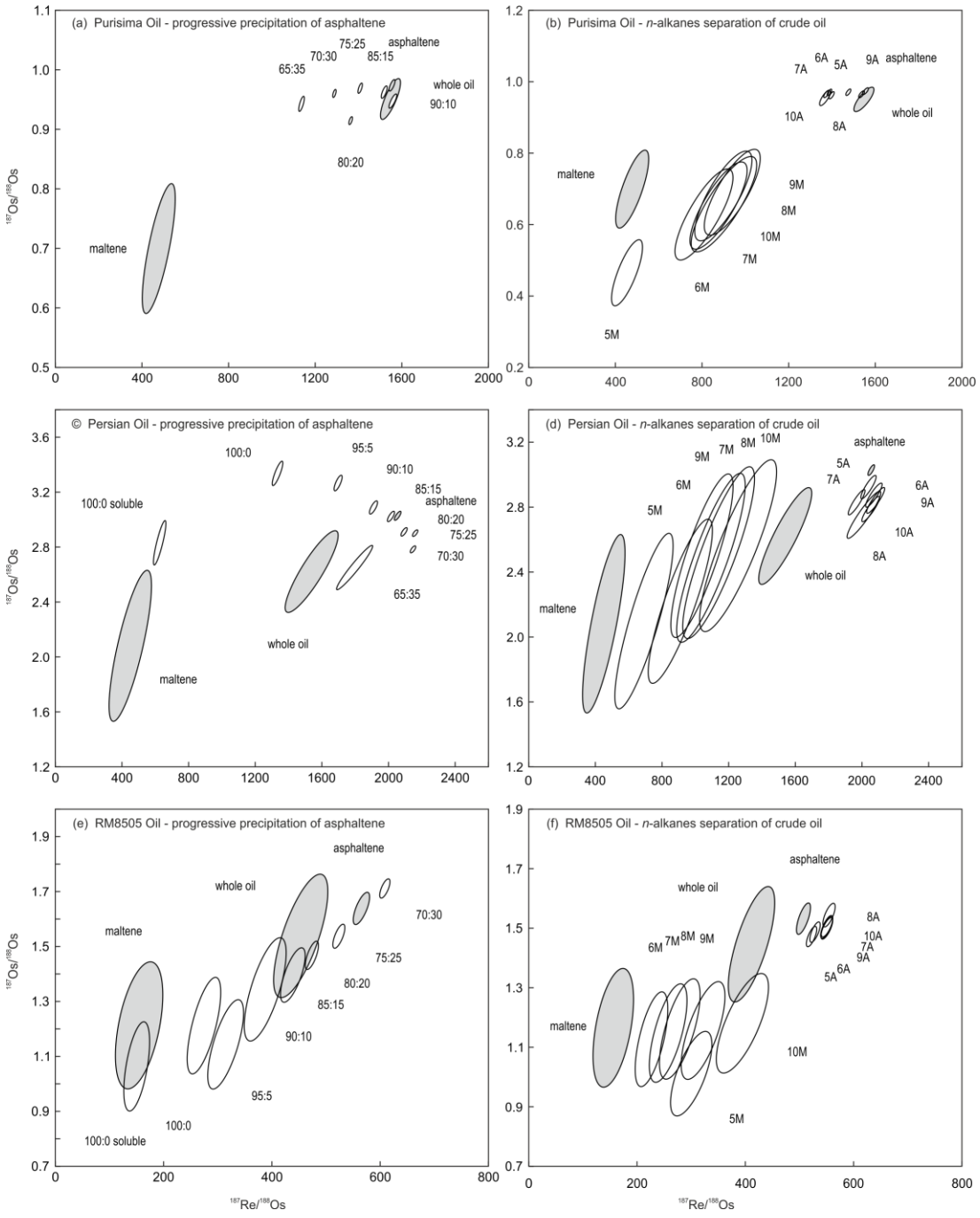
(a) Purisima Oil - progressive precipitation of asphaltene
asphaltene
75:25
70:30
85:15
65:35
whole oil
90:10
80:20
maltene
(b) Purisima Oil - n-alkanes separation of crude oil
6A
5A
9A
asphaltene
7A
10A
whole oil
8A
maltene
9M
8M
10M
7M
6M
5M
© Persian Oil - progressive precipitation of asphaltene
100:0
95:5
90:10
85:15
asphaltene
100:0 soluble
80:20
75:25
70:30
65:35
whole oil
maltene
(d) Persian Oil - n-alkanes separation of crude oil
9M
7M
8M
10M
asphaltene
5A
7A
6M
6A
9A
5M
10A
8A
whole oil
maltene
(e) RM8505 Oil - progressive precipitation of asphaltene
asphaltene
whole oil
70:30
maltene
75:25
80:20
85:15
90:10
95:5
100:0
100:0 soluble
(f) RM8505 Oil - n-alkanes separation of crude oil
asphaltene
whole oil
8A
10A
6M
7M
8M
9M
7A
9A
5A
6A
maltene
10M
5M
187Re/188Os
187Os/188Os

Chapter 5 Conclusions and prospects

The presented research in this thesis consists of three topics with the aim to further the understanding of Re-Os geochronology of crude oil generation and the residence of Re and Os in crude oil. To be more specific, this thesis has contributed matrix-matched reference materials for petroleum Re-Os elemental and isotopic measurements, promoted the understanding of Re-Os geochronology of crude oil generation and oil-source correlation via Os isotopic composition, and proposed how the Re and Os reside within crude oil and the implications on the Re-Os dating with petroleum samples. Accordingly, some potential researches for the future are also proposed.

5.1 Petroleum matrix-matched Re-Os analysis reference materials

The Re and Os abundances and isotopic composition results from the measurements on RM8505 crude oil and the homogeneous asphaltene samples via ID-NTIMS have shown the necessary characteristics to be appropriate reference materials. The NIST RM8505 crude oil contains 1.95 ± 0.25 ppb Re and 24.4 ± 3.5 ppt Os with $^{187}Re/^{188}Os$ ratio of 454 ± 21 and $^{187}Os/^{188}Os$ ratio of 1.517 ± 0.043 for (n = 18, 95% conf.). The homogeneous asphaltene sample contains 16.52 ± 0.48 ppb Re and 166.0 ± 4.4 ppt Os with $^{187}Re/^{188}Os$ ratio of 574 ± 17 and 1.640 ± 0.025 of $^{187}Os/^{188}Os$ ratio (n = 24, 95% conf.). These abundance and isotopic ratio datasets generally follow normal distribution with low relative standard deviations which indicate that sufficient data is acquired with good repeatability. These values are also consistent with the measurement results of two other laboratories on the same crude oil. These conditions validate their use as matrix-matched reference materials for petroleum Re-Os analysis. This work should facilitate inter- and intra-laboratory comparison and method validation of the Re-Os measurements petroleum samples.

With the petroleum matrix-matched Re-Os measurement reference materials, future work can be taken on the development of Re-Os analysis methodology suitable for very low abundance petroleum sample, e.g. samples with lower than 1 ng/g Re and 10 pg/g Os. A large fraction of the worldwide crude oil and bitumens, e.g. the Duvernay oils in Chapter Two, are potentially less abundant in Re and Os than most of petroleum samples in the Re-Os studies taken so far. Accurate and precise Re-Os analyses for these low abundance petroleum samples can promote the application of

this geochronometer to a much wider scope. One of the currently potential ways is to increase the sampling amount. The key step is the digestion. The commonly used digestion vessels have their limits of sample amount to use, i.e. < 200mg for Carius tubes and < 500mg for HPA-S glass vials (Selby et al., 2007; Mahdaoui et al., 2013; Georgiev et al., 2016). The increase of sample amount employed could lead to the rapture of digestion vessels due to the generation of carbon dioxide. Increasing digestion vessel volume or adding hydrogen peroxide can only increase the sample to limited extent (Li et al., 2011; Qi et al., 2013). Ashing/combustion may increase the samples being handled enormously, however, the osmium tetroxide is volatile and the digestion should be in closed systems.

5.2 Re-Os geochronology and oil-source correlation of Duvernay petroleum system

In the Re-Os study of Duvernay petroleum system, the abilities of Re-Os dating the generation of crude oil and correlating oil and source were demonstrated. Besides, significant influence was excluded of the basinal fluids bearing Re and Os on the Duvernay-sourced oil Re-Os systematics. The Re-Os age obtained from Duvernay-sourced oil asphaltene fractions agrees well with the widely accepted perception on the timing of Duvernay formation main maturation stage (Higley et al., 2009; Berbesi et al., 2012). Specially, this Re-Os oil generation age is about 300 million years younger than the source rock deposition. This is so far the largest time span between the deposition and maturation of all the petroleum systems studied by Re-Os for oil generation dating, demonstrating the versatility of Re-Os in the dating of oil generation. The high uncertainty of the Re-Os oil generation age (66 ± 31 Ma) is the joint result of low precision of Re-Os measurement results, limited spread of $^{187}Re/^{188}Os$ values, and the variation in the Os_i values. The similarity between Duvernay formation core samples and Leduc-Nisku oils on the $^{187}Os/^{188}Os$ ranges and weighted averages at 66 Ma is high. Three out of the four other source rock intervals have distinctively different (higher) contemporaneous $^{187}Os/^{188}Os$ values (Creaser et al., 2002; Selby and Creaser, 2003; Kendall et al., 2004; Miller, 2004; Selby and Creaser, 2005; Selby et al., 2007; Finlay et al., 2012). For these multiple organic-rich intervals of Western Canada sedimentary basin, their $^{187}Os/^{188}Os$ values at the same time point, e.g. oil generation, can be discernibly different attributing to the variation of their initial $^{187}Os/^{188}Os$ values inherited from seawater overtime and

the ingrowth of rock $^{187}Os/^{188}Os$ with different $^{187}Re/^{188}Os$ values. The possibly discernible difference could enable the identification of source rock through the comparison with oil initial $^{187}Os/^{188}Os$. The radiogenic Sr of current Leduc and Nisku formation water and diagenetic calcites since Laramide orogeny indicates possibly deep-radiogenic origin of the fluids, e.g. Cambrian and Precambrian strata and crystalline basement (Burke et al., 1982; Connolly et al., 1990; Mountjoy et al., 1999). Such deep strata are highly likely to be very radiogenic with regard to Os, e.g. (Kendall et al., 2004; Kendall et al., 2009). No significant transfer of Re and Os from the deep-originated formation water to the Leduc-Nisku oil is validated through the inspection of current and initial oil $^{187}Os/^{188}Os$ values (from 0.78 to 1.62 and from 0.55 to 1.06, respectively) – or the oils would be far more radiogenic than they currently are.

5.3 Re-Os elemental and isotopic systematics during the fractionation of crude oil and asphaltene

The asphaltene fractions carry the majority of the Re and Os in crude oil. Also, the Re and Os abundances of the progressively precipitated fractions decrease throughout the process. Throughout the progressive precipitation of asphaltene, the $^{187}Re/^{188}Os$ values of the fractions decrease, but can also be similar for the first a few fraction. The $^{187}Os/^{188}Os$ values of the fractions remain similar during the progressive precipitation for most of the samples in this study, but they can also increase and decrease for some samples. Previous studies propose that Re and Os can be bound by stable porphyrins and multiple heteroatomic ligands. Asphaltene is also known to form aggregates easily which can absorb and occlude surrounding molecules. Thus, this study suggests that Re and Os can be bound in free molecules, i.e. the stable porphyrins and compounds containing heteroatoms, and asphaltene aggregates with such molecules absorbed and occluded. The patterns of the $^{187}Os/^{188}Os$ values of progressively precipitated asphaltene fractions will largely depend on which part holds more of the Re and Os, i.e. the free molecules or the asphaltene aggregates.

The change of asphaltene and maltene yields from the separation of crude oil by different *n*-alkanes lead to the difference in their Re-Os abundance and isotopic composition. From *n*-C_7 to *n*-C_{10}, the effect of reducing asphaltene yields with

increasing C number of *n*-alkanes is not as apparent as from *n*-C_5 to *n*-C_7. The reduced yields of asphaltene lead to an increase of Re and Os abundance of the asphaltene and maltene when using higher C number *n*-alkane compared to a lower C number *n*-alkane. However, the $^{187}Os/^{188}Os$ values of the asphaltene fractions from the same oil are basically the same. The $^{187}Re/^{188}Os$ and $^{187}Os/^{188}Os$ values of the maltene fractions from the same oil are different, however, only the maltenes of one of the six oil samples in this study yields a Re-Os age close to the source rock age, i.e. the Purisima oil.

No combinations of the fractions of a single crude oil can consistently yield geologically meaningful Re-Os age for each oil sample of this study. Therefore, the extensive application of using a single oil to obtain meaningful geological dates related to the petroleum system may not be universally viable.

The wax observed in some progressively precipitated asphaltene fractions is thought to be the cause of lower Re and Os abundance than expected, as the typical alkane structure of wax (García, 2000) is not likely to be a host of large amount of Re and Os. Thus for crude oil samples with high wax content, isolating Re and Os poor wax before Re-Os measurements might be helpful for the digestion of more Re and Os abundant fractions. Thus, when dealing with high wax contents samples in the future, it might be worthwhile to isolate wax first before the Re-Os analysis in order to increase the proportion of the more Re and Os abundant fractions to be digested.

For some of the crude oil samples in this study, the $^{187}Os/^{188}Os$ composition of the asphaltene fractions from the progressive precipitation are similar while the $^{187}Re/^{188}Os$ values decrease throughout the process. For such crude oils, there might be the chance to date the event leading to the progressive precipitation of asphaltene through Re-Os analyses, e.g. the injection of CO_2 or methane into oil reservoir.

5.4 References

Berbesi, L. A., R. di Primio, Z. Anka, B. Horsfield, and D. K. Higley, 2012, Source rock contributions to the Lower Cretaceous heavy oil accumulations in Alberta: A basin modeling study: AAPG bulletin, v. 96, no. 7, p. 1211-1234.

Burke, W., R. Denison, E. Hetherington, R. Koepnick, H. Nelson, and J. Otto, 1982, Variation of seawater $^{87}Sr/^{86}Sr$ throughout Phanerozoic time: Geology, v. 10, no. 10, p. 516-519.

Connolly, C. A., L. M. Walter, H. Baadsgaard, and F. J. Longstaffe, 1990, Origin and evolution of formation waters, Alberta basin, Western Canada sedimentary basin. II. Isotope systematics and water mixing: Applied Geochemistry, v. 5, no. 4, p. 397-413.

Creaser, R. A., P. Sannigrahi, T. Chacko, and D. Selby, 2002, Further evaluation of the Re-Os geochronometer in organic-rich sedimentary rocks: A test of hydrocarbon maturation effects in the Exshaw Formation, Western Canada sedimentary basin: Geochimica et Cosmochimica Acta, v. 66, no. 19, p. 3441-3452.

Finlay, A. J., D. Selby, and M. J. Osborne, 2012, Petroleum source rock identification of United Kingdom Atlantic Margin oil fields and the Western Canadian Oil Sands using Platinum, Palladium, Osmium and Rhenium: Implications for global petroleum systems: Earth and Planetary Science Letters, v. 313-314, p. 95-104.

García, M. d. C., 2000, Crude Oil Wax Crystallization. The Effect of Heavy n-Paraffins and Flocculated Asphaltenes: Energy & Fuels, v. 14, no. 5, p. 1043-1048.

Georgiev, S. V., H. J. Stein, J. L. Hannah, R. Galimberti, M. Nali, G. Yang, and A. Zimmerman, 2016, Re-Os dating of maltenes and asphaltenes within single samples of crude oil: Geochimica Et Cosmochimica Acta, v. 179, p. 53-75.

Higley, D. K., M. D. Lewan, L. N. R. Roberts, and M. Henry, 2009, Timing and petroleum sources for the Lower Cretaceous Mannville Group oil sands of northern Alberta based on 4-D modeling: AAPG Bulletin, v. 93, no. 2, p. 203-230.

Kendall, B., R. A. Creaser, G. W. Gordon, and A. D. Anbar, 2009, Re–Os and Mo isotope systematics of black shales from the Middle Proterozoic Velkerri and Wollogorang Formations, McArthur Basin, northern Australia: Geochimica et Cosmochimica Acta, v. 73, no. 9, p. 2534-2558.

Kendall, B. S., R. A. Creaser, G. M. Ross, and D. Selby, 2004, Constraints on the timing of Marinoan "Snowball Earth" glaciation by $^{187}Re–^{187}Os$ dating of a Neoproterozoic, post-glacial black shale in Western Canada: Earth and Planetary Science Letters, v. 222, no. 3-4, p. 729-740.

Li, C., W.J. Qu, D.H. Wang, Z.H. Chen, A.D. Du, and C.Q. Zhang, 2011, Dissolving Experimental Research of Re-Os Isotope System for Bitumen Samples: Rock and Mineral Analysis, v. 30, no. 6, p. 688-694.

Mahdaoui, F., L. Reisberg, R. Michels, Y. Hautevelle, Y. Poirier, and J.-P. Girard, 2013, Effect of the progressive precipitation of petroleum asphaltenes on the Re–Os radioisotope system: Chemical Geology, v. 358, p. 90-100.

Miller, C. A., 2004, Re-Os dating of algal laminites reduction-enrichment of metals in the sedimentary environment and evidence for new geoporphyrins: Master of Science Dissertation, University of Saskatchewan, Saskatoon, Canada, 153 p.

Mountjoy, E. W., H. G. Machel, D. Green, J. Duggan, and A. E. Williams-Jones, 1999, Devonian matrix dolomites and deep burial carbonate cements: a comparison between the Rimbey-Meadowbrook reef trend and the deep basin of west-central Alberta: Bulletin of Canadian Petroleum Geology, v. 47, no. 4, p. 487-509.

Qi, L., Gao, J.-F., Zhou, M.-F., and Hu, J., 2013, The Design of Re-usable Carius Tubes for the Determination of Rhenium, Osmium and Platinum-Group Elements in Geological Samples: Geostandards and Geoanalytical Research, v. 37, no. 3, p. 345-351.

Selby, D., and R. A. Creaser, 2003, Re–Os geochronology of organic rich sediments: an evaluation of organic matter analysis methods: Chemical Geology, v. 200, no. 3-4, p. 225-240.

Selby, D., 2005, Direct radiometric dating of the Devonian-Mississippian time-scale boundary using the Re-Os black shale geochronometer: Geology, v. 33, no. 7, p. 545.

Selby, D., R. A. Creaser, and M. G. Fowler, 2007, Re–Os elemental and isotopic systematics in crude oils: Geochimica et Cosmochimica Acta, v. 71, no. 2, p. 378-386.